UNIVERSITÀ
DEGLI STUDI
DI PADOVA

UNIVERSITA' DEGLI STUDI DI PADOVA

Sede Amministrativa: Università degli Studi di Padova
Dipartimento di Innovazione Meccanica e Gestionale

SCUOLA DI DOTTORATO DI RICERCA IN INGEGNERIA INDUSTRIALE
INDIRIZZO: INGEGNERIA DELLA PRODUZIONE INDUSTRIALE
CICLO XXII

METROLOGICAL PERFORMANCE VERIFICATION OF OPTICAL COORDINATE MEASURING SYSTEMS

Direttore della Scuola: Ch.mo Prof. Paolo F. Bariani
Supervisore: Ch.mo Prof. Enrico Savio
Correlatore: Ing. Simone Carmignato

Dottorando: Alessandro Voltan

Preface

This thesis has been prepared as one of the requirements of the Ph.D. degree.
The work has been carried out from January 2007 to December 2009 at DIMEG - Dipartimento di Innovazione Meccanica e Gestionale, University of Padova, Italy, under the supervision of Prof. Enrico Savio and Dr. Simone Carmignato.
From February 2009 to April 2009, three months were spent at the Interstate University of Applied Sciences of Technology (NTB), Buchs, Switzerland, while in 2008 a month was spent at the Technical University of Denmark (DTU), Lyngby, Denmark.
I would like to thank my supervisors for their inspiration and contributions to my work. Furthermore, I would like to express my gratitude to Prof. Claus Keferstein and all the PWO team for their hospitality and inspiration to my research activity at NTB. Finally, I would like to thank Prof. Leonardo De Chiffre and all the MEK team for the help and all the interesting suggestions during my work.

Padova, January 2010

Alessandro Voltan

Abstract

At the state-of-the-art, the use of Coordinate Measuring Systems (CMS) for verification of geometrical and dimensional tolerances is becoming very wide-spread in industrial manufacturing. Traditional CMMs are generally equipped with mechanical probes, but recent trends are highlighting several limitations of tactile probes, due mainly to the increasing requirement of faster inspection and higher complexity in measurement tasks. In particular, due to the miniaturization of components and the employment of new delicate materials, the use of optical measurement systems is becoming more and more suited for industrial applications. Nevertheless, only a very small percentage of the potential applications for non contact measurement systems is established so far. The main obstacles to a large integration of optical sensors on CMMs can be found in the lack of international accepted specification and verification rules. International standards on performance verification of optical systems are still missing and the existing ones related to mechanical CMMs cannot be applied directly to non contact machines.

For these reasons, the main objective of the present work has been to contribute to the development of methods and artefacts for performance verification of non-contact measuring systems.

The thesis is composed of three main parts.

The first part deals with a study of the state-of-the-art in non contact Coordinate Metrology, including examples of measurements and test on own machines. After a first introductive Chapter related to the productive role of metrology in manufacturing processes, the second Chapter focuses on actual industrial requirements for quality assurance and related non-contact instruments review and classification.

The second part is committed to traceability of non contact Coordinate Systems, including experimental investigations and results on different optical systems. In particular the third Chapter is dedicated to methods, standards and guideline for performance verifications and traceability of non-contact CMS, while the fourth Chapter describes activities related to the development and testing of cooperative calibration artefacts.

The third part is finally dedicated to industrial applications. The newly developed cooperative artefacts, in particular, have been applied within the European Cooperative Research Project OP3MET. During the Project, an innovative optical measuring system for automated inspection of dimensional and geometrical tolerances, including free-form surfaces, has been developed. The contribution of the author has concerned metrological verification and traceability of the new developed system. Particular attention has been paid to the application of the guideline VDI/VDE 2617-6.2: 2005. On the basis of specific experimental results on a laser scanner, the main problems arising in the implementation of testing

procedures were analyzed. The second industrial case reported in this work has been related to the integration of a chromatic sensor into a high precision circular grinding machine. The author of this Thesis participated to the integration-project working directly to the development of a software module for in-line measurement of roundness and automatic correction of systematic errors of the measurement system. After a first phase of modelling and simulation of the measuring process, the developed module has been validated by comparison with results obtained with dedicated roundness equipment and metrological software.
In the last Chapter of the present work, the main results from an industrial inter-laboratory comparison for Coordinate Measuring Machines equipped with optical sensors are presented. The comparison, named *VideoAUDIT*, has been organized and coordinated by the Laboratory of Industrial and Geometrical Metrology of the University of Padova, involving a total of 21 CMMs in Italy and other European countries. As one of the most important result, the comparison has proved that the quality of dimensional measurement results on real industrial workpieces is largely independent on the CMM length measurement performance, as well as the limited ability of most participants to properly evaluate task-specific measurement uncertainty.

Sommario

Allo stato dell'arte, l'uso di sistemi di misura a coordinate (CMS) per la verifica di tolleranze geometriche e dimensionali risulta essere sempre più diffuso in ambito manifatturiero. Tuttavia, l'esigenza relativa alla riduzione dei tempi di controllo, unita ad una maggiore complessità nel task di misura, sta mettendo in luce i limiti dei tradizionali sistemi di misura a contatto. In particolare la miniaturizzazione dei componenti e l'utilizzo di nuovi materiali facilmente danneggiabili rende l'impiego dei sistemi ottici sempre più indicato nell'ambiente produttivo industriale. Tuttavia, alcuni problemi permangono ancora a limitare la diffusione di strumenti di misura ottici per il controllo geometrico e dimensionale. Se da un lato, infatti, sono numerosi i vantaggi che essi presentano rispetto agli strumenti a contatto, dall'altro una maggiore sensibilità a fonti di errore addizionali e un panorama normativo carente rendono difficoltoso l'impiego di questi strumenti. In particolare, la mancanza di metodi standardizzati per la verifica delle prestazioni metrologiche e per la riferibilità delle misure impediscono il confronto con i risultati ottenuti mediante sistemi a contatto o tra sistemi ottici basati su principi di acquisizione diversi.
Il presente lavoro di Tesi ha avuto come obiettivo principale quello di contribuire allo sviluppo di metodi e campioni per la verifica di prestazioni di sistemi ottici, mediante lo studio accurato dell'attuale impiego in ambito manufatturiero e attraverso l'applicazione dei criteri proposti in casi di interesse industriale.
In particolare il presente elaborato risulta essere composto da tre parti.
La prima parte contiene lo studio dello stato dell'arte relativo alla Metrologia a Coordinate non a contatto, con particolare riferimento ai requisiti in ambito industriale, alla descrizione e alla classificazione dei principali strumenti ottici utilizzabili.
La seconda parte del lavoro di Tesi risulta essere invece interamente dedicata alla verifica di prestazioni dei sistemi non a contatto, comprendendo test e risultati ottenuti su diversi sistemi di misura. In dettaglio, dopo una descrizione di metodi, norme e linee guida relativi a criteri di accettazione e verifica di sistemi a coordinate ottici, particolare attenzione viene dedicata allo sviluppo di campioni di taratura.
I nuovi campioni sviluppati sono stati utilizzati dall'autore all'interno del Progetto di Ricerca OP3MET, il primo di tre casi aventi ricaduta industriale riportati nella terza parte del lavoro di tesi. All'interno del Progetto OP3MET, avente per obiettivo principale lo sviluppo di un nuovo sistema di misura 3D mediante scansione laser, l'attività dell'autore ha riguardato prevalentemente lo studio della riferibilità delle misure ottenute, l'applicazione di metodi per la verifica di prestazioni, il calcolo dell'incertezza di misura e lo sviluppo di test specifici per le verifica del nuovo software metrologico sviluppato.

Il secondo caso industriale affrontato durante il lavoro di Tesi ha riguardato l'integrazione di un sensore di misura cromatico in una macchina utensile per rettifica circolare. L'attività svolta dall'autore ha avuto come obiettivo lo sviluppo di un modulo software per la misura di rotondità in linea, in grado di effettuare la correzione automatica dei principali errori sistematici del sistema di misura stesso. Dopo una prima fase di modellazione e simulazione del processo di misura, il modulo software sviluppato è stato validato mediante il confronto con strumenti e software dedicati

Nell'ultimo capitolo del lavoro di tesi vengono riportati i risultati principali del Progetto *VideoAUDIT*, un confronto inter-aziendale tra macchine di misura a coordinate con sensori ottici ideato e coordinato dal Laboratorio di Metrologia Geometrica ed Industriale dell'Università di Padova. Dal confronto, comprendente 21 CMM in Italia e altri paesi europei, è emerso in particolare come la qualità delle misure effettuate su comuni componenti industriali sia alquanto indipendente dalle prestazioni metrologiche del sistema, così come sussistano evidenti problemi da parte degli utilizzatori nel valutare propriamente l'incertezza di misura.

Table of Contents

Chapter 1

Introduction

Following the intensification of the global competition, new and faster measuring instruments are required both in laboratories and production processes. The time saved in developing a prototype of a product contributes to reduce the final cost of the product: for this reason, also quality control and inspection have evolved in recent times, mainly through the introduction of new measuring instruments with increased performances. New challenges in metrology are now represented by the increasing miniaturization of components and the employment of new fragile and deformable materials. Therefore, non-contact measuring systems are becoming more and more used in "productive metrology" for 3D measurements in stead of conventional contact systems.

1.1 PRODUCTIVE METROLOGY

As indicated in [1] "Production" is understood as a "Combination of material and non-material goods for the manufacture and utilization of other goods respectively products". The life cycle of a product includes design, development and testing before or while suppliers are called in and the supply chain is established. Kunzmann et al. define in [2] Production Metrology as "the fundamental tool to gain information and knowledge in all phases of the life-cycle of any product to help linking the separate production processes". For this reason, metrology is not only related to Quality Inspection, but it can be addressed as an actual productive tool. However, it must be productive in an economic way, both cost efficient and relevant to satisfy the single process requirements of information (Fig. 1.1). Dance [3] underlines the productive aspect of metrology: "Knowledge gained through metrology adds value through continuous learning and improvement. Thus if characterization information improves the process, then metrology is a value added step." Several measurement activities are directed to the new product as well as to the new manufacturing process, as:

· new product-oriented measurements for model verification,
· performance and conformity testing,
· new process-oriented measurements for process analysis and qualification,
· equipment qualification, e.g. machine tool verification

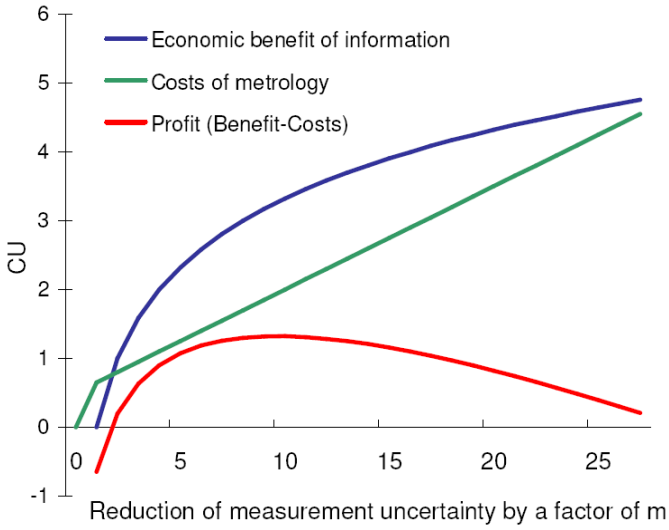

Fig. 1.1: Optimal investment on metrology [2].

Nevertheless, if results coming from measuring equipment are not reliable, their measurements could not be called productive: capability of measuring equipment and process capability are strictly connected in production environment, as shown in Fig. 1.2.

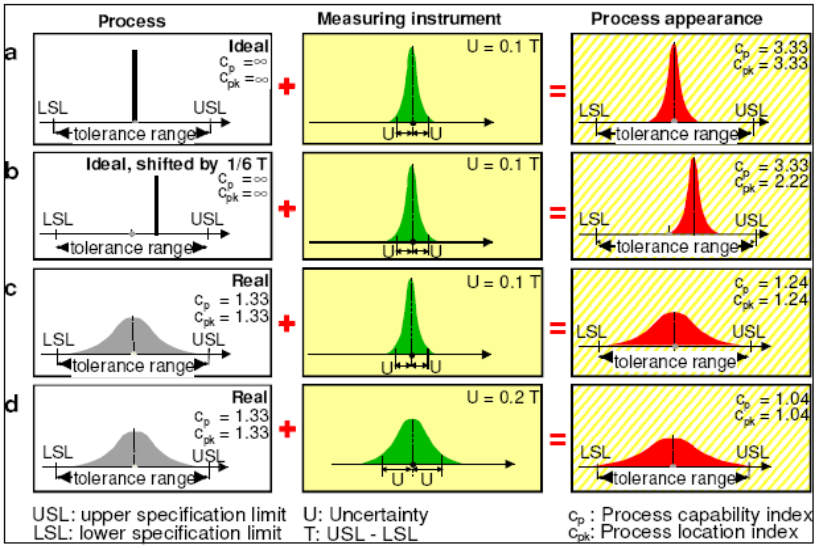

Fig. 1.2: relations between process capability and measuring uncertainty [2].

In this figure is clearly shown as the performance indicators of a process (such as Cp and Cpk) are the sum of two contributions: the capability of the process itself and the uncertainty of the measurement equipment. For this reason, traceability of

measurements becomes a necessary step not only to assure a common code of information but also to contribute to the improvement of the production processes.

1.2 EVOLUTION OF QUALITY, FROM CONTROL TO ASSURANCE AND AUTOMATION

During the last years, quality has moved from the concept of control to the concept of assurance. Quality assurance, moreover, needs new technological instruments such as SPC, in line inspection and integration of quality control while the product is being made. The need for in-process measurements and control has arisen owing to competitive pressure and market pull [4]. The modern consumers or other end users of manufactured goods are now intolerant of inferior quality. Furthermore, in industrial manufacturing of critical goods, such as in pharmaceutical production, 100% inspection is required by regulatory [5]. Because of cost limitations associated with quality control and inspection, the manufacturer must turn to a technological solution that is going in the direction to integrate automatic measurement system directly along the production line [6]. Therefore, manufacturers are obliged to ensure that the highest quality standards are met while reducing costs. The needing of innovation in quality control has lead to an increasing development of systems and sensors that can be used for the automatization of measuring processes [7],[8],[9]. These sensors coupled with computerized control and appropriate software, can be utilized in a feedback arrangement to maintain the process within the allowable tolerance band. All the inspection can be automatized, reducing costs and scraps. In-process sensors can be classified into two major categories: contact and non contact. Non contact sensors have come into greater favour because the lack of contact eliminates wear and deflection, which introduce inaccuracy into the measurements. Different kinds of non contact sensors can be employed in in-process control such as capacitive sensors, eddy current, ultrasound, Computed Tomography, Fiber optic, Optical, etc.
Optical sensors in particular have a number of advantages. First of all that they are truly non contact, in that there are no forces on or connections to the part being measured. They can measure parts of any material and they allow the distance from the sensors to the object being measured to be large. As will be explained in Chapter 2, various optical techniques are used in dimensional measurements.

1.3 COORDINATE METROLOGY

For the inspection of material goods in the industrial production processes, coordinate metrology has gained recognition since its development in seventies [10]. Coordinate metrology deals with measuring technologies performing three-coordinate measurements by means of a Coordinate Measuring System (CMS). Dimension, position and form tolerances can be determined on a Coordinate Measuring Machine (CMM), a CMS with Cartesian architecture. It is basically a question of collecting single points on the surface of a workpiece. The probed

points are all represented by their coordinates (e.g. (x,y,z) Cartesian coordinates). However, these coordinates do not give any information as to the parameters of the workpiece (e.g. diameter, angle etc.) under investigation. Therefore the points have to be combined into substitute geometric elements [11],[12] by applying mathematical algorithms to combinations of single points. The number of sampled points necessary to perform the calculation of the substitute geometric element depends on the geometry. Where a CAD model is available, it can be used as nominal element. CMMs are widely used because of their flexibility and are found in many different roles in the chain of quality assurance in production. First CMMs were developed in the 1950s [11] and they were mainly equipped with tactile probes. During the years, CMMs have evolved integrating also non-contact probes and improving their measuring accuracy and capability. In the following sub-paragraphs CMMs are described in the versions they can now be found.

1.3.1 COORDINATE MEASURING MACHINES WITH TACTILE PROBES

Conventional Coordinate measuring machines (CMMs) are equipped with tactile probes that mechanically contact the workpiece surface. Tactile CMM probes have reached a very high level of accuracy (<0.5μm) and reliability. CMMs in the shape that is known today were developed in the 1950s [11]. The first CMMs were introduced in response to the need for faster and more flexible measuring tools as machining became more complex through the use of numerically controlled machine tools. Almost simultaneously CMMs were developed in England, Italy, Japan and the USA, the first CMMs being operated using solid probes [11]. The invention of the touch-trigger probe in the early 1970s improved the CMMs and their performance dramatically. At the same time the three-dimensional measuring probe head was introduced making continuous scanning possible [11],[12]. Since the end of the 1970s a very fast development of CMMs has been observed [13]. The development in information technology initiated the use of software error correction of CMMs improving their performance. Also the possibilities of measuring more complex items (e.g. small and soft items, gears, freeform surfaces etc.) have increased during the last twenty years. The development of new materials for construction elements has made modern CMMs faster and less sensitive to temperature effects. The versatility of modern CMMs combined with the very fast development has made CMM a widespread measuring instrument.

1.3.2 CONTACT CMMS FOR MEASUREMENTS OF MICROCOMPONENTS

Most accurate contact-CMMs have a Massimum Permissible Error (MPE) of about 1 micron when measuring dimensions up to 100 mm and dimensions of probes employed for the measurements have diameters generally bigger than 0.3mm. For these reasons employment of traditional CMMs in microtecnology is not possible. First of all they are not enough accurate and the dimension of probe are too big if compared with dimensions to be inspected. Nevertheless the

technology employed in coordinate measurement is completely 3D. In the recent past, a series of CMMs have been expressly developed for the measurements of microcomponents. They are equipped with miniaturized probes or optical sensors and are designed following criteria of design for precision. CMMs for microsystems, with measuring range less than 100mm and designed to obtain measuring uncertainty less than 0.2μm, are extensively described in [14] and briefly presented in the following.
A special CMM with a working volume of $1dm^3$ and measuring uncertainty of less than 0.1μm has been designed at the Technical University of Eindhoven [15], [16]. As is possible to notice in Fig 1.3, where the functional scheme of the machine is reported, the accuracy of the machine is achieved using a completely symmetrical design.

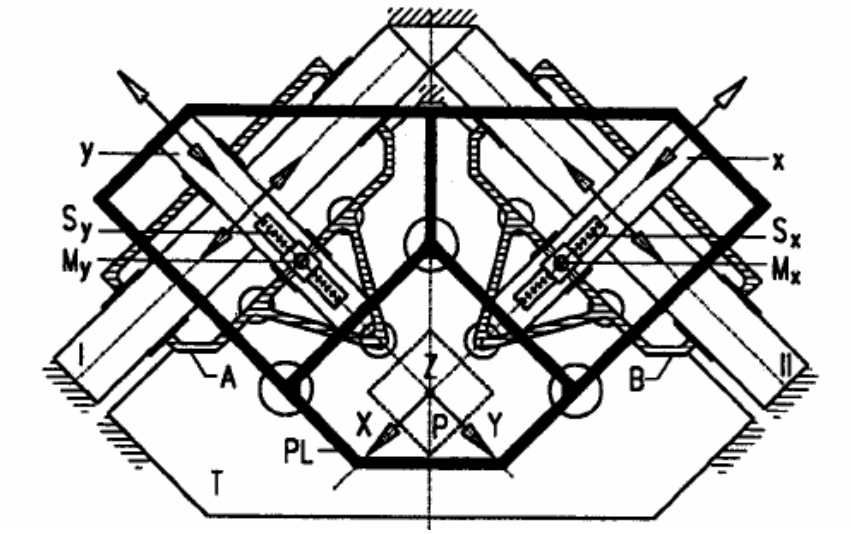

Fig. 1.3:. Schematic of the precision CMM designed at the Technical University of Eindhoven [15].

A CMM for microcomponents has been developed in collaboration between two companies: IBS Precision and The Philips Centre for Industrial Technology CFT. This machine is available from 2004 on the market with the name of Isara® [17] and the manufactures stated a measuring uncertainty of 30nm, with a measuring volume of (100x100x40)mm. The accuracy of the machine is achieved removing the so called Abbe error, keeping the probe fixed and moving only the table, the position of which is measured by laser interferometers. In the UK, at the National Physical Laboratory (NPL), the so called "Small volume CMM (SCMM)" [18],[19] has been developed to be integrated with a traditional CMM. The measuring cube has a 50mm side and an uncertainty target of 50nm. Another solution has been developed by the Physikalisch Technische Bundesanstalt (PTB), where a CMM with a working volume of (25x40x25)mm, with measuring uncertainty less than

0.1µm has been produced starting from a systems already produced by the Werth Messtechnik company. Finally, the so called "nano positioning and measuring machine" has been developed between the Technical University of Ilmenau and the SIOS Messtechnik company [20]. The measuring range is (25x25x5)mm and, as the measuring machine developed by IBS precision, use table movement for measurement respecting the Abbe principle in the entire measuring volume.

1.3.3 NON-CONTACT COORDINATE MEASURING SYSTEMS

In the recent years, many different types of optical sensors have been used. With non contact optical sensors the measurement speed can be increased and therefore a larger number of measurement points can be acquired within a shorter time. Flexible parts can be probed without being deformed and very small structures can be measured which could not be resolved with a conventional tactile probe [21]. Typical optical sensors used on CMMs are triangulation sensors (Fig. 1.4a), autofocus sensors and video probes (Fig. 1.4b). A detailed description of the most used optical sensors will be presented in Section 2.3.

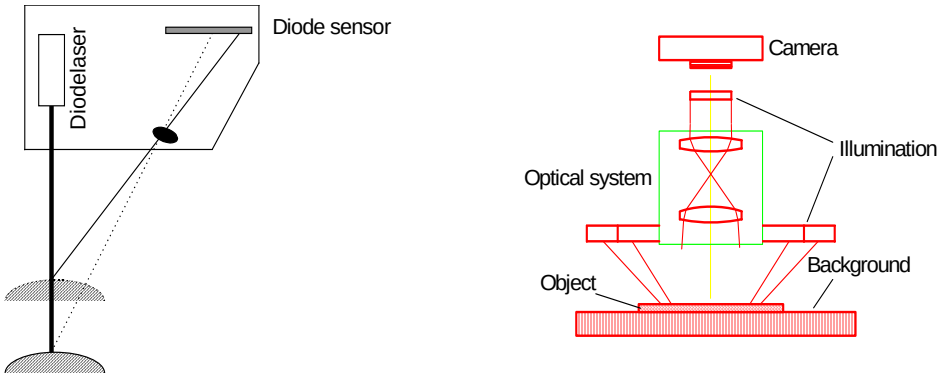

a) b)

Fig. 1.4:. Optical sensors: a) Triangulation sensor, b) Video Probe [22], [23]

1.3.4 MULTISENSORS SYSTEMS

Comparing tactile and optical techniques in production metrology, it is possible to find complementary properties. Soft coatings that should not be touched and thin membranes or cantilevers pose problems for tactile techniques but not for the optical ones. Optical techniques have limitations measuring steep surface slopes, specularly reflecting or transparent or black materials. For ceramics and plastics, light is not reflected from surface but remitted from a volume below the surface, thus causing erroneous optical measures. All of this is not a problem for touch probes. Undercuts cannot be measured optically and planar structures (like chromium on glass) not tactile. Considering the advantages and disadvantages of different sensor types, the trend for CMM manufacturers goes towards multi-

sensor machines, in which mechanical and different optical sensors are combined to measure in a common coordinate system (Figure 1.5).
With the opto-tactile fibre probe [24], characteristics of optical and mechanical probing are combined in one sensor system: a fibre probe with a tip diameter down to 25µm and a probing force down to 1µN mechanically contacts the surface while its position is evaluate by a video camera.

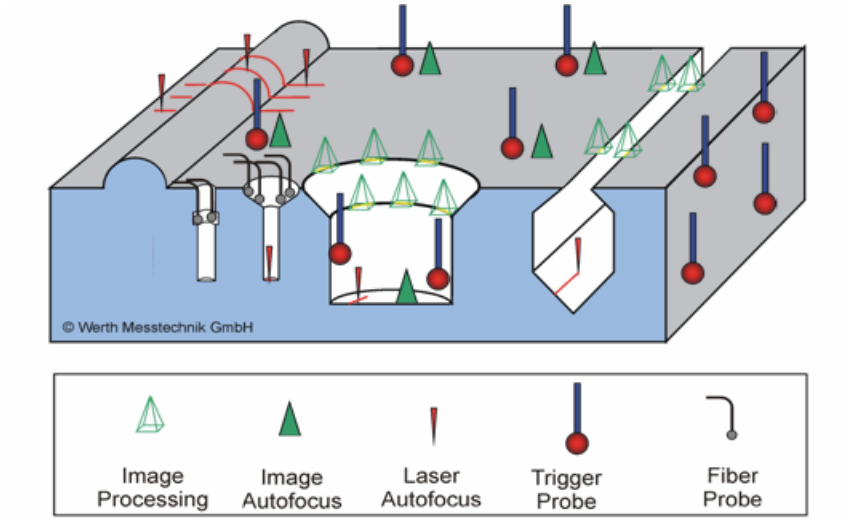

Fig. 1.5: Applications of tactile and optical sensors by a multisensor CMM [25]

1.4 TRACEABILITY OF COORDINATE MEASURING MACHINES WITH OPTICAL SENSORS

Traceability is essential to ensure comparability, accuracy and reliability of measurements.
Traceability of measurements is also a normal requirement of ISO 9000 [26] and ISO 17025 [27]. According to the International Vocabulary of Basic and General Terms in Metrology [28], traceability is "the property of the result of a measurement or the value of a standard whereby it can be related to stated references, usually national or international standards, through an unbroken chain of comparisons all having stated uncertainties".
Traceability is guaranteed by calibration: "a calibration establishes a relationship between the indicated values of a measuring system and the conventional true values of a measurand". Calibration of CMMs according to the definition means determination of correctable and non-correctable errors and uncertainties for all possible measuring tasks in the whole measuring volume of the CMM. This is impossible due to the complexity of the measurement model and therefore the calibration of CMMs for individual measurement tasks, the so-called task related calibration, is recommended. National and international standards have defined

performance verification procedures for acceptance and reverification tests of contact CMMs, which typically involve their ability to measure calibrated lengths (e.g. gauge blocks or step gauges) and form (e.g. calibrated spheres). It is recognized that, without further analysis or testing, these results are insufficient to determine the task specific measurement uncertainty of most measurements (See Section 2.6.1). The application of mere performance verification tests, therefore, does not guarantee full traceability.
While traceability remain a difficult task for contact CMMs, the situation is even worse for optical CMMs [29]. Up to now, in fact, testing procedures and artefacts for performance verifications of non-contact systems are not completely defined by the available international and national standards. Standards regarding contact probing CMMs are not directly applicable to non-contact systems.
Moreover, measuring strategies, illumination, surface structure and geometry of the object, represent additional error sources. Therefore probes and optical CMS cannot simply be characterized only by measurement error limits. **They have to be characterized in a more complex way by their error limits under specified conditions of operation.**

1.5 PROBLEM IDENTIFICATION AND WORK STRUCTURE

Optical coordinate systems are very promising in the field of "productive metrology" and for automatic quality control. To allow a better integration in manufacturing environment, some problems have still to be solved. These problems regard first of all the evaluation of their metrological performances, as a prerequisite for the achievement of full traceability. A seen before, in fact, testing procedures and artefacts for performance verifications of non-contact systems are not completely defined by the available international and national standards while standards for contact systems cannot directly be used for optical systems.
Starting from this consideration, the general aim of the Ph.D. project was to investigate methods for performance verification and traceability of optical coordinate systems, with the main objective to contribute to the international pre-normative research.
In particular the Thesis is articulated in the following way:

In Chapter 2, after having described the actual industrial requirements and typical applications of optical metrology, a short description of the optical sensors mainly used in coordinate metrology and their working principle will be reported. Then, the relation between industrial requirements and metrological performances of measuring equipment will be laid down.
A state-of-the-art study in the field of performance verification and traceability of optical CMMs will be presented in Chapter 3. After a first part related to description and experimental investigation on specific error sources for optical CMS, guidelines, standards and initiatives for standardization of performance verification procedures are described and discussed.
As the influence of the object properties (material and surface characteristics) on the measurement result is much stronger and more difficult to assess for optical sensors than for tactile ones, also suited artefact are needed for calibration and verification of optical systems. In particular the artefact properties should have no significant effects on the parameters to be determined. In Chapter 4 an experimental investigation on "cooperative surfaces" and related results will be presented, paying particular attention to the description of artefacts developed for evaluation of metrology performances of triangulation laser systems.
The newly developed artefacts, in particular, have been applied for the verification of a laser scanner within the European Research Project OP3MET described in Chapter 5. The contribution of the author has regarded mainly the traceability of the system, including both performance verification, uncertainty evaluation and testing of the newly developed metrological software. In particular the national standard VDI/VDE 2617:6-2 [30] has been implemented and studied for metrological verification of the newly developed scanner.

In Chapter 6 another industrial application of optical metrology will be reported, related to integration of metrology instruments directly into the production line. The activities reported in this section have been performed during a period spent by the author at NTB – Interstate University of Applied Sciences of Technology in Buchs, in Switzerland.
Finally, the main results of the *VideoAUDIT* industrial inter-laboratory comparison for Coordinate Measuring Machines (CMM) equipped with optical sensors will be presented in Chapter 7. Beside the evaluation of metrological performances of optical CMMs in industrial environment, an important task of the comparison was to test the ability of participants to determine the uncertainty of their measurements. Important results have been achieved during the comparison, confirming the necessity of more standardization and good practices for optical systems.

Chapter 2

Industrial requirements for quality assurance and instruments review

Today's production is characterized by an increasingly complexity, related mainly to the employment of new materials, miniaturization of products and related components and needs of a lower measuring uncertainty. These aspects have lead to the development of new instruments and mainly optical systems can guarantee the satisfaction of industrial requirements. In this Chapter a short overview of actual industrial requirements is reported and discussed. Then, after having described the most common optical sensors used in coordinate metrology, the relation between industrial requirements and metrological performances of measuring equipment will be laid down.

2.1 INDUSTRIAL REQUIREMENTS FOR QUALITY ASSURANCE

In table 2.1, the most significant results related to an analysis of requirements to quality assurance in the manufacturing industry are reported [31]. The analysis, led by the Department of Mechanical Engineering of the Technical University of Denmark, has been carried out within the OP3MET Project (see Chapter 5) involving 48 industrial companies in Denmark, Italy, Romania, Portugal and Iceland.

The analysis has addressed a number of issues related to tolerance verification on industrial workpieces: typical geometries, materials, dimensions, weight, surface properties, tolerances, current instruments, measuring times, and other requirements for in-line quality control. In particular Table 2.1 shows the range between the companies of Minimum Dimensional Tolerance Values and Minimum Geometrical Tolerance Values that they are used to verify. If, as reported in the table, tolerances to be verified need an increasing accuracy of measuring instrument, from the other side (Fig. 2.1) also faster measuring systems are required by industries. For these reasons, optical measuring systems are becoming more and more widespread in production. In the following section, typical application of optical measuring systems will be presented.

Minimum Dimensional Tolerance Values		
	Min	**Max**
Linear [mm]	0.002	0.100
Angles [°]	0.003	5.000
Edges [mm]	0.040	0.100
Minimum Geometrical Tolerance values		
	Min	**Max**
Straightness [mm]	0.002	0.500
Flatness [mm]	0.002	0.200
Roundness [mm]	0.002	0.200
Cylindricity [mm]	0.005	0.500
Line form [mm]	0.020	0.200
Plane form [mm]	0.010	0.600
Parallelism [mm]	0.010	0.200
Perpendicularity [mm]	0.002	0.500
Angularity [°]	0.010	0.100
Position [mm]	0.010	0.500
Coaxiality [mm]	0.002	0.500
Symmetry [mm]	0.010	0.500
Circular Run-out [mm]	0.010	0.300
Total Run-Out [mm]	0.005	0.300

Table 2.1.: industrial requirements for quality assurance [31].

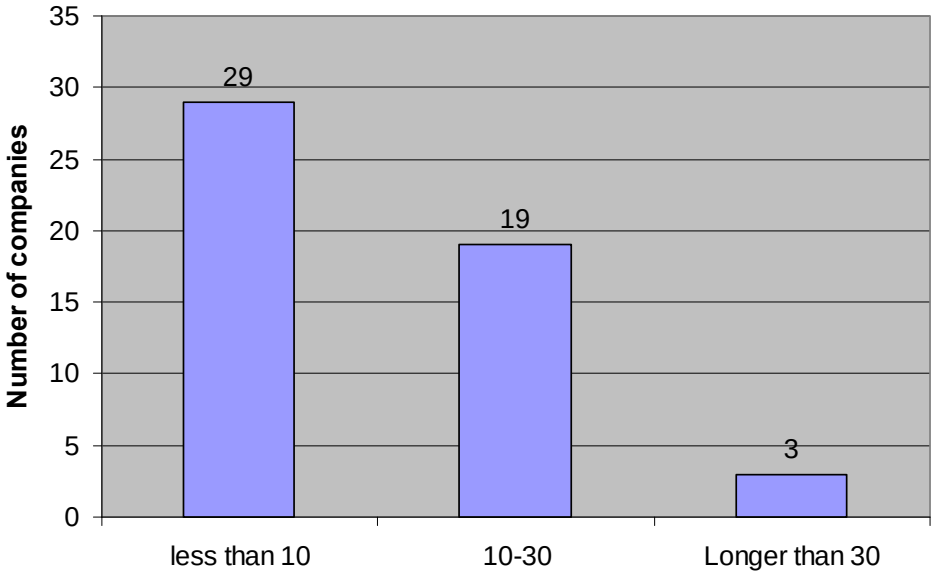

Fig. 2.1: Typical measuring time pr. workpiece in min. [31].

2.2 TYPICAL APPLICATION OF OPTICAL CMMS

Considering the industrial requirements for quality control outlined in previous paragraph, the employment of non-contact CMMs are expected growing in manufacturing industry [8],[9].
Respect to contact systems, in fact, optical instruments present a series of advantages and disadvantages, that are summarized in Table 2.2.

Optical Measuring Systems	
Advantages	**Disadvantages**
• High density measurement data • No deformation by probing force • Possibility to measure deformable parts • Possible to measure area at once • Easy to measure a freeform surface • Measuring results easy to compare with the CAD models	• Generally larger uncertainty • Difficulty in error estimation • Effect of ambient light • Results are influenced by optical properties of the object to be measured • Cost

Table 2.2: comparison between optical and tactile measuring systems.

In general, optical sensors for inspection of parts offer several advantages: higher speed, freedom from damage, decreased maintenance, availability of more information.
The absence of contact makes optical coordinate systems particularly suited for measurements of microcomponents [32]: a typical example of a workpiece that can easily be measured with an optical CMM with a 2D sensor (see Section 2.3) is reported in Fig. 2.1.
Moreover as component become more complex and freeform, non-contact methods become increasingly advantageous respect to tactile CMMs. When inspecting complex freeform shapes with a contact probing method, in fact, only a small number of points are typically measured. Using non-contact methods, instead, a much denser point cloud can be acquired in a very short period of time [33]. This is commonly what is required for the inspection of complex freeform surfaces, where the importance of the accuracy of a single point measurement is coupled with the density of the inspected data and the coverage over critical areas. Dense point clouds can be directly compared to a nominal CAD model and the operator can see instantly (via colour plots) where a part is in or out of tolerance (Fig 2.2).
For all these application of CMMs there is one common requirement: the measurement result must be traceable to the unit ‘meter’ and uncertainty must be stated. Only traceable measurements are valid for formal quality assurance systems.

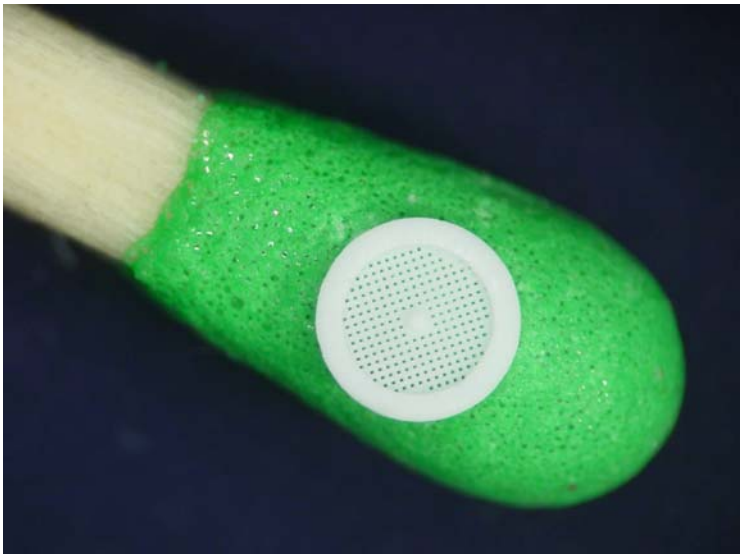

Fig. 2.1: example of microcomponent [34].

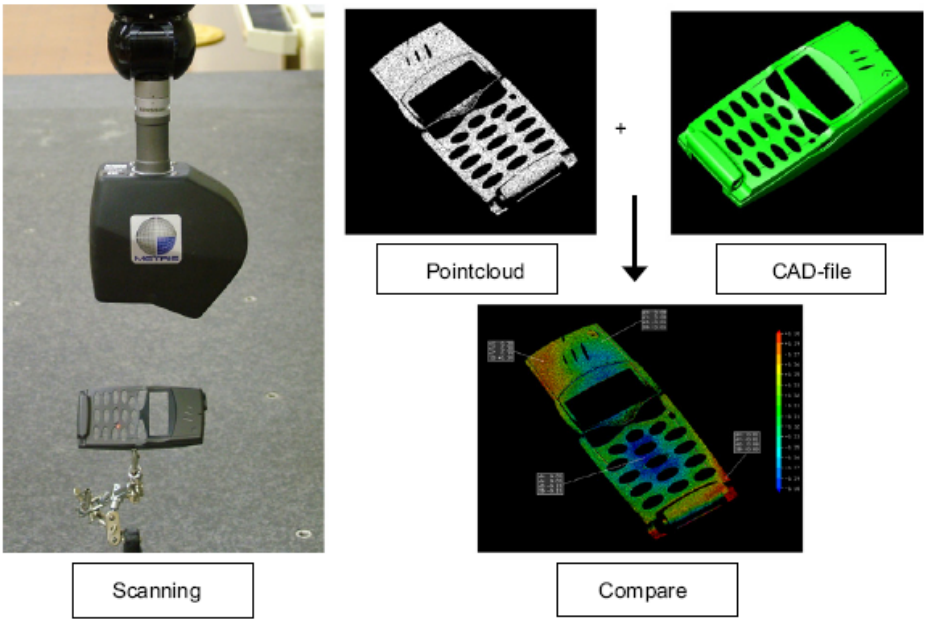

Fig. 2.2: Typical application of a laser line scanner for dimensional control of a freeform surface [35].

2.3 CLASSIFICATION OF OPTICAL SENSORS

In Table 2.2 a method for sensor classification proposed by the OSIS WG3 [36] is shown (see Section 3.5). This classification have been introduced to help users and manufacturers to have an objective method for assuring:

- The understanding of the technology the sensor uses;
- An immediate association of the sensor technology and the measuring task required;
- A fast identification of the sensor technology by mean of an alphanumeric code.

Heading	Type	Classification Criteria	Explanation
Sensor movement requirement	A	Trigger	Must move to acquire data
	B	Stand still	Must not move to acquire data
	C	Scanning	Can acquire data whether moving or not
Point Data Output	1	Point with 1 degree of freedom	r,s or t
	2	Point with 2 degrees of freedom	rs, st, rt or a combination of these in space
	3	Point with 3 degrees of freedom	All r,s,t
	4	Multiple points with 1 degree of freedom	Multiple r, or s, or t
	5	Multiple points with 2 degrees of freedom	Multiple rs, or st, or rt, can be distance sensitive (rt or st) or lateral sensitive (rs)
	6	Multiple points with 3 degrees of freedom	Multiple rst (Point cloud data)
Sensor Data Acquisition Style	I	Simultaneous acquisition of points	Points acquired at the same time
	II	Sequential acquisition of points	Points acquired one at a time, fast or slow
	III	Single Point measurement only	-
Feature Output	YES	Can provide complex feature extraction	Provides geometric feature information (e.g. Gap & Flush)
	NO	Cannot provide complex feature extraction	-
Light source	INT	Internal light source	Active light source
	EXT	External light source	Ambient light source
Technology features	Yes	Active mechanics	-
	No	Does not have active mechanics	-

Table 2.2: Optical sensors classification as reported in [36].

In the national standard VDI/VDE 2617-6 [37] optical sensors are divided into two main groups:

- Lateral sensors;
- Distance sensors.

In the following paragraphs this classification will be used.

2.4 OPTICAL LATERAL SENSORS

Lateral sensors (2D sensors) for coordinate metrology all work on the principle of measurement in the image of the workpiece as seen by a sensor (Fig 2.3). An image is taken by a camera and points detected in this image. The camera is usually a so-called CCD-camera, consisting of an array of photosensitive elements, so-called pixels. Each pixel gives an analogue output which is proportional to the light intensity projected onto the pixel. In this way the image of the surface is digitised into an array containing information on the light intensity of each pixel. This information can be analyzed automatically in a digital picture processing computer. The processing software detects edges based upon transitions from dark to light or light to dark. This system is used to determine the X- and Y-coordinates of the object. After having digitized the picture in principle is an array of numbers which represent the greyscale factor for each pixel. The system can distinguish between a certain number of levels of grey depending on the A/D-converter of the system. Basically the 2D-sensor works only in one plane giving X- and Y-coordinates as results of the measurement. If the Z-coordinate has to be determined this is usually done by video-autofocus or by manually adjusting the focus [38].

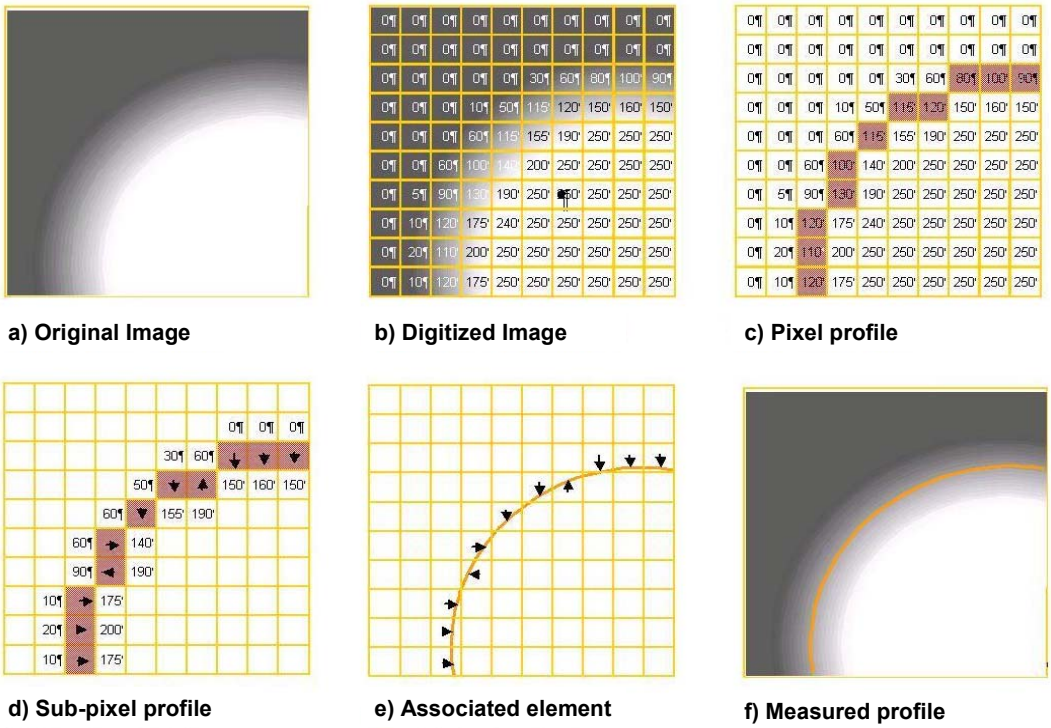

Fig. 2.3: Principle of the CCD sensor [38].

2.5 OPTICAL DISTANCE SENSORS

This section gives an overview of the main optical distance sensors suitable for coordinate measuring systems. According to [30], the sensors are grouped in the following way (see Table 2.3):

- One-dimensional (1D) sensors: needing at least two mechanical moving axis for 3D measurements;
- Two-dimensional (2D) sensors: needing at least one mechanical moving axis for 3D measurements;
- Three-dimensional (3D) sensors: without need for external moving axis.

Three-dimensional methods (w/o external frame of reference)	Methods involving structured lighting	
Two-dimensional methods (involving at least one mechanical axis for three-dimensional measurements)	Methods based on triangulation	Laser light section/ Laser scanning
	Interferometric methods	White-light interferometry
	Focusing methods	Confocal microscopy
One-dimensional methods (involving at least two mechanical axis for three-dimensional measurements)	Focusing methods	Chromatic focusing method
		Laser focusing method
		Video autofocus method
	Methods based on triangulation	Point triangulation
	Holographic methods	Holographic conoscopy

Table 2.3.: Optical distance sensors as classified in [30].

2.5.1 1D SENSORS

2.5.1.1 Point triangulation sensors

The main components of a triangulation sensor are shown in Figure 2.4. A light source (such as a laser diode) emits a collimated laser beam in a specified direction. The beam axis is the measurement line. The surface of the test object causes a diffuse reflection of the light beam. The resulting light spot is projected onto a position detector (such as a position-sensitive photo diode, a differential photo diode, or a linear CCD array) by means of an optical imaging system whose axis is inclined with respect to the laser beam axis.

The angle between the optical axis of imaging system and laser beam is the triangulation angle. The position of the light spot on the detector changes as the distance between the sensor and the test object changes. The sought-for distance between sensor and test object then results from the position of the centre of the light spot on the detector.

Triangulation sensors using CCD-detectors generally yield a better accuracy because the intensity profile of the image can be determined. On the other hand,

for this sensor type, the influence of ambient light cannot be eliminated by a modulation of the laser intensity.
Furthermore, sensors with CCD detectors are more expensive and their measurement bandwidth is smaller.
Typical measurement ranges of triangulation sensors are 2mm to 200mm; they provide relative resolutions down to 10^{-4}. The main uncertainty contributor in most applications is the optical characteristic of the workpiece surface, for example very smooth surfaces cannot be measured because of insufficient diffusely reflected light. Controlling the laser intensity and the sensitivity of the detector can moderate this effect. Errors are also induced by: the slope of the surface (which may produce direct reflections to the detector), volume scattering (e.g. for plastic material), or an inhomogeneous surface texture [22].

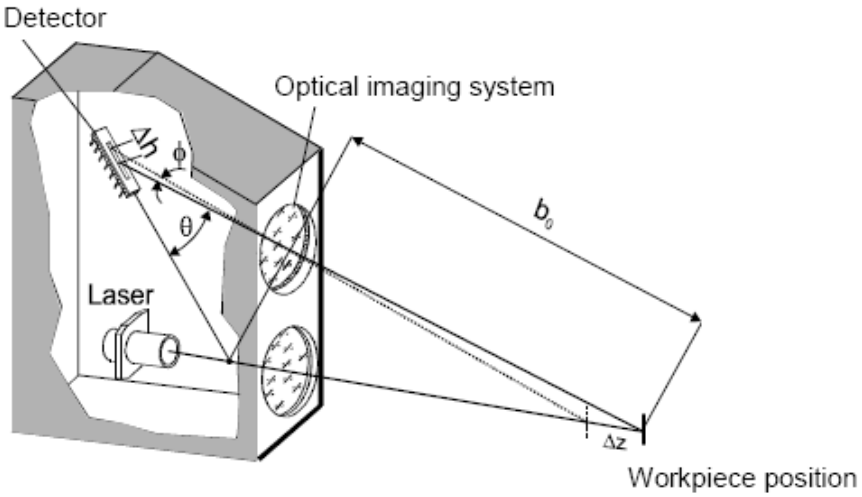

Fig. 2.4: Principle of the triangulation sensor [29].

2.5.1.2 Focusing sensors

In comparison to triangulation sensors, instead of collimated light being projected, in focusing sensors the light is focused onto the surface of the specimen. The reflected light is directed to a focus detector. Depending on the position of the surface relative to the focal point, the outer or inner segments of the focus detector are illuminated. Either the sensor or the objective is shifted in the direction of the optical axis in closed loop control until the surface is in focus. Then the position of the sensor relative to the surface can be determined. The measurement ranges of typical autofocus sensors are small (up to ±250µm) compared to triangulation sensors. On the other hand, autofocus sensors can provide a significantly higher accuracy. On cooperative surfaces, relative repeatability in the order of 10^{-3} to 10^{-4} of the measurement range can be achieved. When sharp edges are measured directly or when the reflectance of the surface changes significantly within the measured profile, an autofocus sensor can produce large errors [22].

There are different kinds of focusing sensors, working with different principles. In the following three different methods are described: (i) Focault method, (ii) Contrast-focusing method and (iii) Chromatic focusing method [30].

(i) Foucault method

The Foucault method is illustrated in Figure 2.5. A laser beam, emitted by, e.g., a laser diode, is focused onto the surface of the test object. The diffuse reflection of the light spot is projected via a beam splitter onto a detector (mostly a linear array of differential diodes).

A diaphragm introduced into the optical path serves to block part of the light beam, making it asymmetrical. This will give rise to a signal in the differential diode as long as the surface of the test object probed does not lie in the focus of the sensor. The detector signal allows for direct determination of the variations in the distance between test object and sensor (measuring sensor). However, the detector signal can also be used as an input signal to control the focusing of the optical imaging system or the sensor as a whole, allowing for scanning of the surface. The position and orientation of the sensor in the frame of reference of the coordinate measuring machine then allows determining the measurement points for detecting the geometry of the object in question [30].

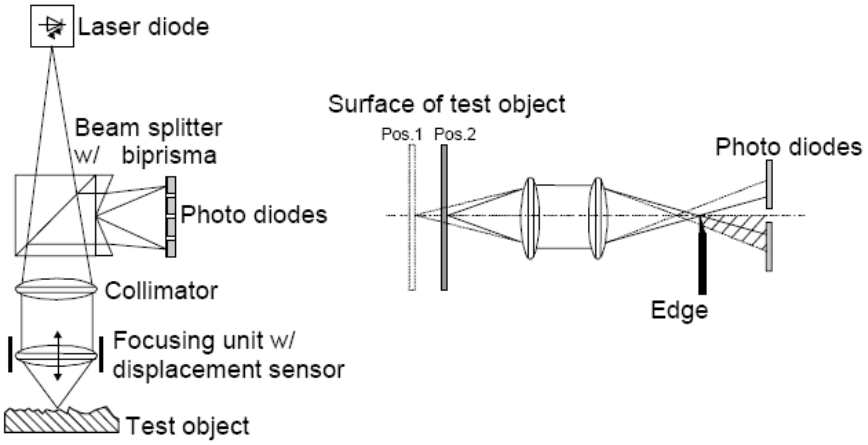

Fig. 2.5: Principle of the Foucault method [30].

(ii) Contrast-focusing method

Contrast-focusing methods are used, e.g., in CCD cameras with image-processing systems. They determine the distance from the surface of the test object by focusing to maximum contrast (image sharpness). This is usually achieved by means of a relative movement along the direction of measurement, between the sensor and the test object (Figure 2.6). While doing so, the position of the sensor and a weighting criterion for the contrast are determined. In addition to the contrast proper, it is possible to use, e.g., acutance (steepness of an edge) or the

spectrum of spatial frequencies. This evaluation is performer for a part of the entire image, whose position and size can be specified by the user.
When the position of greatest contrast has been found, the part of the image under evaluation lies on the optical axis of the sensor, at a known distance in front of the same. This distance is determined beforehand by means of calibration. For enhanced resolution of distance measurement, a best match curve is frequently fitted to the measured contrast values, and the position of the maximum of this curve is calculated in terms of an interpolated sensor position of the focal point.
Image-processing systems are mostly equipped with their own sources of lighting. Furthermore, in order to allow probing of objects with low-contrast structures by means of video autofocus sensors, systems are used which project a high-contrast, sharp pattern onto the object surface, allowing focusing on this projected pattern [30].

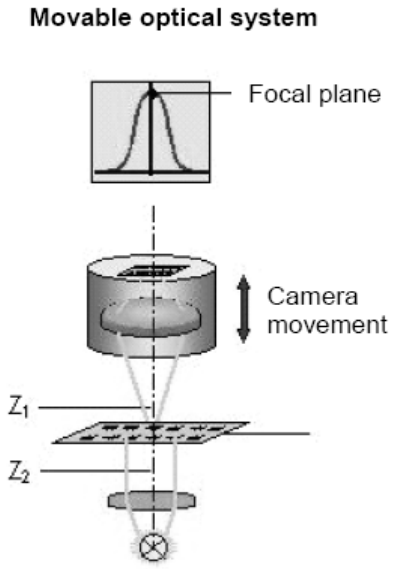

Fig. 2.6: Principle of the contrast-focusing method [30].

(iii) Chromatic focusing method

The chromatic sensor (Figure 2.7) focuses white light using a lens. Due to chromatic aberration of the lens, rather than being collected in a focal point behind the lens, the light is focused in a "focal line" depending on the wavelength of the light. The different colour components of white light are therefore focused at different distances from the sensor and can be detected using a spectrometer. The distance information of the chromatic sensor is determined from the wavelength as detected by the spectrometer.

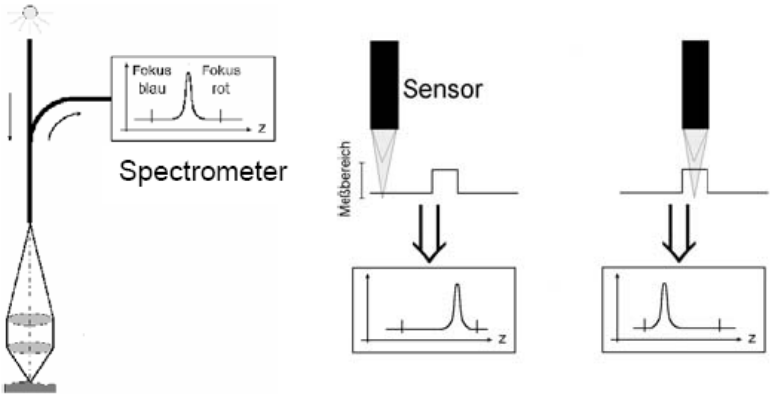

Fig. 2.7: Principle of the chromatic focusing method [30].

2.5.1.3 Holographic conoscopy

The principle of holographic conoscopy is shown in Figure 2.8.

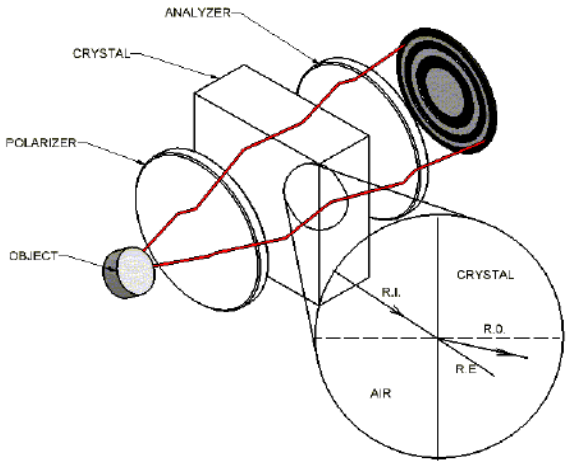

Fig. 2.8: Principle of holographic conoscopy [39].

The sensor contains a laser diode that illuminates the specimen by a quasi-monochromatic light beam.

The light emitted at the spot on the surface passes through a lens and a circular polariser, and then the circularly polarised light passes through a uniaxial crystal (e.g. calcite). The crystal axis is oriented parallel to the optical axis of the lens. As a result, the incident light hitting the crystal at an angle is split into an ordinary and an extraordinary ray. The ordinary refractive index is constant, while the extraordinary refractive index - and so the phase delay between the rays - is a function of the direction of propagation relative to the crystal axis. In a first-order approximation, the different refraction angles of the rays can be neglected because

the difference between the refractive indices is small. The two rays interfere after having traversed the circular analyser (a second circular polariser) and form interference rings. This pattern is detected by a CCD array. The distance between the rings depends on the distance between sensor and specimen. Typical measurement ranges of conoscopic sensors are between 0.6 mm and 70 mm. The relative accuracy is in the order of 10^{-3} and the repeatability in the order of 10^{-4} of the measurement range. Sharp surface slopes (up to 85°) may be measured [39].

2.5.2 2D SENSORS

2.5.2.1 Line triangulation

Line (or light sectioning) triangulation sensors are based on the triangulation principle. In comparison with point triangulation sensors, widening the laser beam through a special cylinder lens or an oscillating mirror generates a "light curtain". The linear array detector used for point triangulation is replaced by a sensor matrix (e.g. a CCD matrix). Image processing algorithms are used to determine the position of the light line, diffusely reflected by the test object, on the sensor matrix. The distance between the laser light sectioning sensor and the test object surface is calculated as for the point triangulation method, extending the evaluation of a point to that of a line.

2.5.2.2 White-light interferometry

In white-light interferometry, the light of a source of white light is first fed into the sensor via a beam splitter, where upon it passes through a microscope with built-in interferometer.

If the path length of the light between lens and test object exactly equals the path length of the light in the interferometer, white-light interference fringes can be seen. Figure 2.9 shows the principle of a white-light interferometer and the interference fringes.

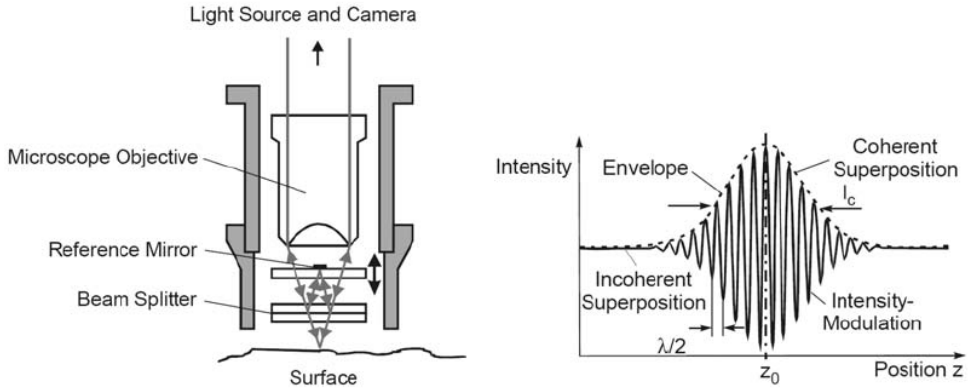

Fig. 2.9: Principle of the Mireau interferometer (left) and light intensity as a function of lens displacement for one pixel (right) [30].

The lens is moved over the working range by means of actuators. The displacement of the lens is recorded precisely by means of position sensing. The position of white-light interference is calculated separately for each pixel, and a conclusion is derived from this with respect to the corresponding measurement point [22].

2.5.2.3 Confocal microscopy

In confocal microscopy (see Figure 2.10), a microscope lens is used to project a point light source onto the test object. If the object lies precisely in the focal point, it reflects the light back along the same path through the lens, and via a beam splitter onto a detector.

Conversely, if the object is out-of-focus, an aperture will prevent the reflected light from reaching the detector. The projected light spot is moved very rapidly across the object, scanning it point-by-point and line-by-line, which allows scanning a measurement plane.

For the lateral scanning of the workpiece surface, different techniques have been developed: the lateral displacement of the specimen, pinholes on a rotating disk (the so-called Nipkov disk), scanning mirrors, arrays of micro lenses and, recently, the Digital Micro-Mirror Device (DMD). Finally, the object is slightly adjusted in height, and the surface scanned again. Stacking the sections thus obtained reveals the three-dimensional structure of the object [22].

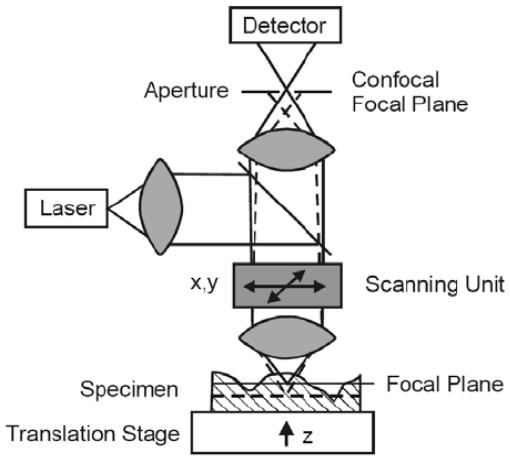

Fig. 2.10: Principle of confocal microscopy [30].

2.5.3 3D SENSORS

2.5.3.1 Photogrammetry

Photogrammetry systems are based on the principle of triangulation. They enable the reconstruction of surfaces by mathematically combining images from different viewpoints. In photogrammetry for large scale metrology, the measured surface is

usually provided with physical markers (e.g. retro-reflective dots) to generate so-called homologous points. A mobile camera records these points from different perspectives [22].

2.5.3.2 Structured lighting

One method using structured lighting is fringe projection. This method is actually a triangulation method and can be regarded as an extension of line triangulation. The method consists in projecting a recurrent pattern of equidistant lines, rather than one single line, onto the test object. This may be achieved by liquid-crystal or Digital Micro Mirror Devices (DMDs). The diffusely reflected line pattern then visible on the object is recorded by a CCD camera aligned at a triangulation angle, Θ, to the axis of lighting (Figure 2.11).

As in the point and line triangulation methods, the height information is contained in the position of the lines on the CCD sensor. In order to ensure unambiguous allocation of the projected lines to those recorded, the lines are projected serially, e.g. according to the Graycode method (Figure 2.12). Enhanced resolution is achieved by using phase-shifting techniques and sub-pixel methods.

A typical measurement volume of structured light systems is in the range of side between 0.1m and 1m. These systems provide a relative accuracy of up to 10^{-4}, which depends on the phase measuring errors, the pixel and image co-ordinate measuring errors and the lateral structural resolution. When applied to the microscopic scale, fringe projection systems can even be used for the measurement of micro-shape and roughness [30].

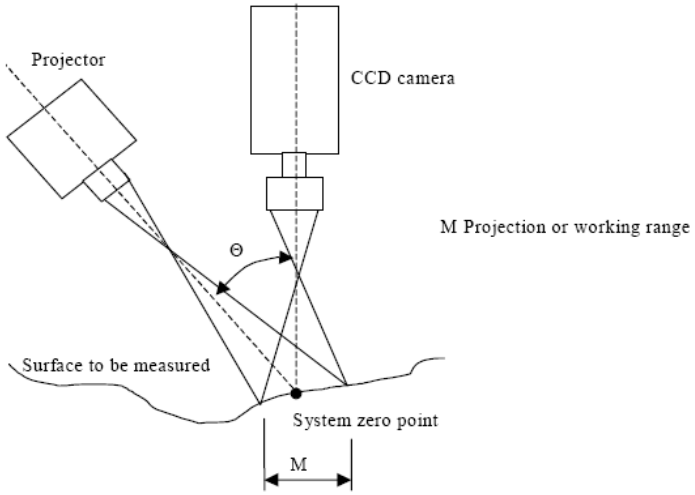

Fig. 2.11: Fringe-projection system consisting of projector and camera [30].

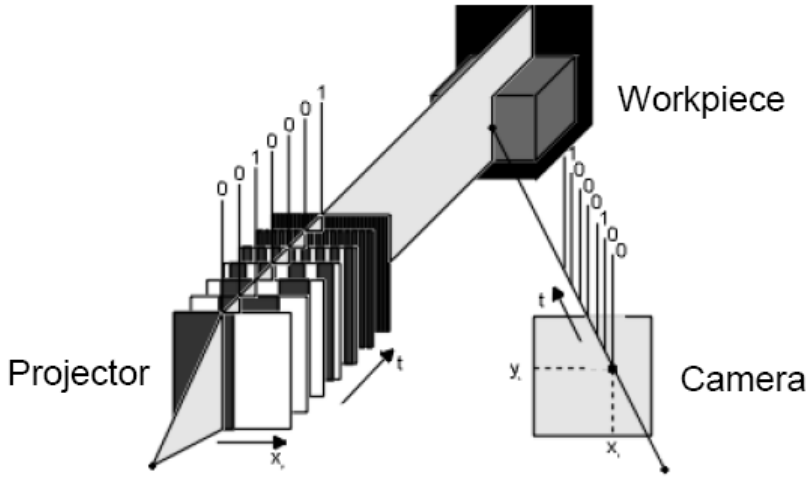

Fig. 2.12: Fringe-projection according to the Graycode method [30].

2.5.3.3 Computed tomography

As a recent development, also Computed Tomography (CT) using x-rays – so far primarily employed in medical diagnostics – may be regarded as a coordinate metrology tool, since it has become a promising technique for dimensional metrology on engineering parts [40],[41]. So far, the main aspects of interest for the industrial application of CT scanning are the non-destructive analysis of faults (like cracks, flaws, shrink-holes) and the material composition inside the volume. Now, in addition, CT allows users to quantitatively measure internal and external geometrical features. Therefore, CT measurements have the potential to substitute and improve some of the measurements currently performed on classical coordinate measuring machines [42]. The cornerstone of X-ray tomography was laid back in 1895, when Wilhelm Conrad Roentgen discovered the X-rays by chance. Forty years later, Godfrey Newbold Hounsfield at EMI invented the first computer assisted tomography scanner.

Although hardware and software of CT systems made great progress within the last 20 years, a basic scanner still consists of an X-ray emitting source, an object manipulator, a detector and electronic and computational devices for data acquisition and back projection.

The visible contrast in CT images is produced by the X-ray absorption of the material and therefore is a function of the local electron density of the object under study. The measurement chain of industrial CT starts with the source where X-rays are emitted either by tubes with defined focal points or linear accelerators. The object to be scanned is located on a rotary table. Depending whether a line (1D) or an area (2D) detector is used, CT systems are capable of measuring 2D or 3D information with one revolution of the part. The first case is referred as 2D CT systems (Figure 2.13), while the second is called 3D CT systems (Figure 2.14).

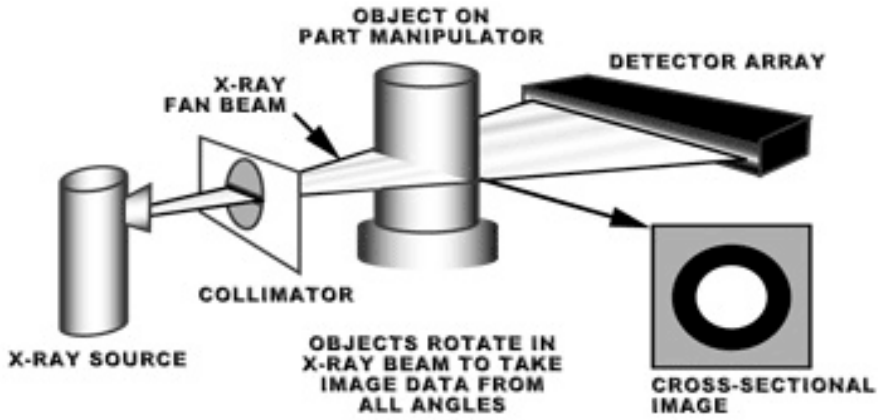

Fig. 2.13: Principle of an industrial CT scanning system with 1D detector [29].

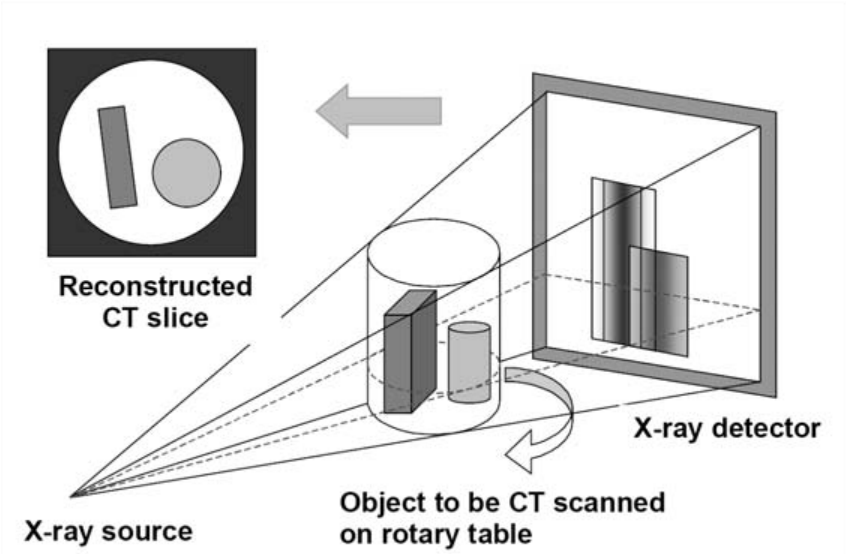

Fig. 2.14: Principle of an industrial CT scanning system with 2D detector [22].

2.6 RELATIONSHIP BETWEEN TOLERANCES TO BE INSPECTED AND METROLOGICAL PERFORMANCES OF THE MEASURING SYSTEM

The choice of the metrological instruments to use is strictly connected to the geometrical and dimensional tolerances to be inspected. In particular to evaluate if an instrument is good enough to perform the requested measurement, it is necessary to specify a "task specific" uncertainty for the system itself. To quantify every "task specific uncertainty" to be tested is necessary to consider the ISO 14253-1 [43]

standard about “conformance and non-conformance with specifications”, in relation with the tolerances to be inspected.
The contents of the standard are here summarized:

In the design or specification phase, e.g. on an engineering drawing, the terms "in specification" and "out of specification" (see 1 and 2 in figure 2.15, line C) *designate the areas separated by the sharp borderlines LSL and USL.*
In the production or verification phase, the meaning of the terms "in specification" and "out of specification" are complicated by the ever-existing uncertainty of measurement. The sharp borderlines (from the design phase) are transformed into uncertainty ranges. Consequently, the conformance and non-conformance zones are reduced by the estimated uncertainty of measurement by means of the uncertainty range (see D in figure 2.15). *The specifications for a workpiece are given under the assumption that they are espected, so that no workpieces or measuring equipment are out of specification.*
In practice, in the verification phase, the estimated uncertainty of measurement shall be taken into account to demonstrate or prove the conformance or non-conformance with a given specification.

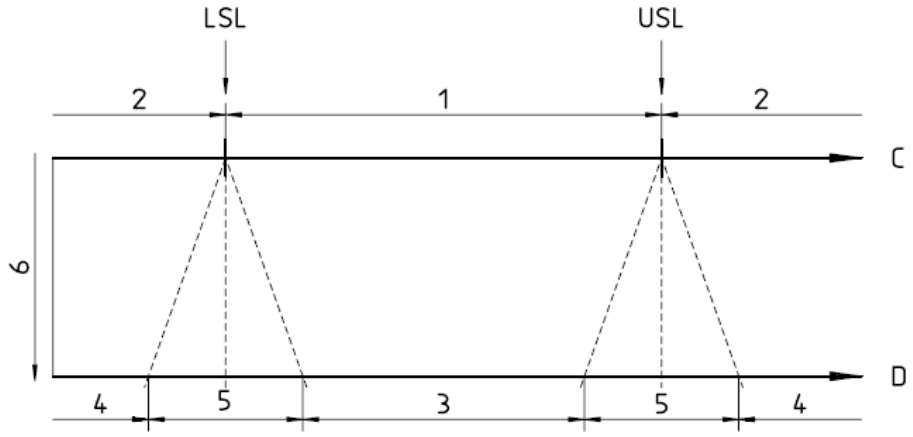

Key
C Design/specification phase
D Verification phase
1 Specification zone (in specification)
2 Out of specification
3 Conformance zone
4 Non-conformance zone
5 Uncertainty range
6 Increasing measurement uncertainty, U

Fig. 2.15: Uncertainty of measurement: the uncertainty range reduces the conformance and non conformance zones [43].

Uncertainty of measurement is variable and is controlled by several components in the measuring process [44].
Consequently, the sizes of the conformance and the non-conformance zones are variable and depend on the estimated uncertainty of measurement, U.

Taking into account these indications, tolerances to be inspected should be translate into appropriate "task specific" uncertainties U; this value has to be chosen in such a way that the ratio U/T is the appropriate trade-off between costs of measuring process and market requirements fulfilment. The "golden rule of metrology" says that measurement task has to be at least lower than 1/5 of the tolerance of the characteristic under consideration and 1/10 for safety or critical application [2].
In Coordinate Metrology it is impossible to specify the uncertainty for all measurement tasks that can be executed by the machine, in any position within its working volume, using any measurement strategy. In particular, traceability establishment requires the estimation of task specific uncertainty, where both the measurement strategy and measurement conditions are well specified. Method for evaluation of task specific uncertainty in Coordinate Metrology will be described in Section 3.4.

2.6.1 Maximum Permissible Error and measuring uncertainty

For every metrological characteristic it is possible to define a **Maximum Permissible Error (MPE)** that, as indicated in [28], is the "Extreme values of an error permitted by specification, regulations, etc. for a given measuring instrument". Starting from this definition, the MPE should be related to the measuring instrument, taking into account the cumulative effect of all the measuring characteristics of the instrument itself. Conformity to MPE defined by the manufacurer is satisfy if the error of indication of the tested instrument is within the limits defined by MPE. Considering the case of Coordinate Measuring System, tests for performance verification are mainly based on the evaluation of the MPE related to length measurements capability of the measuring systems and the MPE for probing system. It is necessary to specify the difference between the MPE and task related uncertainty for a measuring system. The first, in fact, represents a performance characteristic defined by the manufacturer, while the second is following the definition of VIM [28] the "parameter, associated with the result of a measurement, that characterizes the dispersion of the values that could reasonably be attributed to the measurand". Starting form this consideration, performance verification procedures for a measuring system are not enough to guarantee full traceability of a specific measurement.

2.7 CONCLUSIONS

In this Chapter special attention has been paid to the description of the actual requirements in production metrology. Modern production is characterized by increasing complexity, related both to dimensions to be inspected and materials. For this reason optical methods are becoming more and more widespread in production. After the results obtained from a market analysis related to industrial requirement for quality assurance, a description of the most diffused optical sensors used in dimensional metrology have been reported. At the end of the Chapter the relation between performance verification of CMS and tolerances to be inspected have been reported.

Chapter 3

Performance verification and traceability of non contact coordinate measuring systems

The main focus of this chapter goes into methods for performance verification of optical coordinate measuring systems. After a first part related to description and experimental investigation on specific error sources for optical CMS, guidelines, standards and initiatives related to performance verification procedures are described and discussed. Suggested artefacts to be used for performance verification will be discussed in Chapter 4.
Nevertheless, as seen in the previous Chapter, application of performance verification tests does not provide full traceability of measurement: in the last part of the this section methods for traceability establishment will be dealt with.

3.1 INFLUENCE PARAMETERS FOR OPTICAL SYSTEMS

Standards and artefact for performance verification of contact CMMs cannot be directly applied for testing of optical systems. Compared to the general model of error sources for tactile CMMs, in fact, in optical coordinate metrology a series of additional sources of uncertainty is present. Therefore, measuring results of optical systems are influenced by many factors. A list of them is presented in Table 3.1. In particular, many additional error sources take place from the interaction between the optical probe and the object to be measured. The number of these additional influence parameters is large and some of them are of a totally different nature than the ones present in mechanical coordinate metrology.
The first experimental investigation and proposal about test and procedures for performance verification of optical system is related to the Research Project, supported by the Commission of European Communities under the programme for Applied Metrology and Chemical Analysis (BCR), finished in 1994 [45],[46]. In this Project, the experimental investigation was done by means of real measurements and by modelling the error mechanisms in simulates measurements. In all, the behaviour of 11 different probes was analyzed for a total of 35 error mechanisms. Based on the experience gained during the Project, a series of test procedures was developed by the participants, with the aim to provide final users

methods to state the metrological performance of their optical probes. The above mentioned test procedures have been used in supporting the work of national and international standardization committees in developing existing guidelines. In particular, test procedures have been developed taking into account that measuring strategy, illumination, surface structure and geometry of the object determine the errors of optical probes more than in the case of mechanically contacting probes. Probes therefore cannot simply be characterized by measurement errors but they have to be characterized in a more complex way by their error limits under specified conditions of operation. Furthermore the suggested tests determine the performance of the probe itself wherever possible: in cases where it is not possible to separate the performance of the probe from that of the CMM's kinematics system with economic means, the combined errors of CMM and probes are determined (entire "probing process"). In the following paragraphs, specific error sources for lateral sensors and distance sensors are presented, including performance tests introduced in [46] and experimental results obtained by the author.

3.1.1 Influence parameters for lateral Sensors (2D)

All components of the information processing channel, which consists of the illumination, the object, the imaging lens, the CCD-sensor, the evaluation electronics, and the algorithm for image processing, may be disturbed by systematic and random errors (see Fig. 3.1). To evaluate the effect of these error sources on measurement results, in [46] a series of test and artefacts have been reported (Table 3.1).

Performance tests on Optical 2D-probes	
Test	**Artefacts**
Circle test	Circular artefact (ring, chromium deposition on glass..)
Bar test	Thin bar or chromium line on glass
Cylinder test	Cylinder plug gauge
Resolution test	Calibrated periodic chromium on glass bar grids

Table 3.1: performance test for 2D-probes as indicated in (adapted from [46]).

An experimental investigation has been performed by the author on the effects of imaging parameters in coordinate measurements using a video-CMM on two artefacts commonly used for performance verification of optical CMMs: a linear glass scale and an optomechanical hole plate. In particular, the results show the influence of illumination, objective magnification, measuring window size, use of autofocus and image filtering [47]. The investigation has been performed in preparation to the *VideoAUDIT* comparison, reported in Chapter 7, in order to evaluate the influence of measuring strategy and imaging parameters on measuring

uncertainty and on the intrinsic uncertainty of performance verification tests. Other results related to error sources for video Probe are described in [48],[49],[50],[51], [52],[53].

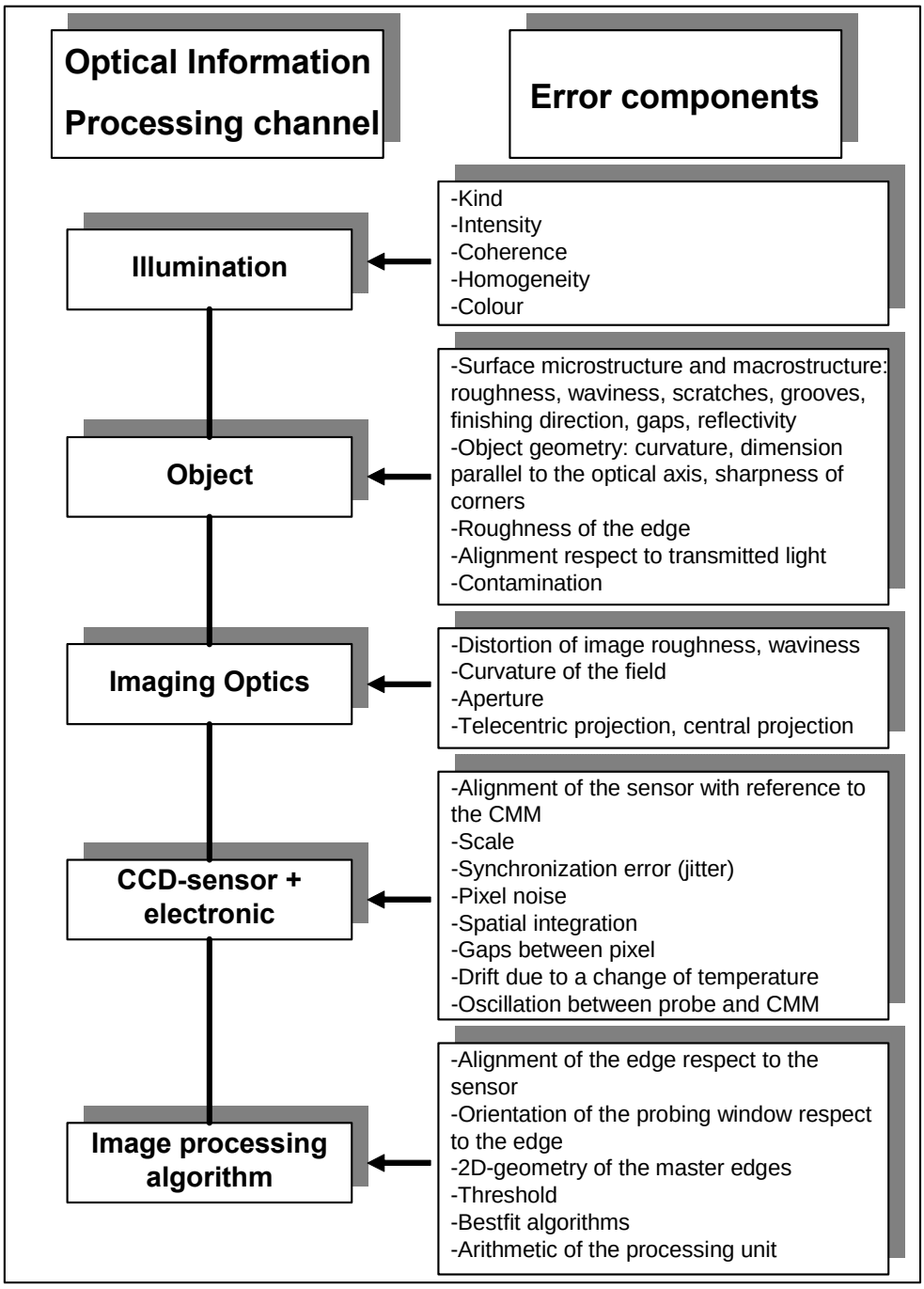

Fig. 3.1: survey in the physical sources of errors of 2D-video probes [46].

The experimental investigation has been performed on a high precision multisensor Coordinate Measuring Machine: Werth Video Check IP 400 (Fig. 3.2). In Table 3.2 the specification of the optical CMMs used in the investigation are reported.

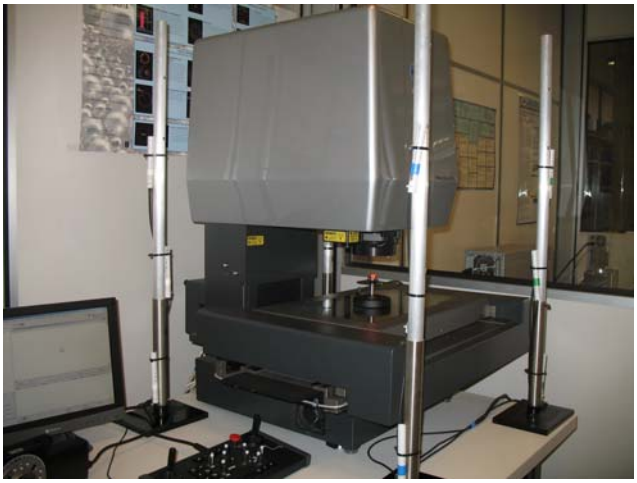

Fig. 3.2: Multisensor measuring system Werth Video Check IP 400, with temperature sensors positioned at the corners of the measuring volume.

Optical Magnification	Digital Magnification	Working distance	Light sources	MPE
1x-10x	1x-400x	59mm	Back light Ring light Coaxial light	E2=1,8+L/250µm, L in mm

Table 3.2: specification of the multisensor measuring system used in the investigation.

The measured artefacts are: a DTU Optomechanical Hole Plate [54] and a linear glass scale. For the Hole Plate, the diameter of hole 17, the diagonal 1-25 and the diagonal 1-15 (Fig. 3.3-left) are chosen as measurands. Holes are measured moving the sensor and acquiring 4 points along the visible profile. For the glass scale, two different distances between the chrome depositions are measured without moving the sensor: a bidirectional distance and a unidirectional distance (Fig. 3.3-right).
The results show the influence of illumination (Fig. 3.4 and Fig. 3.5-left), objective magnification (Fig. 3.5-right), measuring window size (Fig. 3.6), use of autofocus (Fig. 3.7-left) and image filtering (Fig. 3.8-right). As it is possible to notice from the diagrams, bidirectional measurements are more sensible to parameters variation than unidirectional ones.

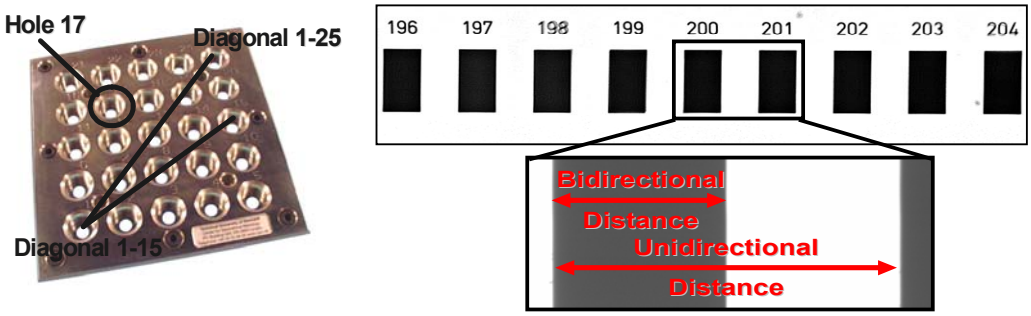

Figure 3.3: (left) Hole Plate; (right) Glass scale with detail on probing strategy.

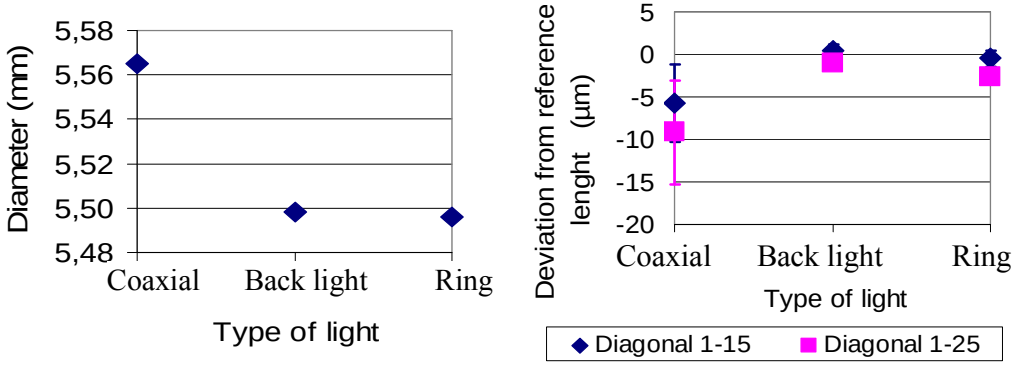

Fig. 3.4: Effect of illumination type on Hole Plate: (left) diameter; (right) diagonals.

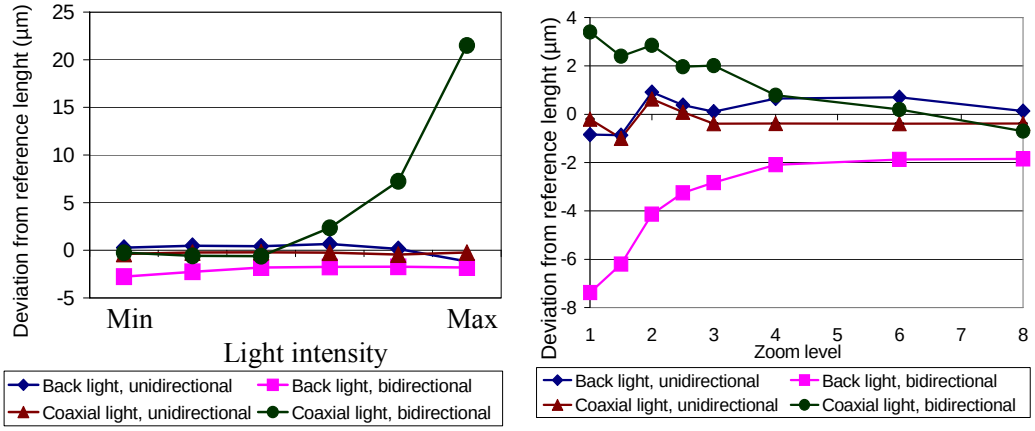

Fig. 3.5: Results on glass scale: (left) light intensity; (right) magnification.

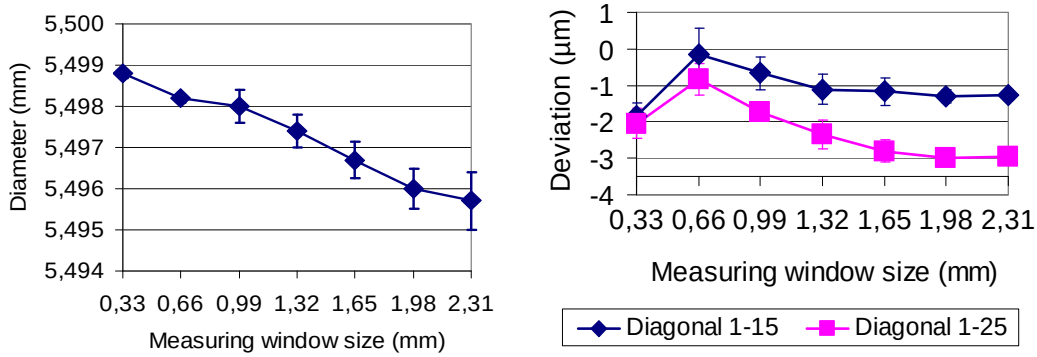

Fig. 3.6: Effect of measuring window size on Hole Plate: (left) diameter; (right) diagonals.

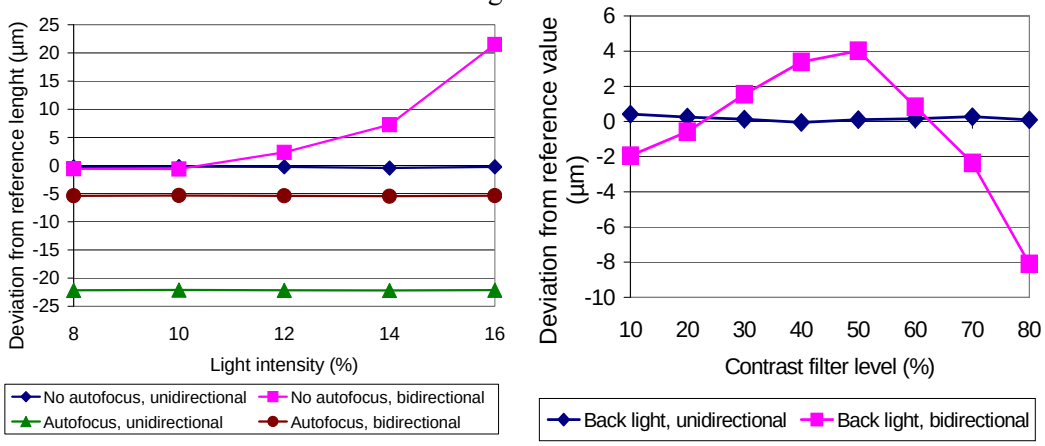

Fig. 3.7: Results on glass scale: (left) autofocus; (right) contrast filtering.

3.1.2 Influence parameters for Optical Distance Sensors

The main uncertainty contributor related to distance measurement sensor is the optical characteristic of the workpiece surface. For example, in most cases, very smooth surfaces cannot be measured because of insufficient diffusely reflected light. Other common errors are also introduced by: the slope of the surface (which may produce direct reflections to the detector), volume scattering (e.g. for plastic material), or an inhomogeneous surface texture. Secondary reflections, specular reflections, volumetric scattering, colour transitions, or ridges left by machining, may lead to gross systematic measuring errors. Further additional uncertainty contributors are environmental illumination and errors in the registration of multiple views. Since the dimension of the object is directly related to the time it takes to scan the object, an error is introduced for a moving object. In Table 3.2 a list of error sources related to optical distance sensor is reported, while in Table 3.3 test suggested in [46] to quantify the effect of measurement errors are listed with the related artefacts.

Error source	Type
Motion of object measured	Systematic and random
Atmospheric effects	Random
Dirt	Random
Environmental conditions	Random
On object	Systematic
Temperature	Random
Surface finish of object	Systematic
Edge-sensing errors	Systematic
Stray light	Systematic and random
Process effect	Systematic and random
Surface slope	Systematic and random

Table 3.2: error sources for distance sensors (adapted from [7]).

Performance tests on Optical 1D-probes	
Test	**Artefacts**
Static Sphere Test	Two test spheres: one metallic matte, one dark matte sphere
Bright-Dark transition Test	Flat artefact which is half matte black and half matte white
Dynamic Scanning Test	Uncalibrated Sphere of a form error <0.1-0.2 times the probe's error limit
Ambient light	Dark object on a white target
Step test (Fig. 3.8)	Artefact with abrupt change of level
Gauge block test	At least six gauge block of different length
Edge focusing test	Circular artefact

Table 3.3: performance test introduced in (adapted from [46]).

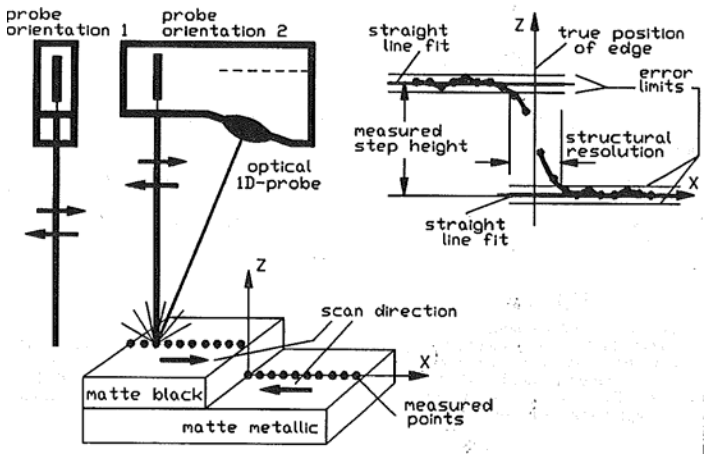

Fig. 3.8: step test [45].

The performance characteristics of some widely diffused sensors, such as those using optical triangulation, are nowadays well known and described in literature [54],[55],[46]. This is not true for other optical sensors, especially those exploiting new techniques, whose performance must be validated by more extensive experimental investigations. Conoscopic holography is one of these, being an upcoming principle in the field of 3D measurement which has not yet been deeply studied [22]. The main advantage of this technique is to be able to measure sharp surface slopes up to 85 degrees [56].
Considering the lack of information and documented tests on conoscopic holography, an experimental investigation has been conducted by the author in order to evaluate the effect on measuring results due to the relative slope between optical axis and surface to be measured [57]. To quantify this effect, a dedicated reference artefact has been designed and developed (fig. 3.9), paying special attention to the optical properties of the surfaces to be measured.

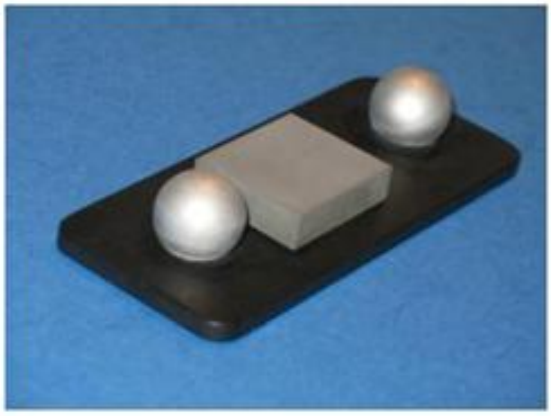

Fig. 3.9: cooperative artefact for optical measuring systems [57].

Fig. 3.10 shows the mean error along the optical axis as a function of the surface slope Θ: the red lines indicate the standard deviation of the calculated errors on 113 independent repeated measurements.

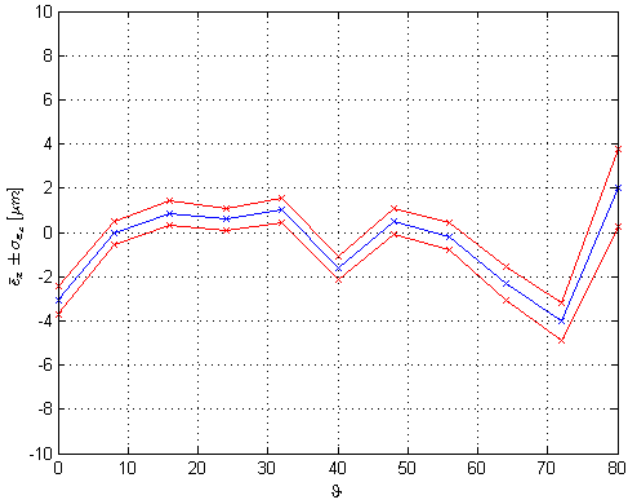

Fig. 3.10: Mean and standard deviation of the error along the optical axis as a function of the surface slope Θ.

3.2 PERFORMANCE VERIFICATION AND ACCEPTANCE TESTS FOR OPTICAL CMM

In the previous sections, some examples of tests for evaluating specific error of optical sensors have been presented. Generally those tests can be used to evaluate the sensor itself but they don't give any information about the metrological performance of all the measuring system.
Tests for performance verification of optical CMM are mainly based on the evaluation of length measurements capability and, as reported in Table 3.4, they can be performed for different purpose [49].

Situation	Necessary action
Purchase of CMM	Acceptance testing
Service on CMM	Reverification
Periodical inspection (short and long intervals)	Interim testing
New hardware or software installation	Reverification
Special or important measurements	Interim testing

Table 3.4: Typical situation for performance verification of CMM [49].

Despite all the progress that has been made in optical coordinate metrology, an enormous need for information and standardization still exists in this field. Up to now, testing procedures and artefacts for performance verifications of non-contact systems are not completely defined by the available international and national standards and method for verification of contact systems cannot be directly applied.

At present, consequently to the lack of internationally standardized rules for optical systems, specifications provided by producers of different systems are given on the basis of not comparable verification procedures. Therefore, users have difficulties in comparing different systems and they don't have clear rules to check metrological performances of systems. In this context, there is a strong need of standardized artefacts and methods for testing optical systems and for making optical measurements comparable to mechanical measurement [29].

3.3 STANDARDS AND GUIDELINE

In the next paragraphs standards, guideline and initiative related to performance verification of Optical Coordinate Systems are reported and discussed.

3.3.1 ISO Standard: 10360 series

No international standards have yet been published. However the ISO Working Group on CMMs (the ISO/TC 213/WG10) is working to the development of a series of standards dedicated to optical CMMs:

Part 7 (CMMs equipped with video probing systems) [58]: the current draft has been developed using the ISO 10360-2 for contact systems [59] as a starting point: this part of ISO 10360 specifies the acceptance test for verifying performance of a CMM used for measuring size. The assessment for MPE_E is performed by comparison of the calibrated values with the indicated values of different material standards of size, each of a different length, measured in different locations or orientations in the measuring volume of the CMM. For MPE_P the assessment is performed measuring a calibrated reference circle (a chromium deposition on glass or a calibrated ring) and determining the range of distances of the measured points from the centre of the Gaussian associated circle.

Part 8 (CMMs with optical distance sensors) [60]: this parts deals with sensors able to measure optically only an axial distance. Also this document start from the indication of ISO 10360-2 and ISO 10360-5 [61] for contact CMMs.

Some questions related to the new standards are still opened: first of all, the probing error is defined in part 5 by the measurement of 25 points over a sphere: generally this kind of sensors acquire thousands of points and use specific filters to reject unwanted outliers. Varying the filter depth every point cloud can be translated into a perfect sphere: which are the specification to consider in terms of filtering? Furthermore, spheres wouldn't be measured by some sensors as the high-sloped surface and the results could be completely different changing the material of the artefact. Which are the best artefact to be employed, taking into account performances, availability on the market, costs and calibration procedures?

Part 9 (CMMs with multiple probing systems) [62]**:** this part is related to multisensor CMMs, equipped for example with a tactile and an optical probe. Also for this part some questions are still opened: for example, if a CMM is

equipped with two contact probes, which is the standards to be used, part 5 or part 9? The standard has the aim to investigate performances of all the system or just the spatial offset of the two probing systems? As for part 8, which are the best artefacts to be used?

3.3.2 VDI/VDE 2617

VDI/VDE 2617 is a German guideline. It has been around since the mid-1980s and has received the most international use prior to the release of the ISO 10360 standard. This guideline specifies characteristics serving to describe the accuracy of CMMs and describes methods for testing these characteristics. In this section particular attention is given to the parts of the guideline that refers to optical sensors:

VDI/VDE 2617 - Part 6:1997 [37] is a general description of acceptance and reverification testing and performance verification of CMMs equipped with optical probes. For acceptance testing the CMM has to pass two tests: one concerning probing error and one related to error of indication for size measurement (see Chapter 5).

VDI/VDE 2617 - Part 6.1:2005 [38] deals specifically with 2D optical sensors and gives an intensive description of function and important influence parameters for the different sensor types.

VDI/VDE 2617 - Part 6.2:2005 [30] is an adaptation of ISO 10360 to CMMs with optical distance sensors. This part of the guideline has newly been released in 2005. The previous version of Part 6.2 (VDI/VDE 2617 - Part 6.2:1999 [58]) was covering only one dimensional sensors, and the procedures described were not in compliance with ISO 10360. The functioning and specifics of the sensors are explained within the standard. The methods for acceptance testing and reverification of optical error and probing error in optical distance sensors are defined in close harmonisation with ISO 10360-2:2001 [58].

3.3.3 Other standards and guidelines

At present, while international standards are not available, some national Organizations, especially in the United States and in Germany, are developing their own guidelines.

In the United States, the B89 Dimensional Metrology Committee of the American Society of Mechanical Engineers (ASME) is working to add to the **ASME B89.4.1** [64], dealing with methods for performance evaluation of tactile CMMs, a new document on non contact probes for CMMs (Project Team 4.14: “Non-Contact Scanning Probes”[65]).

In Germany, the Association of Engineers (VDI) and the National Institute for Standardization (DIN) have been particularly active, publishing many innovative documents. Beside the above mentioned VDI/VDE 2617 series other standards have been published:

VDI/VDE 2634 is another important guideline in the field of optical systems. It is divided in two parts.
VDI/VDE 2634-Part 1:2002 [66] describes practical tests for the evaluation of the accuracy of optical 3D measuring imaging systems with point by point probing. The definition of the parameter "length measurement error" is similar to that in ISO 10360-2.
VDI/VDE 2634-Part 2:2002 [67] contains practically relevant procedures for the accuracy evaluation of 3D systems based on area scanning (whole-field measuring). Definitions of the parameters "probing error" and "sphere spacing error" are defined following ISO 10360-2.
The German standard DIN 32877:2000 [68] applies to optoelectronic length measuring devices for the measurement of distance, profile and form. It defines designations and stipulates requirements and their verification. The triangulation, focusing and shadow image procedures are described in this standard. Original tests and artefacts are defined in the standard, for evaluating some of the parameters of the measuring system that affect the measuring uncertainty.

3.4 EVALUATION OF STRUCTURAL RESOLUTION

Another method to evaluate performance of optical probes is by their Structural Resolution. Structural resolution characterises the smallest structure perpendicular to the direction of measurement that is measurable with the specified probing error. Structural resolution is not already included in the probing error that is determined through typical performance verification tests. For instance, with increasing low-pass effect of filtering, the probing deviation decreases while the structural resolution deteriorates. Structural resolution must, therefore, be considered and specific tests have to be applied in order to determine this characteristic. Measurement results for determining the resolution are not a priori comparable if they were obtained using different methods. In [69] test for evaluation of structural resolution are tested and compared (see Fig. 3.11). In particular the following methods were experimented:

- Edge-structure test from VDI2617-6.2:2005 [30],
- Structure-standard test from VDI2617-6.2:2005 [30],
- Evaluation of Modulation Transfer Function (MTF),
- Evaluation of Point Spread Function (PSF),
- 5.Step-height test from ASME B89.4.14 (1998 draft) [65].

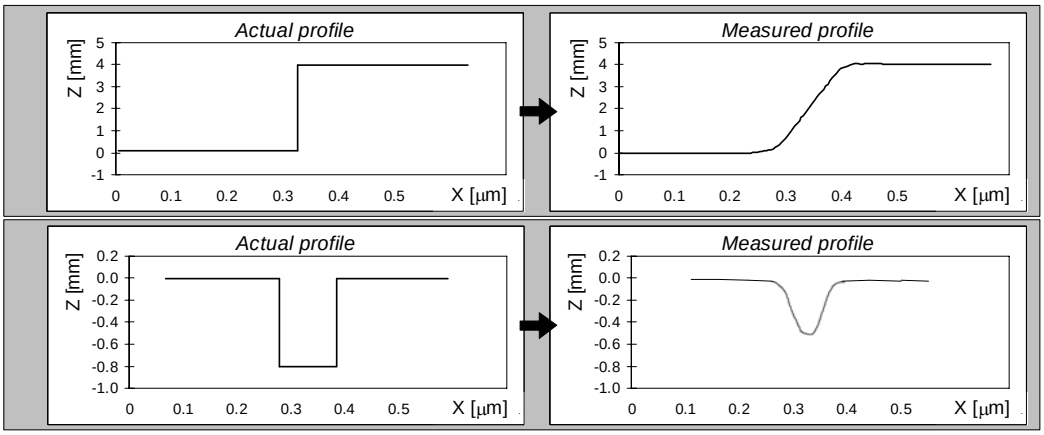

Fig 3.11: Determination of structural resolution by: (a) measuring a step artefact, (b) measuring a structure standard (rectangular groove) [69].

In the same paper, also some newly developed artefacts for structural resolution have been presented [69], (Fig 3.12).

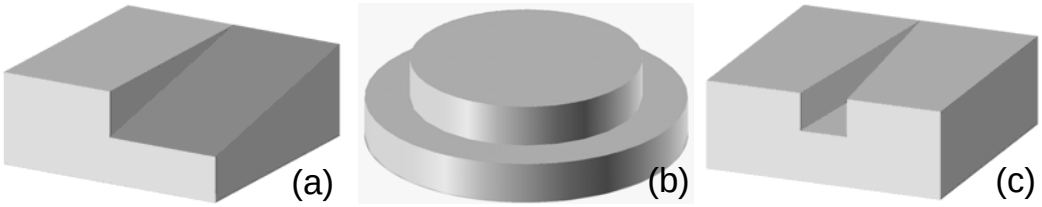

Fig. 3.12: Artefacts: (a) "V-step", (b) "Cylindrical step", (c) "V-groove"[69].

3.5 THE OSIS INITIATIVE

OSIS (Optical Sensor Interface Standard) [36] is an industry initiative with the aspiration to promote development and usage of optical metrology in combination with CMMs [70]. It is an initiative of the leading manufacturers of optical sensors and CMMs. OSIS was funded with the goal of releasing a common interface standard. It is estimated that saved costs in an order of magnitude of several hundreds of thousands Euros are realistic for every integration of a new sensor in a CMM with this standard [71]. Also manufacturers of robots and machine tools can apply this standard to integrate optical sensors much more efficiently then in the past. OSIS activities are supported by the International Association of Coordinate Measuring Machine Manufacturers (IA.CMM) [72].
The objective of standardising the integration of optical sensors into CMMs was split between three working groups, with three different tasks:

- WG1: Mechanical / electrical interface [73];
- WG2: Data integration (Software interface) [74];
- WG3: Classifications, specifications and performance verifications [75].

Concerning performance verification tests, OSIS introduced a four-shell model approach (see Fig. 3.13). The idea is to provide a systematic approach and a set of tests for all shells.

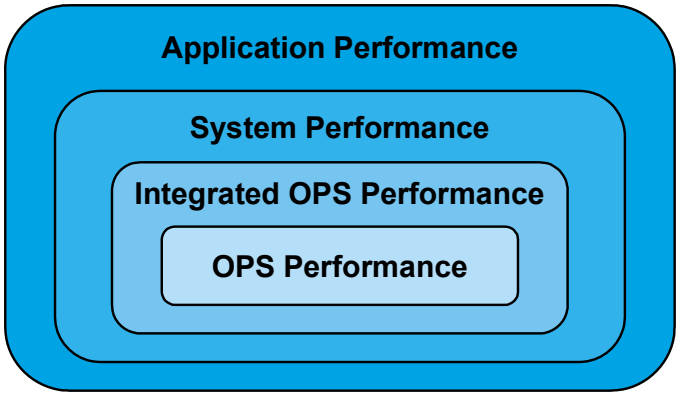

Fig. 3.13: Four-shell model for performance verification [36].

The focus of *shell 1* is on Optical Probing Sensor (OPS) performance. This only includes influences from the sensor itself and tries to eliminate influences from the integration. The performance evaluation for *shell 1* is done before the definition of the target system and on a "mover" of the sensor manufacturer's choice. The results are specification data for the OPS performance. *Shell 2* evaluate integrated OPS performance. This includes all additional influences on the sensor itself after the integration in the intended system. It can include additional data processing not coming from the CMM that combines one or more raw points and position information from the CMM. It also includes any synchronisation problems, electrical disturbances due to cable length, position jitter etc. The "mover" for the test is the CMM on which the OPS is mounted. *Shell 3* spots on system performance and particularly on acceptance test criteria. The reason for this shell is to fill the gap due to the lack of clear interpretations for OPS in the existing standards for the acceptance of CMM equipped with OPS based on system performance. The tests show conformance with the specifications. If performance for certain special applications has to be evaluated, *Shell 4*, application performance, is applicable. This shows system performance on the real work piece with its imperfections (roughness, colour, etc.).
In Table 3.5 the 10 OSIS tests are briefly described. Testing conditions and artefacts are specified in the OSIS document [75], along with each test procedure.

TEST IDENTIFICATION	SHELL			
	1	2	3	4
Test 1 – Repeatability The test gives information about the range of indications for the different shells/stages of integration and use of the sensors: Shell 1: Establishes the basic performance of the OPS Shell 2: Establishes whether integration degrades the basic performance. Shell 4: Workpiece-oriented evaluation of the system.	A	A		A
Test 2 – Local reproducibility This test extends Test 1 to include the influence of micro translations. Shell 1: Establishes the influence of micro translations. Shell 2: Studies the influence of additional functionality due to the OPS integration. Shell 4: Evaluates the influence of the variability of any workpiece/surface and the settings of data processing, filtering, etc.	A	A		A
Test 3 – Reproducibility over operating range This test extends Test 1 and Test 2 to include the influence of distortions within the operating range.	A	A		A
Test 4 – Probing deviation over feature range Test 4 gives an indication of systematic and random errors of the OPS for shell 1, shell 2 and shell 4 over the specified feature range.	A	A		A
Test 5 – Point to point probing error on spheres This test is based on the standard ISO 10360-2 [61] and provides an industry accepted MPE (Maximum Permissible Error) parameter and a method to compare OPS performances with contacting probes.			A	
Test 6 – Scanning probing error on spheres This test is based on the international standard ISO 10360-4 [76]. By the measurement in scanning mode of spheres, this test gives a method to compare OPS performances with scanning tactile probes.			A	
Test 7 – 2D probing error on rings This test is based on the guideline VDI/VDE 2617 Part 6.1 [38] and is applicable only for edge point sensitive OPS. The measurement of a circular sharp edge is required.			A	
Test 8 – Multi-orientation test The test is based on the standard ISO 10360-5 [61], Multistylus test. This test shows the influence of different orientations of the OPS (e.g. on an articulating head) and provides a method for OPS to compare performances with contacting probes.		A	A	
Test 9 – Dynamic range This test quantifies the ability of an OPS to provide measurement results under measurement conditions where the basic optical signal (reflection from the work-piece) gets lower (e.g. darker or more slanted surfaces) or higher (e.g. high reflectivity surfaces).	A	A	A	A
Test 10 – Probe Coordinate system stability The position of the probe co-ordinate system relative to the machine coordinate system can vary over time. This test explores if the position of the probe co-ordinate system relative to the machine co-ordinate system moves during a specific time interval.		A	A	

Table 3.5: OSIS tests (A: applicable)

In [77], OSIS procedures for acceptance and performance verification have been tested by the author in order to evaluate strengths and weaknesses of the proposed verification method using a Multisensor CMM (Werth Video-Check IP-400, Fig. 3.2) equipped with two different optical sensors: a video sensor and a conoscopic laser. In Fig. 3.14, is reported as example the experimental set-up used by the author to performed Test 9 –Dynamic Range, while Fig. 3.15 shows results related to Test 10 - Probe Coordinate system stability.

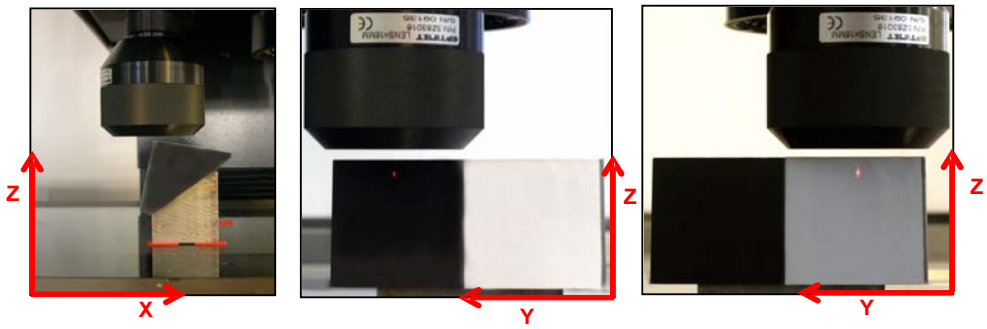

Fig. 3.14: Test 9 performed with the conoscopic laser sensor.

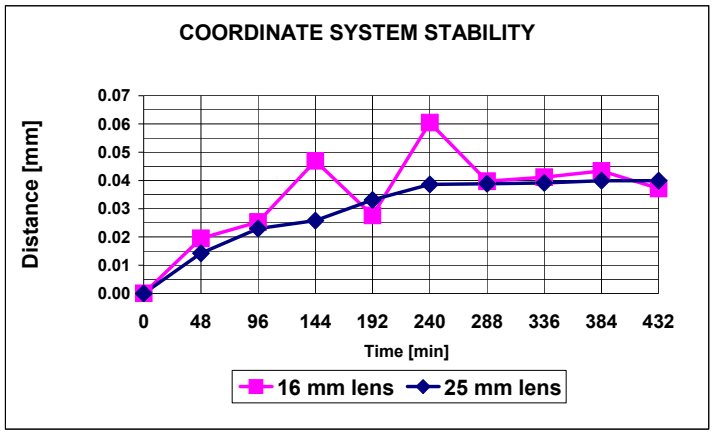

Fig. 3.15: Probe coordinate systems stability.

3.4 TRACEABILITY AND TASK-SPECIFIC UNCERTAINTY ASSESSMENT

Performance verification procedures for acceptance and reverification tests of CMMs, without further analysis or testing, are insufficient to determine the task specific measurement uncertainty of most measurements. The application of mere performance verification tests, therefore, does not guarantee full traceability (performance verification of MPE is a necessary but not sufficient condition for full traceability).

Traceability establishment requires the evaluation of task specific uncertainty, where both the measurement strategy and measurement conditions are well

specified. A correct statement of the uncertainty is required also from the GPS series of standards. In particular, ISO 14253-1 [43] states that a proper uncertainty statement is necessary in order to conclude that products are within or outside of specification.
The reference documents for uncertainty assessment is the Guide to the Expression of Uncertainty in Measurement (GUM). In ISO 14253-2 [44] the Procedure for Uncertainty Management (PUMA) is introduced. PUMA *is a practical, iterative procedure based on the GUM for estimating uncertainty of measurements without changing the basic concept of the GUM and it is intended to be used generally for estimating uncertainty of measurement and giving statements of uncertainty for:*

- *single results of measurement;*
- *comparison of two or more results of measurement;*
- *comparison of results of measurement with given specifications [i.e. maximum permissible errors (MPE) for a metrological characteristic of a measurement instrument or measurement standard, and tolerance limits for a workpiece characteristic, etc.], for proving conformance or non-conformance with the specification.*

Furthermore the Technical Committee ISO/TC 213 "Dimensional and geometrical product specifications and verification" is currently defining a new series of standards, the ISO 15530, describing standardized methods for the evaluation of CMMs measuring uncertainty [78],[79] As it is now intended, ISO 15530 will consist of the following parts under the general title "Geometrical Product Specification (GPS) – Coordinate measuring machines (CMM): Techniques for determining the uncertainty of measurement":

- Part 1: Overview and general issues
- Part 2: Use of multiple measurement strategies
- Part 3: Use of calibrated workpieces or standards
- Part 4: Use of computer simulation
- Part 5: Use of expert judgement.

At the time being, the only published parts are ISO/TS 15530-3:2004 [78], which deals with CMMs uncertainty assessment using calibrated artefacts and ISO/TS 15530-4:2008 [79] that deals with uncertainty assessment using computer simulation.
Another standards based on multiple measurements strategies is under development (ISO/CD TS 15530-2 [80]). In the following the different procedures will be described.

3.5.1 Substitution method (ISO 15530-3)

The substitution method operates with two main elements:

- workpiece to be measured,
- calibrated reference object.

These two objects must be similar within certain limits. The measurement of the calibrated reference object yields directly the errors associated with specific measurement task. Thus the errors associated with the parameters of the measured object due to the accuracy of the CMS (including its software) can be determined directly. Calibrations of this kind are only valid for objects with essentially the same geometrical form and size as the reference object used, measured in the same location, the same environmental conditions and using the same measurement strategy. Table 3.7 gives the similarity requirements of substitution method for CMMs in accordance with ISO/TS 15530-3:2004 [78]. When using the substitution method in connection with optical CMS the same requirements are still valid. However, taking into consideration the additional influence parameters that are active, the number of similarity requirements increases. A list of some additional similarity requirements is given in Table 3.7.

Requirements by 15530-3 for contact CMMs		
Subject	**Requirements**	
Dimensional characteristics	Dimensions	Identical within: ± 10 % beyond 250mm; ±25mm below 250mm
	Angles	Identical within ± 5/
Form deviations and surface texture	Similar due to functional properties	
Material (e.g. thermal expansion, elasticity)	Similar due to functional properties	
Measuring strategy	Identical	
Probe configuration	Identical	
Additional similarity requirements in optical coordinate metrology		
Subject	**Requirements**	
Surface (microstructure)	Orientations of texture similar. Surface roughness parameters (3D preferably) identical within ± 10% Colour identical	
Surface (macrostructure)	Curvature identical within ± 10% Inclination identical Sharpness of edges identical within ± 10%	
Illumination	Type identical Intensity identical	
Imaging optics	Identical	
Settings of optical features for image processing	Identical	

Table 3.7: similarity requirement of substitution method

Performing a comparator-type calibration procedure is relatively straightforward. The procedure involves a sequence of measurements, performed in the same way and under the same conditions as the actual measurements. The only difference is that instead of the workpiece to be measured, the calibrated object is measured. The reference object is measured several times by the CMS. Here it is good practice to make small changes in the location of the object and the measurement strategy to establish the sensitivity of the measurements to small differences between the final application of the measurement and such a calibration. In general, no analysis of errors associated with the CMS is required.
The differences between the results obtained by the measurement procedure and the known calibration values of the calibrated object are used to estimate the uncertainty of the measurements.
According to ISO/TS 15530-3:2004 [78], the user must perform a relevant number (at least 20) of substitution measurements under the various conditions he might expect while measuring real workpieces. When performing the measurements, basically three uncertainty contributions have to be taken into account. They are described by the following standard uncertainties:
• u_{cal}: standard uncertainty resulting from the uncertainty of the calibration of the calibrated workpiece stated in the calibration certificate;
• u_p: standard uncertainty resulting from the substitution procedure as assessed by repeated measurements (calculated as the standard deviation of the measured values);
• u_w: standard uncertainty resulting from material and manufacturing variations (due to the variation of expansion coefficient, form errors, roughness, elasticity and plasticity).
In addition, a systematic error, b, can be considered separately.
The expanded measuring uncertainty, U, of any measured parameter is calculated from these standard uncertainties as:

$$U = k \times \sqrt{u_{cal}^2 + u_p^2 + u_w^2} + b$$

The coverage factor, k, may be chosen as $k = 2$ for a coverage probability of 95%.
Because of the experimental approach, the substitution method is simple to perform, and it provides realistic statements of measurement uncertainties. However this method has also some limitations. They can be summarised as: the availability of artefacts with sufficiently defined geometrical characteristics, stability, reasonable costs, and the possibility of being calibrated with sufficiently small uncertainty. One important drawback is the necessity of a reference workpiece, which is calibrated with an uncertainty lower than the CMS under investigation. Due to the general nature of coordinate measuring systems, many

calibrated artefacts would be required resulting in a need for a huge number of gauges, where storage, maintenance, cataloguing, and calibration of gages is a major expense.
Some researchers have developed general "gages" that imitate particular part features that are critical. Good illustrative examples are given by Pfeifer [82] and Sammartini [83],[84] (Fig. 3.16).

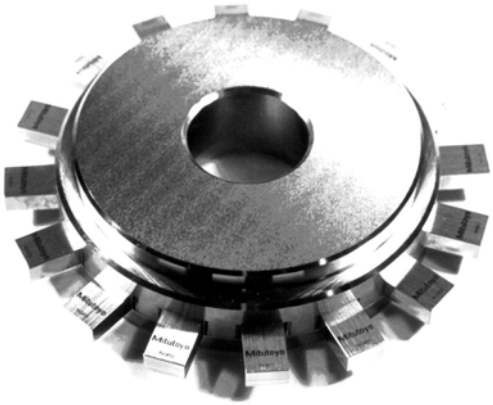

Fig. 3.16: The "Gauge Block Gear" by Sammartini [83].

Similar "modular gages" may be used to investigate CMS uncertainties when measuring free form surfaces. In [85],[86] the so-called modular free-form gauge (MFG) is proposed. The idea under the MFG concept is to simulate a freeform measurement with the measurement of surfaces on regular objects, combined in a manner that represents the shape of interest as closely as possible. The selection of regular objects and their combination is depending on the typical use of the particular CMM; it should cover the typical range of curvature in the working space. An advantage of this solution is the possibility to calibrate the artefact with well-known methods on high precision measuring instruments. The measurements of regular features such as planes, angles, spherical and cylindrical surfaces, etc. can be carried out also using other types of measuring equipment (simpler and fully traceable), and a comparison of measurement results is possible. The approach is still metrologically correct if a proper estimation of the additional measuring uncertainty is carried out to take into account the decreased similarity between calibrated object and actual workpiece. The principle of the MFG is illustrated in Fig. 3.17.

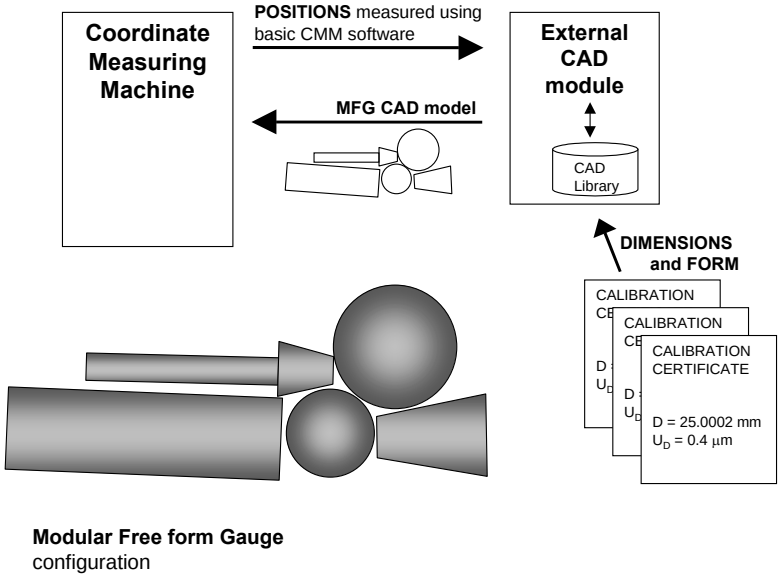

Fig. 3.17: Principle of MFG [86].

3.5.2 Parametric approach and computer simulation methods (15530-4)

The error synthesis approach is based on an analysis of the errors introduced in the various components of a CMS (the so-called parametric errors) and their effect on the errors in the measurand.

A task-related calibration according to the error synthesis approach usually consists of the following three phases:

1. Assessment of the CMS's parametric errors. This involves the assessment of the geometric and probing errors of the CMS and their response to variations in the environmental conditions as specified in the certificate. Only those error sources that are active for the specific measurement task under consideration need to be estimated.
2. Calculation of the errors in the measured coordinates of each single measured point. These errors are obtained by superposition of the parametric errors. The errors calculation is performed for each point specified in the measurement strategy, as obtained using a particular probing strategy, under specified environmental conditions.
3. Assessment of the errors in the measured feature. This is done through combination of the errors in the measured coordinates of the measured points to the errors in the measurands, taking into account the estimation software of the CMS.

Phases 2 and 3 may be performed by computer simulation. Here the goal is to construct a model of sufficient complexity to simulate the propagation of the parametric errors to errors in the measurands, as determined by the measurement task and measurement strategy. Computer simulation enables the simulation of

many measurement strategies by modelling the kinematics, dynamic and thermal characteristics of the measuring system.
Various names have been given to the simulation methods, including the "Virtual CMM"[87],[88], "Virtual Instrument"[89], "Simulation by Constraints"[90], the "Expert CMM"[91], or simply Monte Carlo simulation [92]

3.6 OTHER METHODS

3.6.1 Uncertainty estimation using multiple measurement strategies

The estimation of measurement uncertainty using uncalibrated objects, proposed in ISO/TC213/WG10 Draft ISO/TS 15530-2 [80], is based on the principle of experimental assessment of uncertainty by multi-position measurements of the workpiece. Nevertheless the objective is different, since the main purpose is to quantify the uncertainty of an actual measurement on produced parts.
This part of ISO 15530 provides a practical technique for the combined experimental and analytical uncertainty assessment. This technique is based on measuring the uncalibrated measurement object in multiple positions and orientations and with varying distributions of measuring points. An average result from all measurements is calculated. This is used as the calibration value in all cases where the measurand is not a distance or size etc. In those cases where the measurand is a distance, size etc., the average error of length measurement has to be measured, using a standard of distance or size. The average result from all measurements containing distance, size etc. are corrected for this average error of length measurement. A standard uncertainty is calculated from the results in each object orientation. The quadratic average of these standard deviations is taken as the uncertainty contribution from the repeatability of the CMM and from the form deviations and roughness of the object. The standard deviation of all the averages for each of the object orientations is calculated. This standard deviation yields an estimate for the uncertainty contribution from the errors of geometry of the CMM. Finally all contributions are combined and expanded to yield the task-related measurement uncertainty. In [93] this method have been used by the author to evaluate measurement uncertainty on plastic parts using video probe. In Table 3.8 all the uncertainty contributors considered by the author are reported.

Error source	Determination method	Taken into account by:
CMM geometrical errors	Averaged by multiple measurements strategy	U_{geo}: considered in uncertainty budget
Repeatability	Evaluated in multiple measurements strategy	U_{rep}: considered in uncertainty budget
Handling and clamping	Evaluated in multiple measurements strategy	U_{rep}: considered in uncertainty budget
Object alignment	Evaluated in multiple measurements strategy	U_{rep}: considered in uncertainty budget
Linear scale factor	Measurement of a standard of length	E_L: compensation of measurement results U_{corrL}: considered in uncertainty budget
Video probe errors and effect of lighting conditions	Measurements of standards of size (internal and external diameter)	E_D: compensation of measurement results U_D: considered in uncertainty budget
Thermal effects	Uncertainty budget.	U_{temp}: considered in uncertainty budget

Table 3.8: uncertainty contributors considered by the author in [93].

3.6.2 Sensitivity analysis

In cases where a clear analytical solution can be formulated for the measurand as a function of measurement parameters, it is relatively easy to follow the prescription of the GUM. As specified in the GUM, one must first list each uncertainty source, quantify each source according to its magnitude by a standard deviation, determine its sensitivity coefficient and correlation with other uncertainty sources, and add the product of each standard uncertainty by its sensitivity coefficient, in quadrature, and report the combined standard deviation with a coverage factor, typically, of two. This technique is quite useful when a well-defined mathematical model of the measurement process can be ascertained.

3.6.3 Expert judgment

The GUM recognizes type B uncertainty determinations, which represent an educated estimate based on expert judgement. Experts with significant experience with a particular measurement process and/or a specific CMM may very well be able to realistically estimate the uncertainty strictly as a type B source. This technique may be used to estimate a single uncertainty source, the effect of a group of sources, or the entire uncertainty budget. It may be the only technique available when measurement data and mathematical models of the measurement are unavailable. An approved (registered or accredited) expert will make estimates

– instead of mathematical models, simulated data, or related performance testing data – that make up the input into the error budget feeding into the sensitivity analysis calculation.
Expert Judgement is normally applied when mathematical models, artefacts for substitution techniques, etc. are not readily available. Expert judgement is also normally applied in conjunction with Sensitivity Analysis methodology, and hence could be considered a special case of Sensitivity Analysis.
Expert Judgement is the subject of one of the ISO 15530 parts that are going to be developed by ISO/TC213/WG10. This draft international standard shall specify: (i) the requirements of the expert judgement uncertainty assessment procedure, (ii) the basic experiential and academic background of "experts" exercising judgement and estimating magnitudes of errors comprising the error budget and (ii) the methodology for "synthesizing" individual components of the error budget.

3.6.4 Statistical estimation

High-volume manufacturing is inherently incredibly efficient from an economic point of view and provides considerable data to allow statistical evaluation of measurement results. In such situations CMMs are often used for routine sampling purposes on parts that are produced in very large numbers. The measurement results from nominally identical features can be compiled to develop a history of measurement results for a particular process and a particular part on a particular (or set of) measuring machine(s) that is (are) being used for process control. Because the measurement results include not only production variability and measurement uncertainty, they perhaps do not reflect true measurement variation, but the variance derived likely overestimates the variation due to the measurement process. Also, it is possible that the results include some measurement bias and its uncertainty. However, if the historical data cover a reasonable time span and the produced parts function as intended, it is sufficient to assume that the estimation of uncertainty from this procedure is adequate for the intended end use of the product .

3.6.5 Hybrid methods

There may be applications where a combination of some of the different methods described above is appropriate. One of the most complete treatments of CMS uncertainty using a combination of sensitivity analysis and expert judgement was due to Salsbury [94]. He categorized uncertainties into components from the machine, probe, part, and repeatability. Next the relationships between the uncertainty components and the geometric dimensioning and tolerancing "call outs" were qualitatively evaluated, i.e., would a specific error affect a specific tolerance or not. Application of this technique involves picking a tolerance required on the drawing, determining the uncertainty values that apply, estimating

a value of the uncertainty using standard acceptance test results, measured repeatability, or expert opinion, multiplying by sensitivity coefficients (when required), and adding the results in quadrature. Using this technique clearly requires more understanding than the simulation methods mentioned above, but it has the advantage that it clearly spells out uncertainty sources, which should aid in operator education.

3.5 CONCLUSIONS

In this chapter an overview was given on the current state-of-the art about performance verification of optical coordinate systems.
Error sources in optical coordinate metrology were examined, considering separately the main contributors related to lateral sensors and distance sensors. The influence of measuring parameters, such as illumination, windows size and magnification were discussed through experimental investigations performed by the author using a Video CMM, while the effect of surface slope has been investigated using a conoscopic holography laser.
Guidelines, standards and initiatives for standardization of performance verification procedures were described and discussed. Consequently to the lack of internationally standardized rules for non-contact systems, specifications provided by producers of different systems are often given on the basis of non-comparable verification procedures. Therefore, users have difficulties in comparing different systems and they don't have clear rules to check metrological performances. In addition, the characteristic uncertainty contributors for non-contact methods are often not well known or documented.
Therefore, new methods and artefacts for testing optical systems and for making optical measurements comparable with mechanical measurement are required. To fulfil this lack of standardization, the international cooperation "OSIS" (Optical Sensor Interface Standard), has been started between the main manufacturers and users of optical sensors. In order to contribute to the standardization of methods and artefacts, tests proposed by the OSIS Project have been performed by the author on an high accuracy multisensor CMM.

Chapter 4

Artefacts development for performance verification of 3D optical systems

The influence of the object properties (material and surface characteristics) on the measurement result is much stronger and more difficult to assess for optical sensors than for tactile ones. For the comparability of measurements and the traceability to the unit of length, accepted standards and artefacts are needed. In particular the artefact properties should have no significant effect on the parameters to be determined.
In this Chapter artefacts for performance verification of 3D systems are reported and described focusing mainly on experimental investigation about optical properties of cooperative surfaces. As results of the investigation a series of artefacts has been developed for performance verification of 3D laser systems (Chapter 5).

4.1 ARTEFACT FOR 3D SYSTEMS

As already discussed, only a few standards for the assessment of performance verification of non-contact CMMs have been published so far. The most famous one is German guideline VDI/VDE 2617 Part 6.2 [30]. In this standard, the performance tests are similar to the tests in ISO 10360 Part 2 [59]. For this reason, also proposed artefact for performance verification are same as the gauges defined in ISO 10360 Part 2.
In Fig. 4.1, the following artefacts that can be used both for Coordinate Measuring Systems, are shown:

a) Ball bar [58];
b) Ball cube [95];
c) Tetrahedron [96];

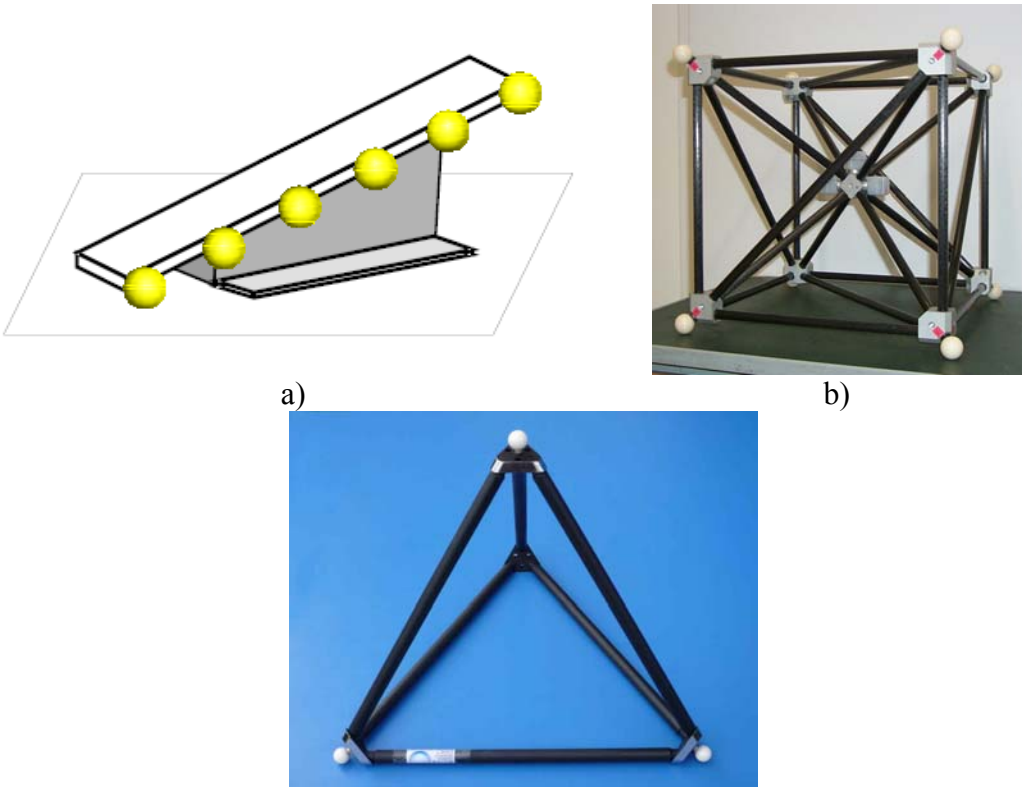

a) b)

c)

Fig. 4.1: typical artefacts for performance verification of coordinate systems.

For non-Cartesian CMMs, VDI/VDE 2634 [66],[67] series is available. For non-contact CMMs, those having Cartesian translation stages are not common, therefore most instruments will be assessed by VDI/VDE 2634 series. In VDI/VDE 2634 series [67], a ball bar are used for the size test, but the diameters of the balls are defined as 10 to 20 % of the measurement volume of the instrument; it does not look a double ball bar rather a pair of dumbbells (fig. 4.2). For example for the instrument having measurement volume of 1m, spheres of 10 to 20cm diameter are needed. Because precise, lightweight, and inexpensive spheres of this size are not easily available, this standard is not commonly used. Geometrical parameters to be measured in this standard are the distance between the spheres and the deviation from the Gaussian associate (least square fitting) ball.

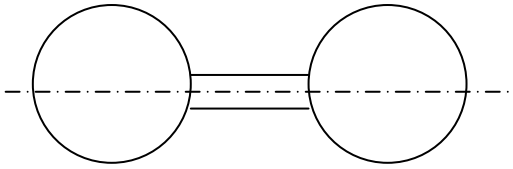

Fig. 4.2 - Schematic of artefact proposed by VDI/VDE 2634 [67].

The guideline, also, to determine the flatness measurement error, proposes rectangular parallelepipeds made of ceramic, steel, aluminium, or other suitable materials with a diffusely scattering surface.
Other artefact have been presented by different authors, as shown in Fig.4.3 [33], [35],[97],[98],[99],[100]. These artefacts have been introduced to evaluate the behaviour of the separate sensors, without considering the performance of the entire system.

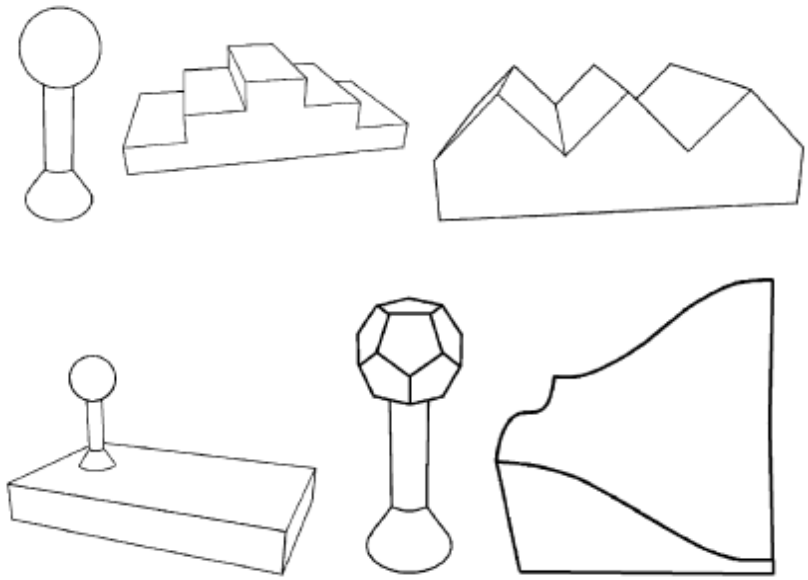

Fig. 4.3: artefact for performance verification of optical sensors [35].

The main difference between artefact for tactile systems and optical systems is related to the surface finish of the gauges itself. Generally, guidelines don't give indication about optical properties and surface finishing of the artefact.
To cover this lack of indication, in the OSIS document [75] a series of requirements has been stated, putting particular attention to the optical properties of artefact's surfaces (Table. 4.1) and indicating standards and guideline taken as reference.
Besides the optical properties of the surface, to be extensively used, calibration artefact have to satisfy the following requirements:

- To be opaque and avoid light penetration
- To be sufficiently hard to permit also contact measurement and calibration
- To be economically available on the market

Parameter	Characteristic	Measuring parameters	Referring Standard
Material	Recommended: Steel 100Cr6 Material number: 1.3505 (for ball bearings)	-	DIN 17350 ISO 3290: 1998 (preferred nominal ball diameters)
Diameter	(30.000±0.011)mm Grade: G20		DIN 5401: 1999 Maß- und Formgenauigkeit, Rauheit
Form error	<2µm (it is recommend to use a ratio between MPE_{Tij} and form error of at least 5:1)	RON_T	DIN 5401: 1999 Maß- und Formgenauigkeit, Rauheit ISO/TS 12181-1
Roughness	Rz = (3.0±2.0)µm		EN ISO 4287:1998 EN ISO 4288:1998 ISO 11562:1996 DIN 5401: 1999 Maß- und Formgenauigkeit, Rauheit
	RSm = (50±25)µm		EN ISO 4287:1998 EN ISO 4288:1998 ISO 11562:1996 DIN 5401: 1999 Maß- und Formgenauigkeit, Rauheit
Reflectance	At 650nm = (50±10)%	to be measured at least in 5 positions over the sphere	ISO 2813: 1994: Paints and varnishes determination of specular gloss of non-metallic paint films at 20°, 60°, 85° ISO 7668: 1986: Anodized aluminum and aluminium alloys—measurement of specular reflectance and specular gloss at angles of 20°, 45°, 60° or 85°
Relative tilted reflectance	(-10/10) < (300±100)% (10/30) < (45±10)% (20/40) < (25±10)% (30/50) < (15±5)%		

Table. 4.1: OSIS requirements for artefacts [75].

4.2 COOPERATIVE SURFACES

As seen before, optical properties of surfaces significantly influence the performance of non-contact sensors. The optimal surface type for scanning purposes would be a totally lambertian surface with a high reflection index [101], [102]. However, most common artefacts have surfaces with specular-reflective or translucid behaviour (Fig. 4.4). With translucid surfaces (Fig. 4.5), light reflects as

in a lambertian surface, but it goes through the material until a certain depth. The higher the light power, the deeper the light penetrates inside the material. In addition, the light scatters inside the material, so that a camera looking at it 'sees' laser reflections sourcing from inside it [103].

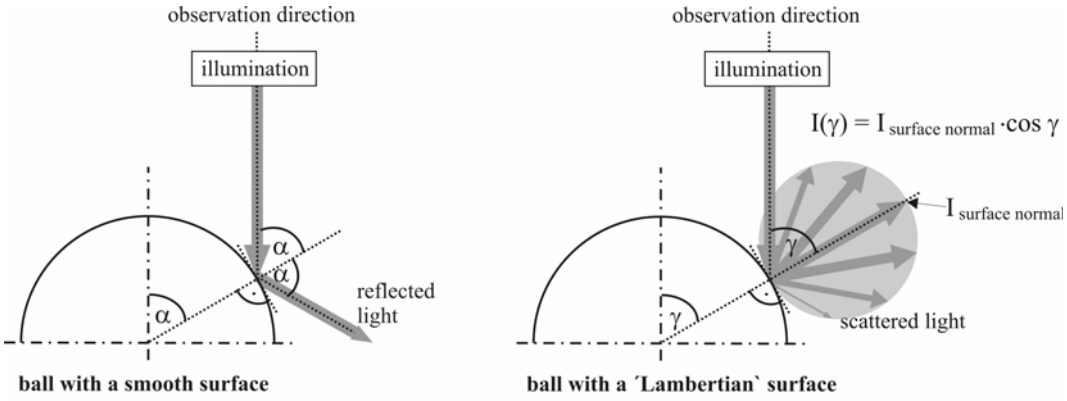

Fig. 4.4: Slope-dependence reflection/scattering behaviour of a smooth surface (left) and a "Lambertian" surface (right) [102].

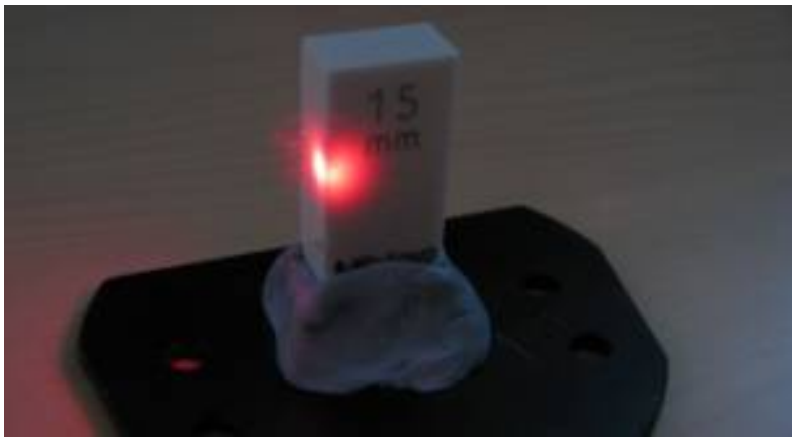

Fig. 4.5: Translucid surface, zirconium gauge block

In the following sections an experimental investigation carried out to develop suited verification artefacts for 3D laser scanner is presented. These activities have been performed within the OP3MET Project (see Chapter 5).

4.3 EXPERIMENTAL INVESTIGATION ON COOPERATIVE SURFACES

The purpose of the first investigation was to test different surfaces of different materials and coatings. Tests will cover both surfaces already used today in calibration or testing, and surfaces that are supposed to behave nearly as a lambertian surface.

In the Table 4.2 the list of the most important tested materials is reported.
The experimental investigation has been carried out using a prototype of triangulation laser scanner built by the Danish company 3Shape [104], (Fig. 4.6).
To compare the optical behaviour of different materials, the laser ray that impinges the surface was analyzed. In particular the following parameters have been considered for the evaluation:

(i) the value of tracking mean, that is the average of the intensity of all the pixels of the CCD impressed by the light
(ii) the standard deviation of the intensity in the direction perpendicular to the direction of the laser
(iii) the ratio between these two values.

Sample n°	Material
1	Deposition of Chromium on glass
2	White sprayed turned steel
3	Sandblasted Aluminium
4	Turned Aluminium
5	Coating of TiN on turned steel
6	Lapped steel
7	Acid-etched steel

Table 4.2: Samples of different materials.

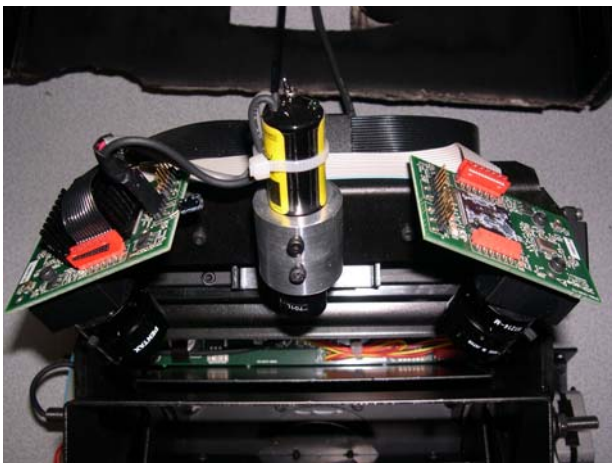

Fig. 4.6: Laser scanner used for the investigation

The intensity of the light ray is Gaussian (Fig. 4.7) in the direction of the width, so the standard deviation informs if the laser stripe is sharp or large and blurred. The ideal parameters for a cooperative surface are (i) a high value of tracking mean (the surface doesn't absorb too much the laser), (ii) a low value of standard

deviation (a light narrow and clear stripe) and (iii) a behaviour independent by the direction of observation (a lambertian surface).

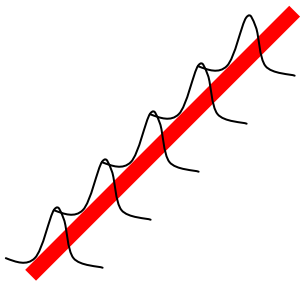

Fig. 4.7: Gaussian behaviour of the stripe light

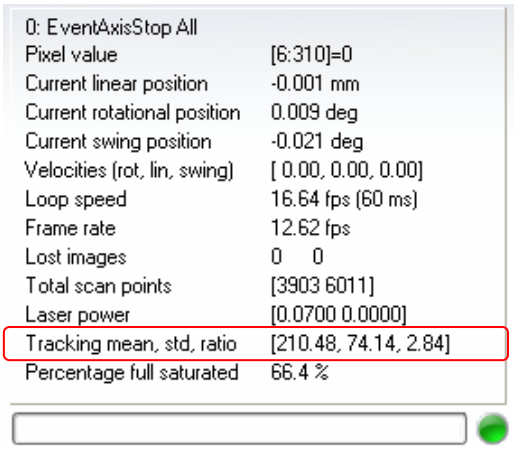

Fig. 4.8: Output of the scanner for every image

Each material have been tested at different distances from the source of light: every two millimetre from the reference level of 0mm (the position on the rotation plate) to 40mm of height. Similar tests are executed in [105], [106], [107].
For every position the power of the laser that minimizes the percentage of full saturated pixels have been used. Then data related to (i) the tracking mean, (ii) the standard deviation, (iii) the percentage full saturated (Fig. 4.8) and (iv) the laser power have been collected. Tests were repeated in two different relative position between the sample and the laser plane: in the first position the laser was perpendicular to the sample while in the second it was inclinated of 45°.
All tests and results are presented in [108]. In particular during the experimental investigation the effect of surface treatment (mechanical and chemical) was analyzed.
In the following tables, the average values of TM, SD stripe, ratio and laser power of the different materials in the two position, are compared. In addition the standard deviation of the tracking mean values is reported for every material.
The average value is fundamental to understand the optical behaviour of the surface in terms of transmission, reflectivity and absorption. An high value of the tracking mean is desired because it means that the laser light is reflected and not transmitted or absorbed. The standard deviation is important because expresses if a surface is lambertian or not: if it is low the material is quite lambertian (diffusive) because the behaviour not changes with the direction of observation.

	TM	SD stripe	Ratio	L power	Sd TM
Deposition of Chromium on glass	174	50	3.5	0.076	14.6
White sprayed turned steel	195	31	6.3	0.068	8.1
Sandblasted aluminium	206	34	6.3	0.070	14.3
Turned aluminium	90	46	2.0	0.068	24.4
Coating of TiN on turned steel	132	58	2.4	0.069	28.6
Lapped steel	175	48	3.7	0.071	15.1
Acid-etched steel	134	70	1.9	0.071	19.4

Table 4.3: Average values, laser perpendicular to surface.

	TM	SD stripe	Ratio	L power	Sd TM
Deposition of Chromium on glass	155	58	2.7	0.101	13.8
White sprayed turned steel	231	20	13.8	0.069	11.3
Sandblasted aluminium	225	25	48.5	0.071	11.9
Turned aluminium	156	56	5.6	0.072	36.6
Coating of TiN on turned steel	144	56	2.6	0.077	16.2
Lapped steel	204	38	5.4	0.070	12.9
Acid-etched steel	\	\	\	\	\

Table 4.4: Average values, laser inclinated of 45°.

From the tables it's evident that the three best materials are:

- white sprayed surface
- aluminium sandblasted
- acid-etched steel

In particular the white plane represents the best surface because it possesses:

- high value of tracking mean that indicates a surface that reflects the greater part of the light (low absorption and transmission);

- low value of standard deviation of the pixel's value on the stripe (SD stripe) that indicates a sharp and narrow laser stripe;
- high value of the ratio between TM and SD stripe that means that the surface is cooperative;
- low value of standard deviation of TM values measured at different heights and from different cameras, that indicates a quite lambertian surface.

Furthermore from tables is quite evident as surface treatments change the optical behaviour of the material. In particular, a big difference is present between aluminium and aluminium sandblasted (Table 4.5):

- the value of tracking mean becomes double
- the ratio becomes six times greater
- sd TM reduces consistently

	TM	SD stripe	Ratio	L power	Sd TM
Turned aluminium	90	46	2.0	0.068	24.4
Sandblasted aluminium	206	34	6.3	0.070	14.2

Table 4.5: Average values for aluminium, laser perpendicular to surface.

The same effect is present for steel. Steel is a material really common in precise reference artefacts, strong, tough and can be dimensionally stable. One of the best methods that has been found for improving the surface properties of stainless steel is by acid-etching. The acid-etching procedure will be described in the section.
It's important to clarify that the aluminium sandblasted behaves in a similar way in the two different relative laser positions whereas the aluminium changes considerably its behaviour with the incident angle; this shows that the block made of aluminium is non-lambertian. In the same way the acid-etched steel shows a behaviour really better than the steel.
At results of the first preliminary study, it was decided to investigate more deeply the white artefact and the steel acid-etched one.
Steel is preferred to aluminium for different reasons:

- It is harder, tougher, more thermally and dimensionally stable;
- It is easily available with the proper tolerance: ball bearings are made of steel, have excellent dimensional properties (form error <5μm, grade 3) and are relatively cheap.
- Moreover acid etching is preferred to sandblasting as it is a cheaper way to treat the surface and, as discussed later, it is quiet easy to obtain an uniform surface with low form error.

4.4 SURFACE TREATMENT FOR IMPROVING THE OPTICAL PROPERTIES OF STEEL

The acid used for the treatment of steel has the property to change dramatically the optical properties of the surface. To develop new artefacts, a series of common ball bearing was used for investigation. In the first experiments it was noticed that after some hours the spheres changed their colour because they oxidized (see Fig. 4.9).

Fig. 4.9: From left to right: steel sphere without treatment, immediately after the acid-etching and after some hours.

To avoid oxidization of spheres, stainless steel has been used and subjected to the acid treatment. First of all it was noticed that the white appearance, after acid-etching, is more evident than for the not stainless steel (Fig. 4.10).

Fig. 4.10: Stainless steel balls with (left) and without (right) acid treatment.

Also after a long period (at least 4 days) the sphere keeps its surface properties: it does not oxidize (Fig. 4.11).

Fig. 4.11: Acid-etched stainless steel after 4 days.

Surface roughness has been measured using an Atomic Force Microscope, in order to evaluate if the obtained spheres satisfy OSIS requirements (Table 4.1). For surface without treatment (Fig. 4.12a), the average value of roughness was Rz = (0.12 ± 0.1)µm (not in good agreement with OSIS indication), while after acid-etching (Fig. 4.12b) the average value was Rz = (1.14 ± 0.1)µm

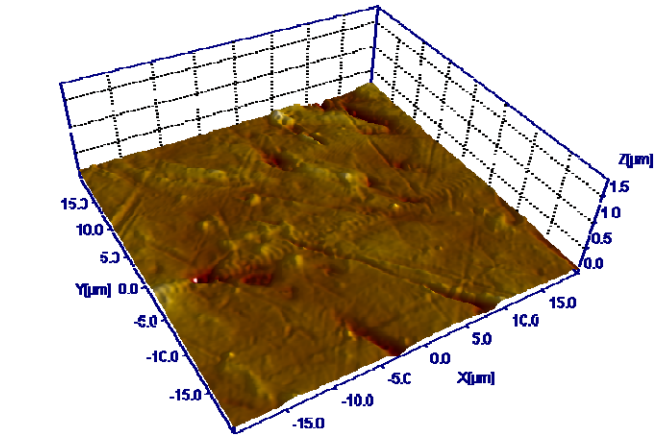

a)

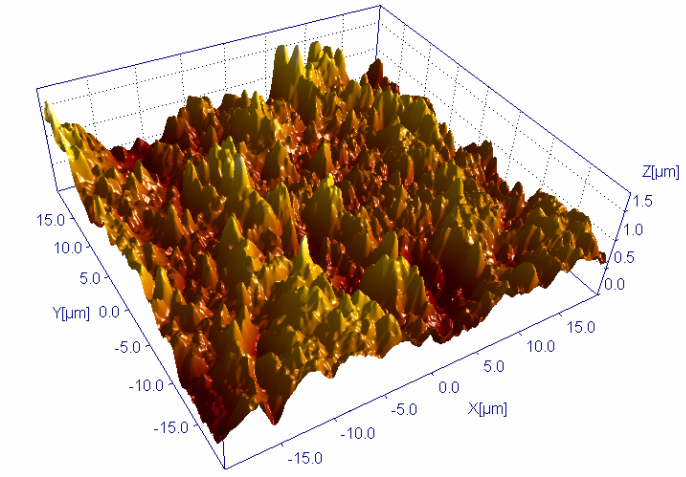

b)

Fig. 4.12: surface topography of steel sphere a) before and b) after the acid etching.

The next problem to investigate was the effect of the acid treatment on the form of the spheres. The ball bearing was measured with an high accuracy contact CMM Zeiss, before and after the acid-etching.
From the Table 4.6 it's evident that the geometry of the balls is not corrupted by the acid treatment.

	Diameter [mm]	Form error [mm]
Before treatment	22.220± 0.001	0.005± 0.001
After treatment	22.218± 0.001	0.006± 0.001

Table 4.6: Dimensions of stainless steel balls before and after treatment.

4.5 COMPARISON ON SPHERES

The major conclusion of the previous section is that a ball bar with white or acid-etched stainless steel spheres can be the proper artefact to verify performance of the scanner laser. For this reason, a series of different spheres were measured with the laser scanner and then results related to diameter and form error where compared with calibrated values obtained with the contact CMM. The scanner gives in output a file .stl (Fig. 4.13); this file was analyzed with the specific software 'I-DEAS 8 Freeform Modeler', the data were fitted with a sphere and then the deviation (form error) between the real data and the ideal sphere was diagnosed.

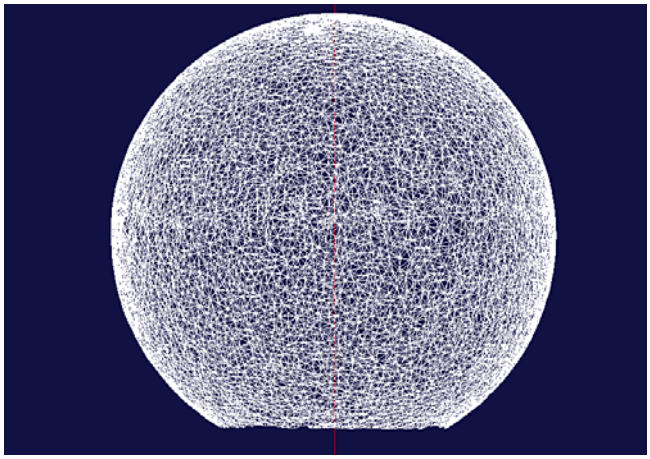

Fig. 4.13: Output .stl of the scanner opened with I-DEAS.

Six different spheres were tested:

1 - a white ball made of zirconium;
2 - a acid-etched stainless steel ball;
3 - a lapped stainless steel ball without treatment;

4 - a sandblasted steel ball;
5 - a sphere made of alumina without treatment;
6 - a sphere made of white sprayed alumina.

In the Table 4.7 there are the results of the investigation:

	Scanner laser		**CMM**		**Deviation scanner – CMM**	
Sphere	Diameter	Form error	Diameter	Form error	Diameter	Form error
1	14,857	0,119	15,000	0,003	-0,143	0,116
2	22,167	0,061	22,207	0,007	-0,039	0,054
3	21,647	3,239	22,221	0,005	-0,574	3,234
4	9,830	0,467	9,982	0,014	-0,152	0,453
5	9,926	0,055	10,019	0,024	-0,093	0,031
6	9,966	0,064	9,993	0,003	-0,027	0,061

Table 4.7: Diameter and error form of spheres measured using the scanner or the CMM.

About the sphere nr. 1 the scanner gives a good reproduction of the object because the point cloud is complete without holes and the form error is satisfying. The value of diameter measured by the scanner is smaller than that measured by the CMM; this happens because the zirconium is a bit translucid (Fig. 4.14), therefore it absorbs the laser ray and the CCDs see laser reflections sourcing from inside it and not from the surface.

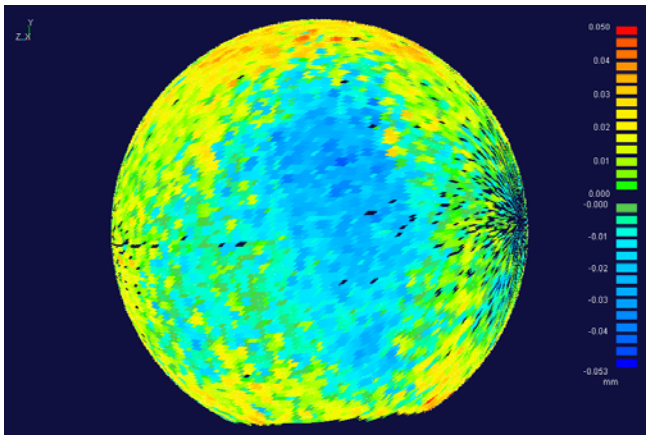

Fig. 4.14: Deviation of the actual sphere nr. 1 (zirconium) from the ideal sphere.

Really impressive are the differences between the not acid etched steel sphere and the one subjected to acid treatment. As proved with the tests on the laser stripe, the acid-etched sphere has excellent optical properties. This is evident also from the point clouds (Fig. 4.15, Fig. 4.16): the first one is complete whereas the second one is incomplete with few points and many outliers.

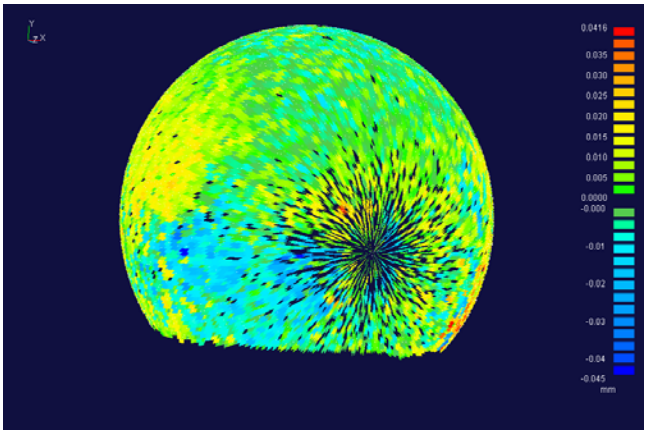

Fig. 4.15: Deviation of the actual sphere nr. 2 (acid etched steel) from the ideal sphere.

It's important to underline that the acid-etched sphere's diameter value, measured with the laser scanner, is similar to the one measured with the CMM (22.167mm; 22.207mm); the same consideration for the error form (0.061mm; 0.007mm). So the sphere made of acid-etched stainless steel can be considered an optimal artefact.

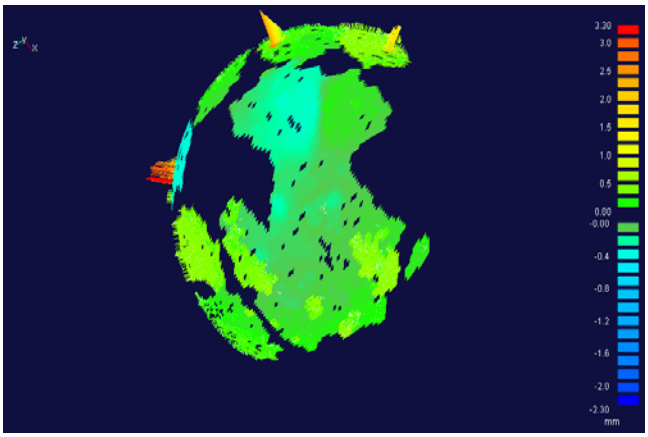

Fig. 4.16: Deviation of the actual sphere nr. 3 (steel without etching) from the ideal sphere.

Additionally it was observed that the sphere nr. 4 (sandblasted steel) measured with the scanner has an elevated value of form error. In fact the image has lot of holes, it's incomplete and has few points (Fig. 4.17) because of the optical properties of the material; the scanner sometimes 'sees' points in the wrong place and sometimes doesn't even see the points.

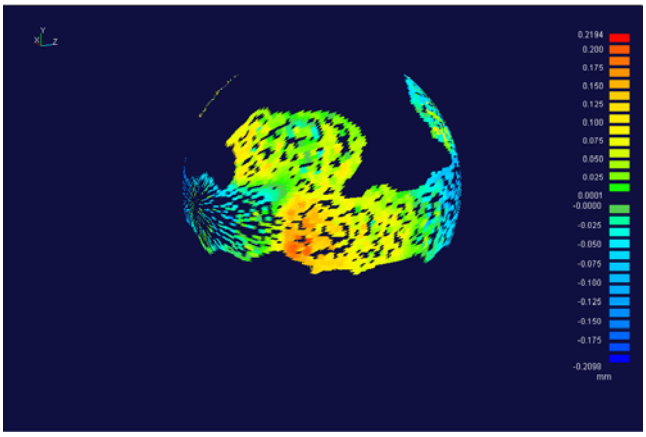

Fig. 4.17: Deviation of the actual sphere nr. 4 (sandblasted steel) from the ideal sphere.

The spheres made of alumina are quite well reproduced by the scanner because the point cloud has just some holes (Fig. 4.18 and Fig. 4.19), but they behave in a different way in terms of laser absorption: the diameter of the alumina sphere, measured by the scanner, is smaller than that measured by the contact CMM. (-0.09mm). Whereas the sprayed alumina sphere absorbs less laser power, in fact the deviation scanner-CMM diameter is only 0.027mm. Moreover the form error of this sphere is considerably smaller than the one of alumina sphere (0.003mm against 0.024mm).

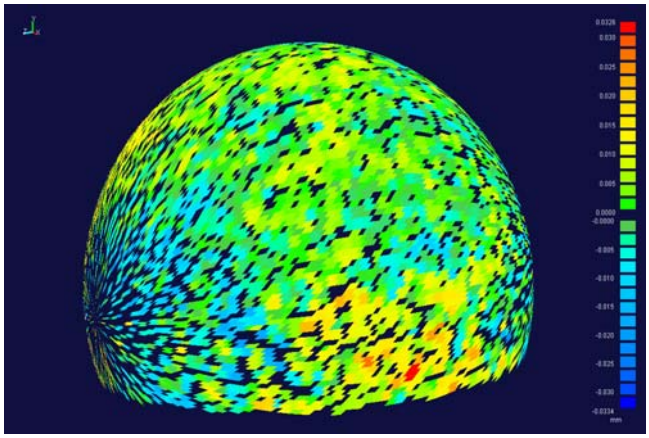

Fig. 4.18: Deviation of the actual sphere nr. 5 (alumina) from the ideal sphere.

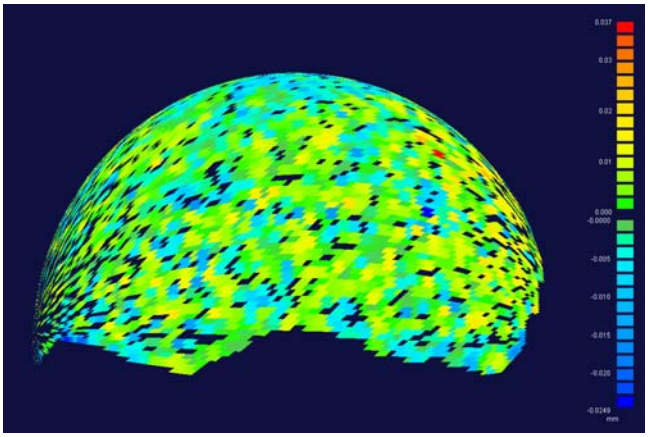

Fig. 4.19: Deviation of the actual sphere nr. 6 (sprayed alumina) from the ideal sphere.

4.6 DEVELOPMENT OF ARTEFACT

As seen in the previous sections, optical properties of different materials have been tested in order to find a cooperative surface for artefact development. From the investigation it was found that the most suited artefact for performance verification of the laser scanner is a ball bar with spheres having white surface or surfaces made of acid-etched stainless steel.
Concerning the material of white spheres, translucid zirconium can't be used because it absorbs the laser ray; the alternative solution is to use balls made of alumina (Al_2O_3), white and matte, with the attention to verify the optical behaviour. In Fig.4.20 is shown a ball bar made with spheres of sprayed alumina used for evaluating for performing a test procedure similar to ISO10360-2 [59] on the laser scanner (see Section 5.2.1).

Figure 4.20: Ball bar with spheres made of alumina

Furthermore, acid-etched steel, is very promising not only for the optical behaviour but also as it is easy to produce and can be used also for artefact with different shapes.
Starting from these considerations, a series of artefact has been developed by the author for performance verification of triangulation laser system. For example, in Fig. 4.21 a prototype of artefact for rotary table verification (ISO 10360-3) is shown, while in Fig. 4.22 the same spheres have been used for a ball bar prototype.

Fig 4.21: First prototype of artefact for ISO10360-3 test adapted for optical scanner.

Fig 4.22: Prototype of ball bar artefact for ISO10360-2.

Also gauge block can be easily treated by acid etching. In Fig. 4.23 an artefact produced using to spheres and one gauge block is reported. This kind of artefact have been used to evaluate the effects of surface slope on measuring results, as introduced in Section 3.1.2, also for triangulation laser system [109].

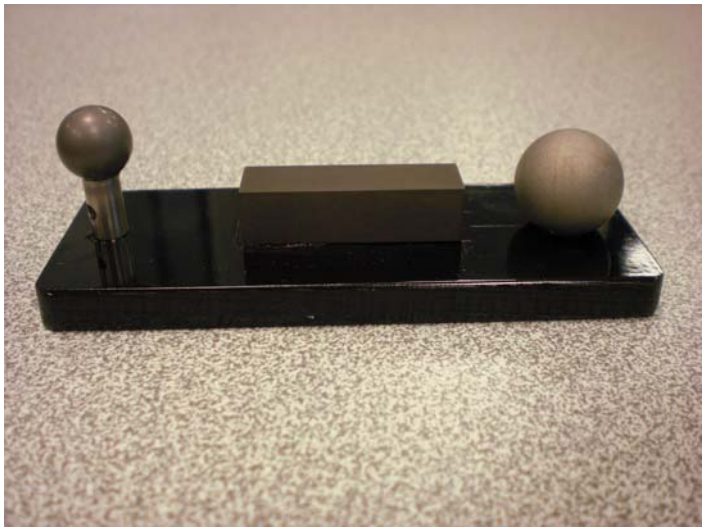

Fig. 4.23: artefact made with two sphere and one gauge block.

Chapter 5

The OP3MET Project: metrological validation of a 3D laser scanner

In this Chapter results from the European Co-operative Research Project OP3MET are reported. The Project, started in November 2006 and ended in November 2008, has led to the development of a new 3D laser scanner for automatic in-line measurements. The contribution of the author has regarded the traceability establishment of the system, including both performance verification, uncertainty assessment and testing of the newly developed metrological software. In particular the national standards VDI/VDE 2617-6.2:2005 has been implemented to evaluate the metrological performances of the system. Beside the main activities performed in connection with the Project, some comments to the standard are presented.

5.1 THE OP3MET PROJECT

The European Co-operative Research Project, named "OP3MET" (Optical 3D Metrology - Automated in-line metrology for quality assurance in the manufacturing industry) has been carried out between November 2006 and November 2008, with the main objective of developing an innovative laser scanner for automated quality control of dimensions and geometries on 3D products, including freeform surfaces and metallic or plastic parts. The Consortium working to this Project was composed of 3 SMEs, 3 end-users and 4 RTD performers, from 5 different European Countries (Denmark, Italy, Portugal, Romania and United Kingdom).
Compared to the state of the art, the main innovative contributions addressed by the newly developed measuring systems are:

- *Adaptive scanning technology facilitating a true 'one- button system':* A novel adaptive technology [110] in combination with a multi-axis positioning system automatically rescans the occluded areas not covered by the initial scan. The adaptive technology is versatile with respect to part geometry and material. The technology can also be used to automatically create sequence files for the initial scan. These elements will enable a true 'one-button solution', i.e. the user only needs to press a single button to scan a new part.

- *Improved accuracy, possibly comparable to those of touch probe coordinate measuring machines:* The improved accuracy covers both improved sampling accuracy and suppression of noise, e.g. originating from specular reflections, speckle effects or half-occlusions.
- *Metrological traceability and standardisation:* Development of procedures and artefacts for metrological performance verification and traceability establishment.
- *Versatility with respect to part geometry and materials in particular freeform metal and plastic parts:* The new system will allow measurement of features and materials that cannot be measured using conventional optical methods.
- *Laser system:* A novel laser system removing or suppressing most of the laser related noise created by the current lasers. The laser related noise is one of the largest error sources.
- *Low system cost:* The low system cost is obtained through innovative low cost design, minimised production cost and applying low cost components compensating for the inaccuracy in software. As a consequence, significant lower end-user prices are estimated than for existing comparable systems.
- *User-friendly metrology software:* The challenge of creating an intuitive and simple user interface, which can be operated with a very limited amount of training, is too often underestimated. A simple user interface for 3D software heavily relies on sophisticated algorithms, which reduce the need for the manual "tuning" of parameters and other manual interaction such as placing corresponding points on several models.

An exhaustive description of the system is reported in [111], including architecture, hardware and software description. In the following special attention will paid to the metrological performances verification and traceability establishment.

5.2 METROLOGICAL PERFORMANCES VERIFICATION

As seen in the previous Chapters, there are no internationally recognised standards, testing procedures and artefacts directly applicable to verify the metrological performances of non-contact systems. There are numerous studies on the modelling and calibration of a laser scanner [112],[113],[114],[115],[116] but the recommended way is to follow the standards ISO 10360-2 [59], ISO 10360-7 (draft) [58] and the German engineering guideline VDI/VDE 2617 – Part 6.2:2005 [63],[117]. In all these standards, performances of systems are evaluated considering two main parameters:

- MPE_P = extreme value of the probing error permitted by specifications, regulations etc. for the system;
- MPE_E = extreme value of the error of indication of a system for size measurement E, permitted by specifications, regulations etc. for the system (Fig. 5.1).

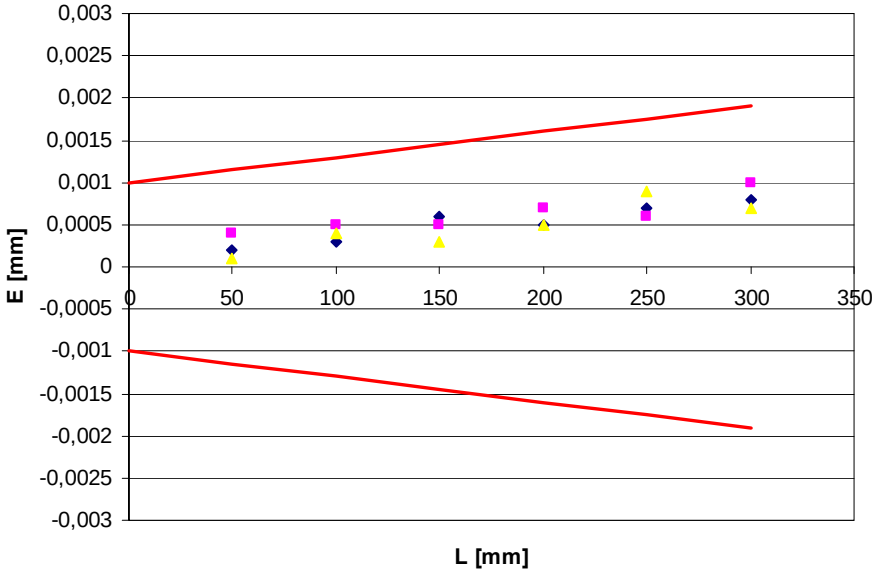

Fig. 5.1: Example of performance verification results for measuring of size.

VDI/VDE 2617-6.2 [30] is the most useful document available in this field because it is a guideline for the application of ISO 10360-2 to coordinate measuring machines with optical distance sensors and it refers also to laser scanners based on the triangulation principle.

5.2.1 VDI/VDE 2617 Part 6.2

This guideline gives specifications for coordinate measuring machines with optical distance sensors, and defines methods for the testing of these instruments. It is in close harmonisation with ISO 10360-2 [59], and provides the necessary additional specifications for the use of optical sensors such as:

- artefacts to be used as an alternative to gauge block;
- comparability of the characteristics where alternative artefacts are used;
- comparability of the characteristics where probing strategies differ for different sensors.

About artefacts, the guideline specify that test spheres of ceramics or steel have to be used to determine the probing error; according to ISO 10360; the sphere's diameter has to be between 10 mm and 50 mm. The procedure and the evaluation of the probing error are analogue to that of ISO 10360-2 [59].
The error of indication for size measurement is determined using artefacts including material standards of size, such as ball bars having two or more spheres.

Measuring of the spheres shall be performed using points distributed as evenly as possible over the entire surface of the sphere. The measurement line of the sensor shall be, if possible, aligned perpendicular to the sphere surface.
The guideline expressly explains that the error of indication for size measurement differs from the sphere-distance error: when the sphere-distance error is determined, the probing error is not included completely in the characteristic. This is due to averaging effects in the calculation of the regression sphere, which result from the large number of permissible measurement points. This measurement is not directly comparable to measurements using gauge blocks. In order to ensure comparability, a short gauge block may be measured additionally. Alternatively, the correction may be obtained from the probing error measurements.
The guideline gives two methods to take into account the averaging effect and compensation of bias errors encountered in measurements of sphere positions, to allow comparison with measurements of individual points on a plane (gauge block):

A - The error of indication for size measurement, E, is obtained from the difference between the test length, L_{ka} (indicated value), and the calibrated sphere distance, L_{kr} (true value), of the artefact plus the signed value of error in size (diameter), PS, and probing error in form PF:

$$\text{Case 1: } (L_{ka} - L_{kr} + PS) > 0 \qquad E = L_{ka} - L_{kr} + PS + PF$$

$$\text{Case 2: } (L_{ka} - L_{kr} + PS) = 0 \qquad E = +PF \text{ or } E = -PF$$

$$\text{Case 3: } (L_{ka} - L_{kr} + PS) < 0 \qquad E = L_{ka} - L_{kr} + PS - PF$$

B - The error of indication for size measurement results from the difference between the test length (L_{ka}) and the calibrated sphere distance (L_{kr}), of the ball bar, plus the error of indication for size measurement resulting from the pertinent measurement of a short gauge block (E_E):

$$E = L_{ka} - L_{kr} + E_E$$

5.2.2 Artefacts

As suggested in ISO 10360-7 [58] and in VDI/VDE 2617 – Part 6.2:2005 [30], a ball bar with six alumina spheres has been used as reference artefact (Fig. 4.21) for the evaluation of the error of indication for size measurement. The diameter of the spheres is 10mm and the roundness error is typically less than 2 microns. The bar is made of carbon fibre composite, solid, unidirectional in longitudinal

direction, pultruded. Its expansion coefficient is $(0\pm0.5)\text{x}10^{-6}$ K^{-1}, like all uni-directional carbon fibre bars.
For the evaluation of the Probing error (Method A), an acid etched steel sphere have been used while, a short acid etched gauge block has been used for the error of indication E_E (Method B), (Fig. 5.2).

Fig. 5.2: Acid-etched gauge block.

5.2.3 Experimental investigation

An experimental investigation on procedures and artefacts proposed by the guideline VDI/VDE 2617-6.2: 2005 [30] was carried out using the newly developed laser scanner equipped with a 2D laser-triangulation sensor. The work was carried out with the aim of contributing to the standardization of verification methods and determining the applicability of the proposed artefacts and procedures, with particular focus on limitations arising in the implementation of tests, and to verify the metrological performances of the indicated laser.
The experimental investigation included the implementation of the most important tests proposed in the VDI/VDE guideline: (i) test for determination of the probing error and (ii) test for determination of the error of indication for size measurement. The results from such tests are briefly presented and discussed in the following.

5.2.4 Probing Error

In [63] the Probing error PF is equal to the range of distances of the scanned point from the centre of the Gaussian associated sphere:

$$PF = R_{\max} - R_{\min}$$

As an additional characteristic, the error in size, PS, is determined. This quantity is the difference between the measured and calibrated diameter of the sphere, respectively D_a and D_r :

$$PS = D_a - D_r$$

The tests for the determination of the probing error were performed on a calibrated sphere with nominal diameter D = 22 mm, according to VDI/VDE

2617-6.2: 2005 [30]. The investigation revealed that the values obtained for the probing error are particularly influenced by two factors:

- value of the maximum slope angle α (see Fig. 5.3), which is the cone angle of the spherical bowl containing the measured points considered for determining *PF*;
- algorithms and filtration methods employed for data elaboration.

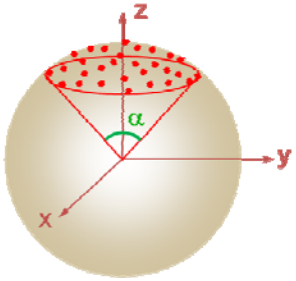

Fig. 5.3: Schematic illustration showing the cone angle α on a calibrated sphere. The red dots schematize the points measured by the probing sensor [111].

Table 5.1 illustrates the influence of the maximum slope angle α on the probing error *PF*. From this and other similar tests, it can be inferred that the probing error is strongly dependent from the angle α chosen for the test.

Angle α	Probing error, PF
20 deg.	0.028mm
40 deg.	0.034mm
60 deg.	0.042mm
80 deg.	0.053mm

Table 5.1: Variation of the probing error PF depending from the chosen value of the angle α [111].

The influence of the algorithms and filtration methods employed for data elaboration is clearly visible from the comparison of Fig. 5.6a and Fig 5.6b. Figure 5.6a shows the data obtained measuring the sphere with the laser scanner using a simple elaboration algorithm, without further filtration. Figure 5.6b, instead, show the data obtained when using a different elaboration algorithm, including linear filtering. The probing error determined in the first case is PF_1=0.18 mm, while in the second case is PF_2=0.06mm. In both cases the probing error *PS* remains well below 0.01mm.

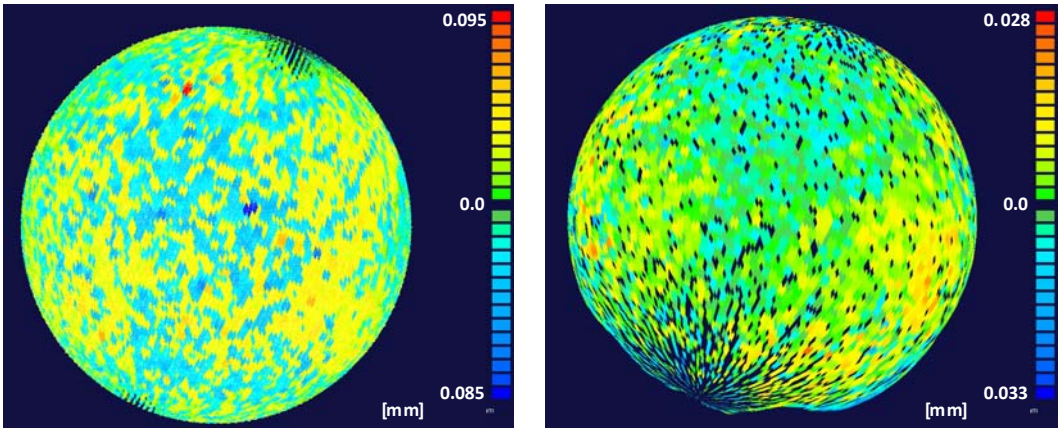

a) b)

Fig 5.4: a) Measurement data obtained using a simple elaboration algorithm, without further filtration, b) Measurement data obtained using an elaboration algorithm including linear filtering.

5.2.5 Error of indication for size measurement

The tests for the determination of the error of indication for size measurement were performed on the calibrated ball bar shown in Fig. 4.21. As suggested by the guideline, the spheres were measured using points distributed as evenly as possible over the entire surface of the spheres and as symmetrically as possible to a plane that is perpendicular to the measurement line and goes through the spheres centres. Figure 5.5 shows the results obtained in one of the tests performed on the laser scanner.

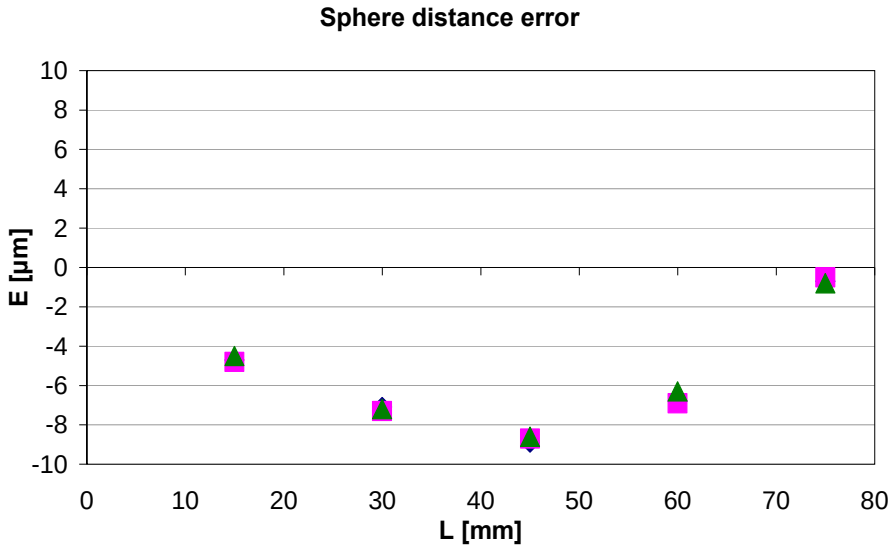

Fig. 5.5: Sphere-distance error, *SD*, determined through the measurement of five test lengths measured three times each.

This diagram reports the values of the so-called sphere-distance error, *SD*, which is defined as the difference between (1) the measured distance between two sphere centres and (2) the calibrated distance between the same two sphere centres. In the diagram, there are actually present 15 measurements, which result from the measurement of 5 lengths per 3 repetitions (as specified in VDI/VDE 2617-6.2:2005 [30] for testing one of the seven positions to be verified within the measurement volume).
As mentioned in the previous section 5.2.1, VDI/VDE 2617-6.2:2005 [30] specifies that the sphere-distance error cannot be used instead of the error of indication: the averaging effect and compensation of bias errors encountered in measurements of sphere distances shall be taken into account additionally to allow comparison with measurements of individual points on opposite faces of a gauge block. In order to ensure comparability, the VDI/VDE guideline specifies that a correction must be added to *SD*, using one of the following two methods: (A) correction obtained from the evaluation of the probing error (B), additional measurement of a short gauge block for each test length. The first method, however, is not always applicable; for example it is typically not applicable when the measuring sensor is not equipped with an articulating system.
In Fig. 5.6 and Fig. 5.8 the results related to the application of Method A and Method B are reported. Figure 5.6 shows the calculation of the error of indication for size measurement (*E*) obtained from the sphere-distance error (*SD*), given in Figure 5.5, plus the signed value of the probing error for form (*PF*) and the probing error for the size (*PS*). In Figure 5.7, the error of indication for size measurement (*E*) is obtained adding to the sphere-distance error (*SD*), the error of indication for size measurement resulting from measurement of a short gauge block (E_E). In Table 5.2 values used for the calculation are reported:

Parameter	Value
PF	60 μm
PS	1.2 μm
E_E	6.9 μm

Table 5.2: Parameters used for the evaluation of the error of indication.

Comparing the graphs reported in Fig. 5.6 and Fig. 5.7 is possible to notice that, using the verification procedure specified in VDI/VDE 2617-6.2:2005 [30], the value obtained for the error of indication for size measurement can be dominated by the influence of the probing errors. In Fig. 5.6, in fact, in which Method A has been used, the error E results much higher than in Fig. 5.7. This is due to the fact that VDI/VDE procedure asks to add the probing errors to the sphere-distance errors for taking into account a single point measurement. However, for many optical sensors actually there exist not a single point measurement and the measurements of a short gage block is not feasible without an articulated arm.

Moreover, depending on the algorithms used for points reconstruction and filtering, probing errors can be much bigger than sphere-distance errors, so that the error of indication, *E*, can be completely masked by the probing error, *PF*. In Fig. 5.8 the error of indication is calculated using method A without the probing error *PF*.

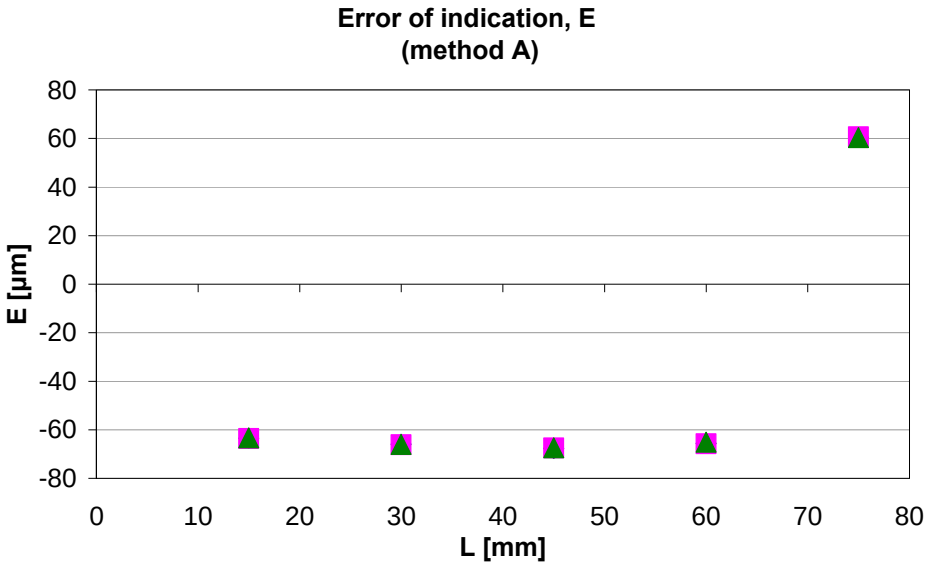

Fig. 5.6: Error of indication for size measurement, method A.

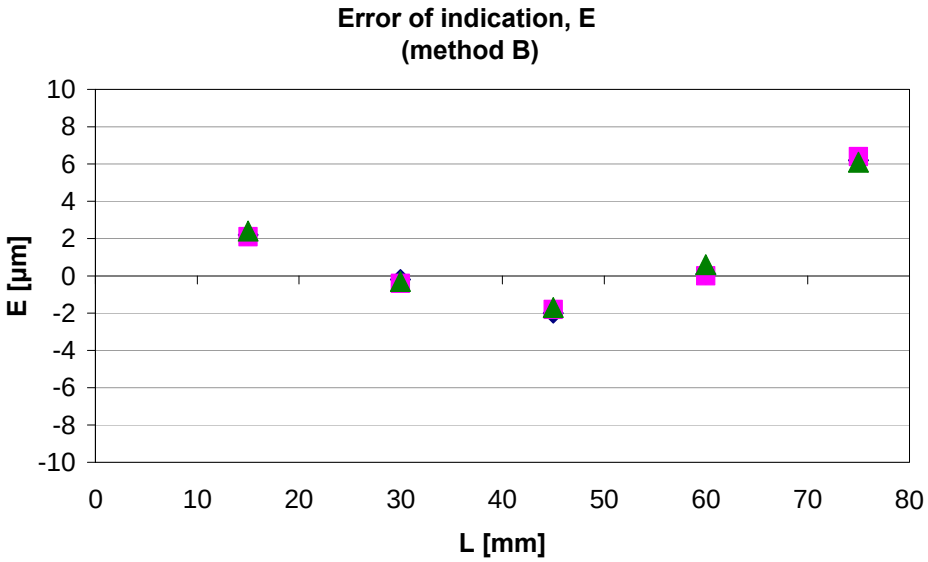

Fig. 5.7: Error of indication for size measurement, method B.

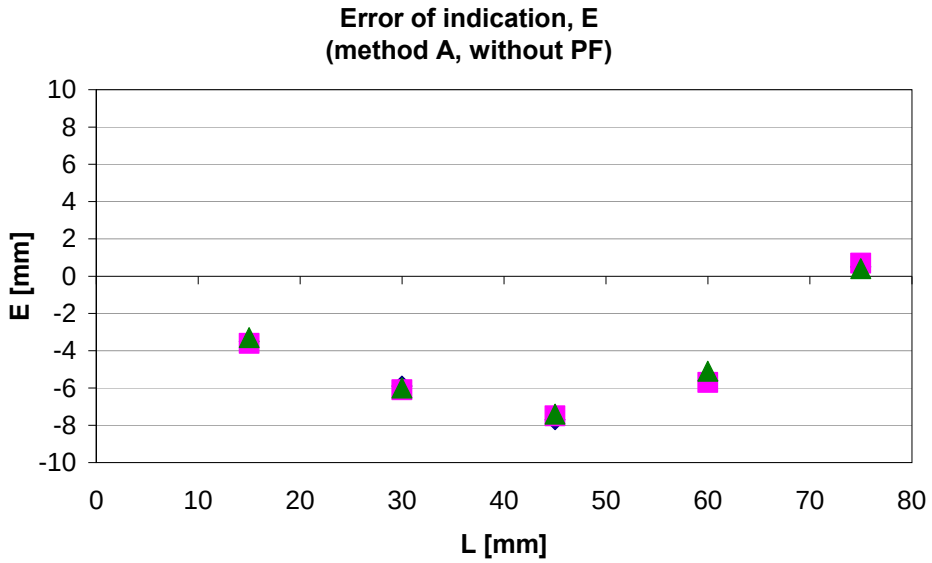

Fig. 5.8: Error of indication for size measurement, method A, without adding the Probing error *PF*.

5.3 TRACEABILITY ESTABLISHMENT

In order to achieve full traceability, metrological performances evaluation is not enough, but also task-specific uncertainty has to be stated (Chapter 3).
The task-specific measurement uncertainties were determined applying an adaptation of ISO/TS 15530-3:2004 [78]. The substitution method operates with two main elements:

- workpiece to be measured
- calibrated reference object.

These two objects must be similar within certain limits, specified by the standard. The measurement of the calibrated reference yields directly the errors associated with specific measurement task. Calibrations of this kind are only valid for objects with essentially the same geometrical form and size as the reference object used, measured in the same location, the same environmental conditions and using the same measurement strategy (See section 3.5.1). The procedure involves a sequence of measurements, performed in the same way and under the same conditions as the actual measurements. The only difference is that instead of the workpiece to be measured, the calibration object is measured. The differences between the results obtained and the known calibration values of the calibrated object are used to estimate the uncertainty of the measurements.

According to ISO/TS 15530-3:2004, the user must perform a relevant number (at least 20) of substitution measurements. When performing the measurements, basically three uncertainty contributions have to be taken into account. They are described by the following standard uncertainties:

- u_{cal}: standard uncertainty resulting from the uncertainty of the calibration of the calibrated workpiece stated in the calibration certificate;
- u_p: standard uncertainty resulting from the substitution procedure as assessed by repeated measurements (calculated as the standard deviation of the measured values);
- u_w: standard uncertainty resulting from material and manufacturing variations (due to the variation of form errors, roughness, elasticity,…).

In addition, a systematic error, b, can be considered separately.
The expanded measuring uncertainty, U, of any measured parameter is calculated from these standard uncertainties as:

$$U = k * \sqrt{u_{cal}^2 + u_p^2 + u_w^2} + |b|$$

The coverage factor, k, may be chosen as k=2 for a coverage of probability of 95%. There are two kinds of uncertainties: type A and type B. Type A uncertainties are those that are evaluated by statistical means, and type B are those that are estimated by 'expert' opinion. The uncertainty of measurement procedure (u_p) is evaluated with method A, the uncertainty of calibrated workpiece (u_{cal}) is evaluate with method B, and the uncertainty from workpiece influences (u_w) can be estimated with method A or B (see section 3.5.1). Because of the experimental approach, the substitution method is simple to perform, and it provides realistic statements of measurement uncertainties. However this method has also some limitations. They can be summarized as: the availability of artefacts with sufficiently defined geometrical characteristics, stability, reasonable costs, and the possibility of being calibrated with sufficiently small uncertainty.
In order to determine the measuring uncertainty for typical production parts, two different parts were selected: one metallic and one plastic part (both shown in Fig. 5.9). For both parts it was decided to measure the diameter and the roundness of a cylindrical feature.

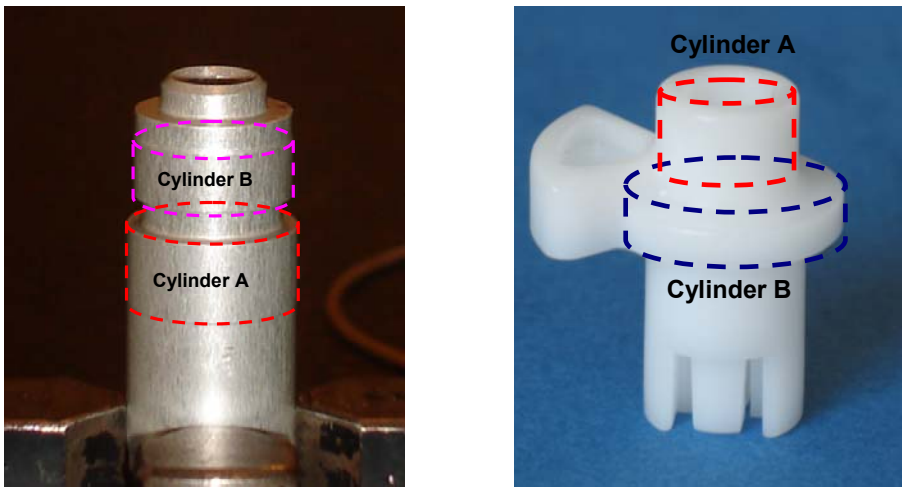

a) b)

Fig. 5.9: workpiece selected for uncertainty calculation using the substitution method.

In our case the workpiece to be measured and the calibrated reference object are the same object, so that the uncertainty from workpiece influences (u_w) is zero.
Both the workpiece have been calibrated using a high accuracy contact CMM; results related to the uncertainty calculation are reported in Table 5.3 and Table 5.4 for both the workpieces.

	Cylinder A		Cylinder B	
	Diameter	Form error	Diameter	Form error
K	2	2	2	2
ucal	2.2	2.5	2.2	2.5
Up	2.4	3.7	1.8	4.6
Uw	0	0	0	0
B	0.7	52.1	-1.5	57.5
U	**7.2**	**61.0**	**7.2**	**67.9**

Table 5.3: Measuring uncertainty for metallic part (results expressed in µm).

	Cylinder A		Cylinder B	
	Diameter	Form error	Diameter	Form error
K	2	2	2	2
ucal	2.2	2.5	2.2	2.5
Up	12.4	96.3	16.6	315.3
Uw	0	0	0	0
B	-203.3	556.5	-184.0	745.9
U	**228.5**	**749.1**	**217.4**	**1376.5**

Table 5.4: Measuring uncertainty for plastic part (results expressed in µm).

The values given in the tables reveal that for the laser scanner under testing the measuring uncertainties are very different depending from the type of measurement and the workpiece material.
In Table 5.3 the strong difference between geometrical and dimensional measurements could approximately be inferred also from the difference between the characteristics *SDE* and *PF*: for the nominal distance close to the workpice diameter, in fact, the laser scanner has *SDE* =4µm and *PF*=60µm. This example confirms that keeping the probing error and the sphere-distance error distinct could be more significant, rather than putting all together in only one characteristic.
It shall be noted that the measurement uncertainties obtained for the measurement of the plastic part is much bigger than that obtained for the metallic part; this is due to the translucency of the plastic material. This translucency causes the penetration of the laser below the external surface until a certain depth, so that the light scatters inside the material and the measuring system actually detects laser reflections sourcing from inside the workpiece.

5.4 SOFTWARE EVALUATION

The software package performs metrological operations according to ISO GPS standards. To achieve the goal of a simple user interface, the developed application uses right-click popup menus (context-sensitive). The menu presented contains only items that are valid choices for the CAD element that the user right-clicked on. There are relatively few icons permanently visible on the screen. The symbols in the context menu are GD&T standard symbols. An example is shown in Figure 5.10.

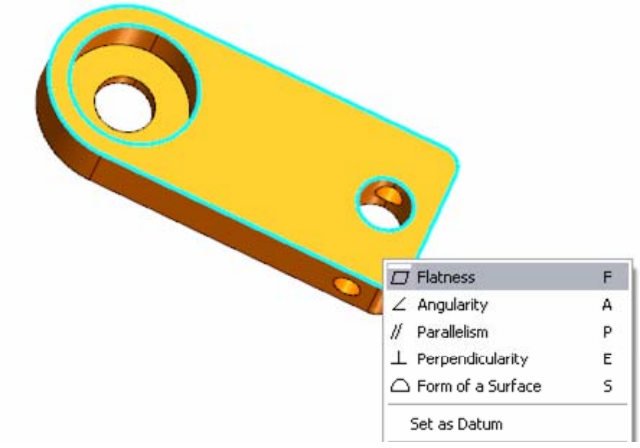

Fig. 5.10: Context menu presented when clicking on a plane within the CAD model. Only applicable GPS measurements are displayed [111].

Besides the formal GPS measurements, the software also supports the traditional dimension measurements (point-point distance and diameter, plane-point distance, etc). Furthermore, there are qualitative/visual analysis functions, like cross sections, as shown in Figure 5.11.

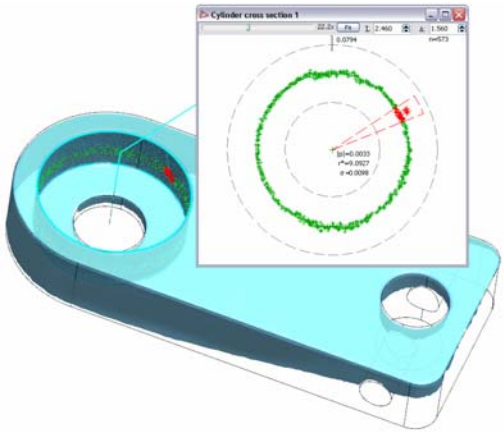

Fig. 5.11: Cylinder cross section and evaluation of roundness. The band of green points highlighted in the 3D scene is that plotted in the 2D plot [111].

The developed metrological software has passed the accuracy certification test performed by PTB (German National Metrological Institute). Such test verifies the accuracy of calculations performed by the software on simple geometries (e.g. calculation of the diameter of a spherical point-cloud) [118]. However, the developed software covers all measurements and tolerances defined within the GPS system, and not only basic tolerances on simple geometries. For this reason, the software was additionally tested in order to verify that all the tolerances that the software can elaborate are correctly evaluated according to ISO 1101 [119] and other ISO standards. The additional tests were performed using artificial point-clouds of known coordinates: for each geometrical tolerance to be investigated a simple 3D model with a known deviation (example for flatness is reported in Fig. 5.12) has been constructed and compared with a reference model. The results of the comparison and graphic output given by the software have been analyzed taking into account the related standards for GD&T calculation.

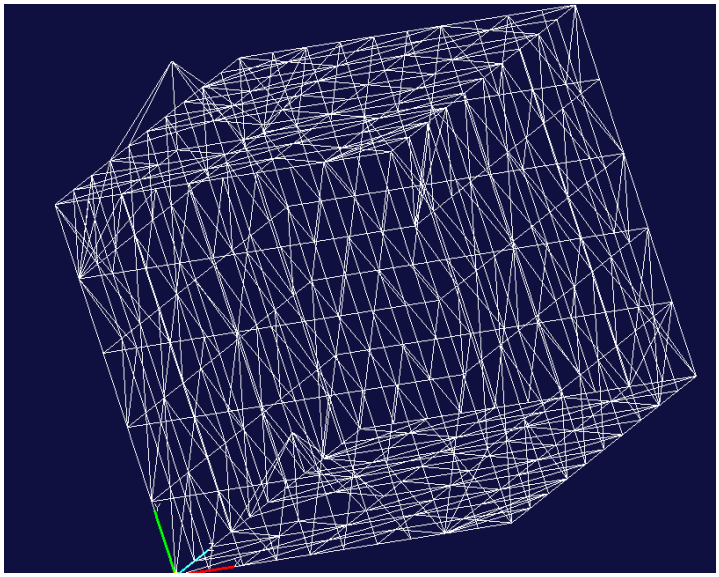

Fig. 5.12: Stl model used for the flatness evaluation.

In Fig. 5.13 the flatness tolerance calculated with the new developed software is shown with the related graphic visualization. In this figure it is possible to notice that there is a difference between the nominal value of the deviation (1 mm) and the software output (1.008mm). Similar errors were found for the verification of other tolerances, such as in the case of roundness, coaxiality and parallelism evaluation [120]. In those cases, results of investigation have been used to improve software algorithms.

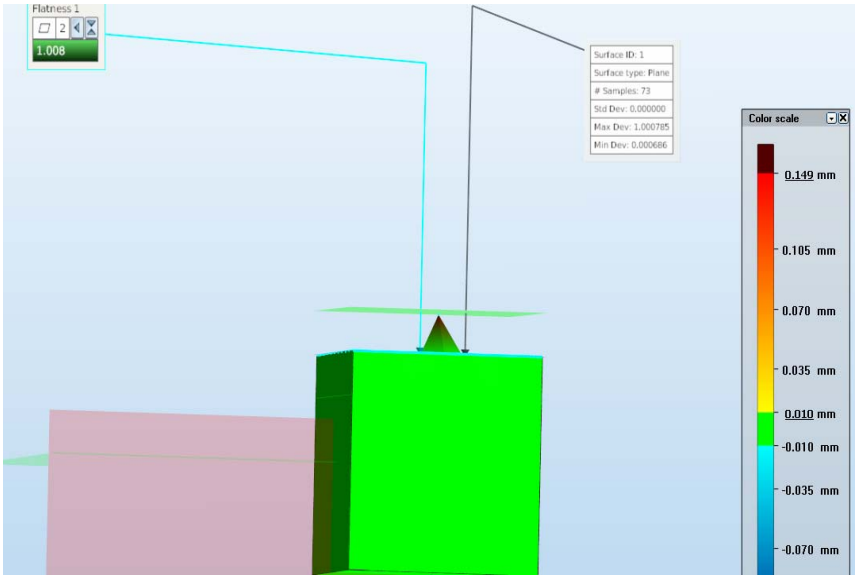

Fig. 5.13: Flatness evaluation.

5.5 CONCLUSIONS

In this Chapter, the main results of the European Co-operative Research Project 'OP3MET' have been presented. During the Project, an innovative optical measuring system for automated inspection of dimensional and geometrical tolerances, including freeform surfaces, has been developed.

The contribution of the author has concerned metrological verification and traceability of the newly developed system. In particular, in this Chapter, an experimental investigation was presented on procedures and artefacts for testing metrological performances of coordinate measuring systems equipped with optical distance sensors. Particular attention was given to the guideline VDI/VDE 2617-6.2: 2005 [30]. On the basis of specific experimental results on a laser scanner, the main problems arising in the implementation of testing procedures were analyzed. In particular it was demonstrated that, when using ball bars, the error of indication for size measurement, E, may be completely masked by the probing error, PF. Furthermore the value of the probing error is extremely influenced by the algorithms and filtration methods implemented in the measuring system.

Traceability was established and the measurement uncertainty was determined for specific tasks by means of an adaptation the ISO 15530-3: 2004 [78] procedure. Generally, geometrical measurements, such as roundness, presented higher uncertainty, due to a higher influence of the probing error.

Also the influence of the object material has been evaluated: due to the translucency of the plastic material, in fact, the measurement uncertainties obtained for the measurement of the plastic part was much bigger than that obtained for the metallic part. This translucency causes the penetration of the laser below the external surface until a certain depth, so that the light scatters inside the material and the measuring system actually detects laser reflections sourcing from inside the workpiece.

Special attention has been paid to the evaluation of the newly developed software. Even if metrological software are tested and certificated, such tests verify only the accuracy of calculations performed on simple and well defined geometries. In this Chapter, a method to test metrological software by mean of synthetic data has been described. The proposed method has been used to improve and correct the new software.

Chapter 6

Optical sensor integration: an application

An higher integration of the measuring systems into the production line can lead to increase efficiency of manufacturing processes by shorter response time. The earlier an error in the production can be detected, in fact, the lower are the consequences. The development of new and more accurate optical measuring sensors in the last few years has lead to new applications, more and more oriented to real time inspection of workpieces during their production. In this Chapter an industrial application related to the integration of optical sensors for in-line measurements is reported. The activities described in this Chapter have been performed by the author during a 3 months period at NTB-Interstate University of Applied Sciences of Technology, Buchs, Switzerland. The main task of the work was the development of a software tool for the in-line measurement of roundness of workpiece obtained by circular grinding.

6.1 SYSTEM DESCRIPTION

Grinding process, and in general abrasive processes, are considered to be highly complex to be modelled and, as they are non-stationary processes subject to variation along the time, the only way to assure quality in production is a constant monitoring of the process itself. For examples, common disturbances that affect cylindrical grinding machines (CGM) are tool wear, temperature drifts, path control deviations, etc. This leads to loss of productivity and to dimensional deviations in the workpiece. A variety of monitoring tools can help to improve the grinding process [121]. In order to allow dimensional control of workpieces during manufacturing, contact probes have been integrated in the past into machine tool giving good results but shown also high limitations such as:

- tip wear;
- contact forces cannot be neglected;
- sensitivity to machine dynamics resulting in low measurement speed;
- incapacity to measure non circular profiles.

Otherwise, the opportunity to use stable and robust non contact sensors for process control, would be extend the employment of CGMs also for manufacturing and control of non cylindrical parts. Starting from this consideration, at NTB a new optical sensor system was integrated into such a grinding machine, making it possible to take measurements for quality assurance, optimisation of the grinding process and reduction of setting-up and machining time [122].
As described in [122] the new developed CGM integrates a chromatic sensor (see Section 2.5.1.2) able to measure also in hostile environments and capable of investigate different kind of materials (fig. 6.1). The distance measurement sensor is arranged on the wheel head in the grinding machine (fig. 6.2). This can automatically be put in place for measuring, as an alternative to the wheel head; otherwise it is located in the rear portion of the cabin.

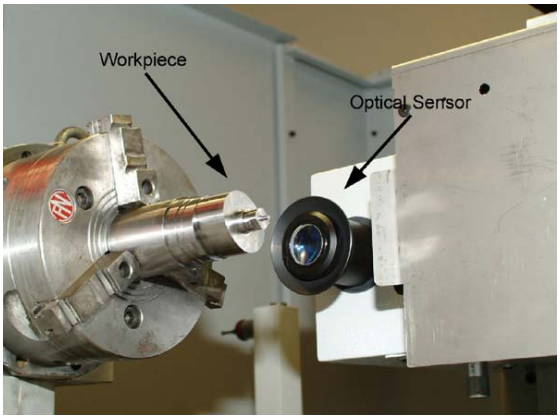

Fig 6.1: Cylindrical grinding machine with integrated optical sensor and workpiece [122].

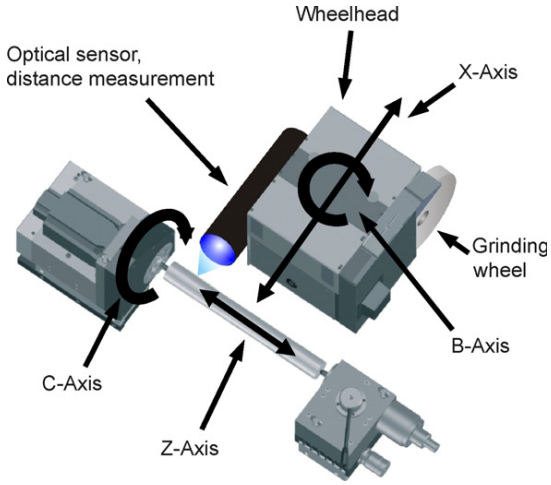

Fig 6.2: Arrangement of the optical sensor on the wheel head in the CGM [122].

For measurement of roundness, the sensor is kept fixed and the workpiece is turned by the spindle of the machine. In this way the chromatic sensors is able to record the profile deviation within the measuring range. Synchronisation of the turning axis (C-axis in fig. 6.2) with the sensor acquisition allow to construct the profile of the workpiece in polar coordinates.

6.2 PROBLEM IDENTIFICATION

As described in the previous paragraph, the chromatic sensor integrated into the CGM is able to measure the form error of the workpiece evaluating the range of the measured points along the X-axis (see Fig. 6.2). In this way the result of the measurement is the addiction of different contributors: the profile of the object itself, its eccentricity respect to the turning axis, the eccentricity of the turning axis, the misalignment of the sensor respect to the turning axis, etc..
Furthermore, as shown in Section 5.5, the result of a measurement is due not only to the measurement system used for the acquisition but it depends in large part to the software tools and algorithms employed for the calculation.
For this reason, after the chromatic sensor was integrated into the new prototype machine, the next part of the Project has regarded the development of a metrological software able to give measuring results in agreement with the reference standards. In this direction the contribution of the author of this Thesis has regarded the development and the validation of a software tool for in-line measurement of roundness and correction of systematic errors.
In particular the following activities have been performed by the author:

- Errors modelling and simulation of their influence on measurement data;
- Development of algorithms for roundness calculation as requested in ISO 4291:1995 [123];
- Development of algorithms for data filtering as indicated in ISO/TS 12181-2:2003 [124];
- Development of algorithms for errors correction and compensation;
- Validation of the developed software by comparison with others metrological software;
- Measurement on real workpieces.

6.3 ERRORS MODELLING

As seen before, the output of the chromatic sensor is a profile where the actual shape of the workpiece is distorted by the systematic errors of the measurement system. In order to measure the roundness of a grinded part, it has to be possible to separate and compensate the effect of the external deviations from the roundness itself. For this reason the main sources of error have been studied and modelled. Then, this mathematic model have been used to simulate the measuring process and develop a “Generator” of synthetic data.

In the following points the main error sources which have been considered are explained.

(i) Eccentricity

The eccentricity between the Machine Coordinate System (MCS) and the actual rotation axis of the workpiece causes an error in the roundness measurements as shown in Fig. 6.3.

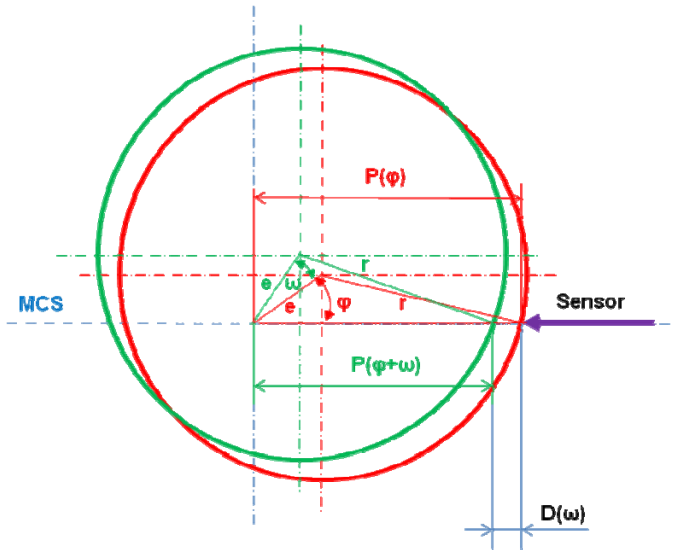

Fig 6.3: effect of eccentricity.

At the starting point, the workpiece (red profile) has an eccentricity of amplitude e and phase φ respect to the MCS. The sensor output is null in this position. After a rotation of ω (green profile) the sensor measure a deviation D(ω) that can be calculated in this way:

$$D'(\omega) = P(\varphi + \omega) - P(\varphi) =$$

$$= [e \cdot \cos(\varphi + \omega) + \sqrt{(r^2 - (e \cdot \sin(\varphi + \omega))^2)}] +$$

$$- [e \cdot \cos(\varphi) + \sqrt{(r^2 - (e \cdot \sin(\varphi))^2}]$$

The reported formula can be used for the generation of data points in case of absence of displacement between sensor and MCS (see point ii). This model takes only the eccentricity of the work piece into account. The path of the centre of the work piece is considered as a perfect circle, the deviation in the spindle motion is neglected. Eccentricity may be due to also to a deviation between work piece axis and the turning axis (fig. 6.4). In this case the amplitude of eccentricity is not constant in the different section of the work piece. By evaluating the eccentricity

at different z-positions, the deviation of the work piece axis and the turning axis can be calculated and corrected.

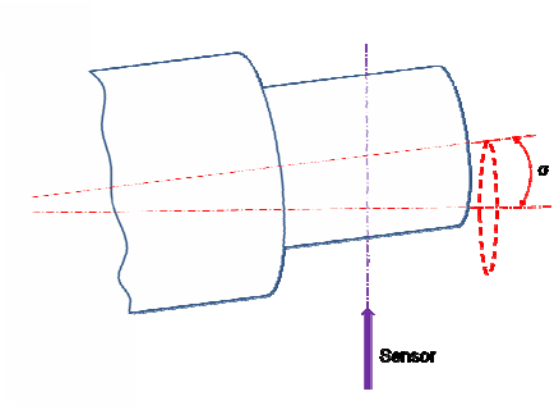

Fig. 6.4: deviation between work piece axis and turning axis.

(ii) Sensor misalignment

The wrong relative position between the measuring sensor and the Machine Coordinate System (MCS) can generate an error in the measurement of roundness that is correlated with the eccentricity and the roundness of the workpiece itself. If the eccentricity is null and the workpiece's profile is a perfect circle, the sensor measures always the same distance and no error is introduced. In Fig. 6.5 a model for the evaluation of the correlated effect of eccentricity and sensor misalignment is shown.

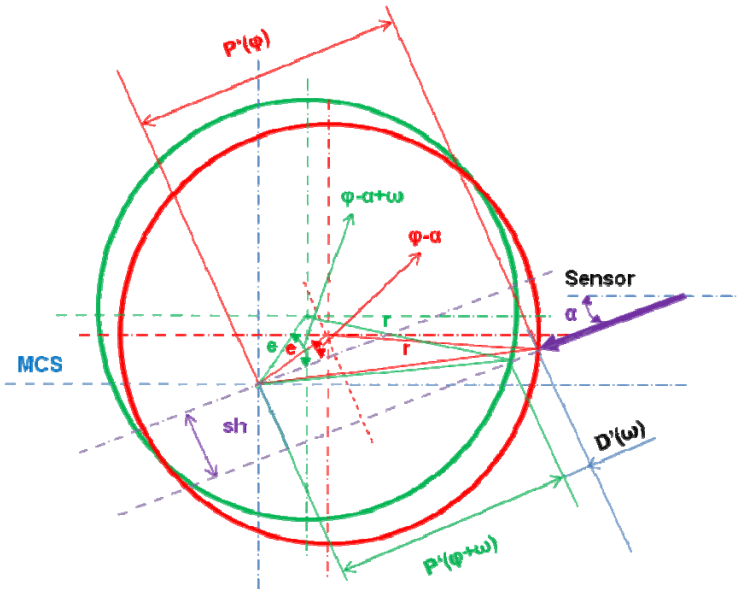

Fig. 6.5: effect of sensor misalignment and eccentricity.

At the starting point, the workpiece has an eccentricity of amplitude *e* and phase φ, while the sensor is tilted with an angle α related to the MCS. Also an offset *sh* between sensor and MCS is present.
The sensor output is null in this position. After a rotation of (ω) the sensor measure a deviation D'(ω) that can be calculated as:

$$D'(\omega) = P(\varphi + \omega) - P(\varphi) =$$
$$= [e \cdot \cos(\varphi + \omega - \alpha) + \sqrt{(r^2 - (e \cdot \sin(\varphi + \omega - \alpha) + sh)^2)}] +$$
$$- [e \cdot \cos(\varphi - \alpha) + \sqrt{(r^2 - (e \cdot \sin(\varphi - \alpha) + sh)^2}]$$

Another form of sensor displacement is the angle between the sensor and the turning axis of the workpiece (see Fig. 6.6). This displacement has the effect to amplify the amplitude of the measured signal: also this aspect has been taken into account for the simulation.

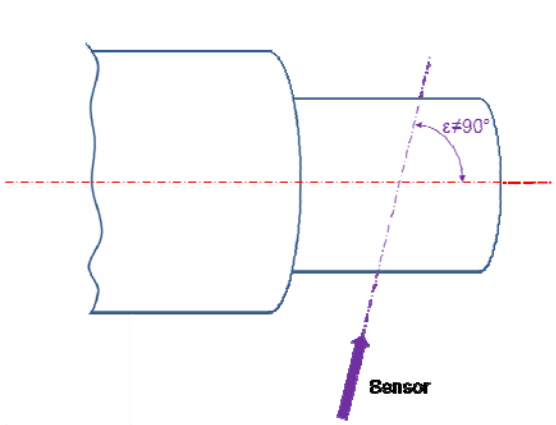

Fig. 6.6: Sensor misalignment in relation to the turning axis.

(iii) Noise

The measured signal is composed by harmonics with low frequency and harmonics with high frequency. Harmonics with low frequency are correlated with diameter, eccentricity and roundness while high frequency harmonics are mainly due to sensor noise, vibrations and other not systematic errors. For the evaluation of roundness, the effect of high frequency harmonics has to be taken into account. After the elimination of the eccentricity, the high frequency harmonics could be filtered using a proper filter (Gauss, Tschebyscheff, 2RC).

(iv) Environment conditions

The temperature of the environment could cause a drift in the sensor position. Generally the effect is the same as in point (ii).

(v) Sensor calibration

The optical sensor has to be calibrated before measuring a workpiece, in order to give a correct output. For this an adequate calibration procedure should be used, in order to obtain the calibration factor for data correction. In Section 6.4.4 a procedure and the relative artefact for calibration will be introduced.

6.3.1 Simulation and data generation

Based on the error sources considered in Section 6.2.1, a "Generator" of synthetic data was developed (Fig. 6.7). Aim of the Generator was the simulation of the measuring process with its main influences, in order to obtained data close to real situation without working directly on the machine prototype.

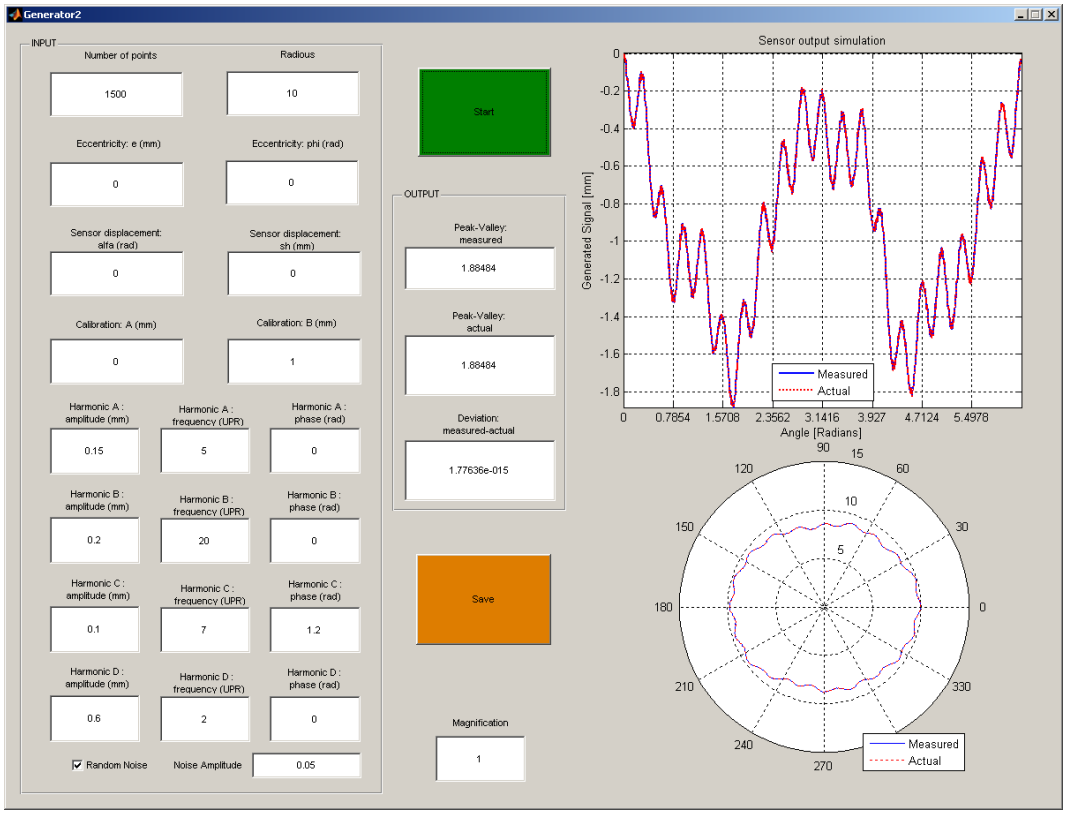

Fig. 6.7: Generator of synthetic data.

The Generator was programmed using MATLAB (Version: 2008a) and compiled in an executable .exe-file, to have the opportunity to run the program on different computers. After having set up the most important parameters for the measuring process in the Graphical User Interface the pro-gram calculates the "synthetic" measuring data, considering these parameters and gives as output two .txt-file. The first one is related to the virtual workpiece profile while the second is related the same profile as it results with the addiction of the error sources described before.
In fig. 6.8 an example of Generator output is reported, where the red profile represents the real profile of the workpiece and the blue one the way it appears with an eccentricity of 0.5mm. The same profile are reported in the polar plot shown in Fig. 6.9.

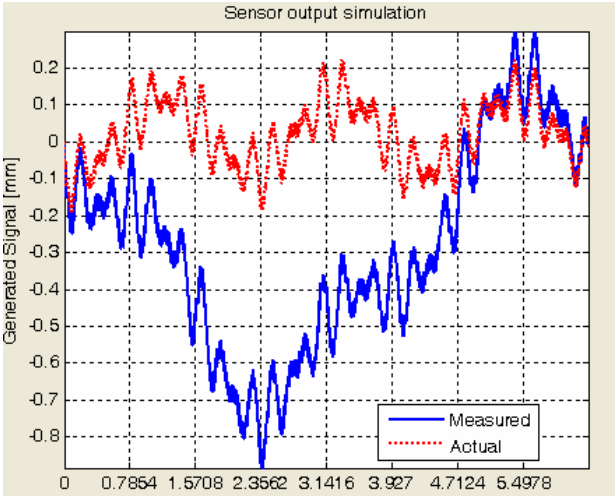

Fig. 6.8: Example of generated signals.

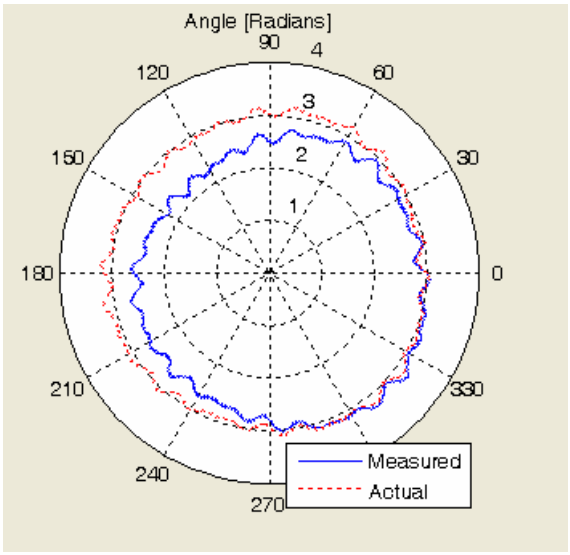

Fig. 6.9: Polar plot of the generated signals.

Profiles generated in this way have been used as input for the evaluation of the Software Module presented in the next section.

6.4 SOFTWARE DEVELOPMENT FOR IN-LINE ROUNDNESS MEASUREMENT

As main result of the activities performed within the Project, a Software tool (SW-Module) has been created, able to calculate roundness as required by reference standards and correct systematic errors (in Fig. 6.10).

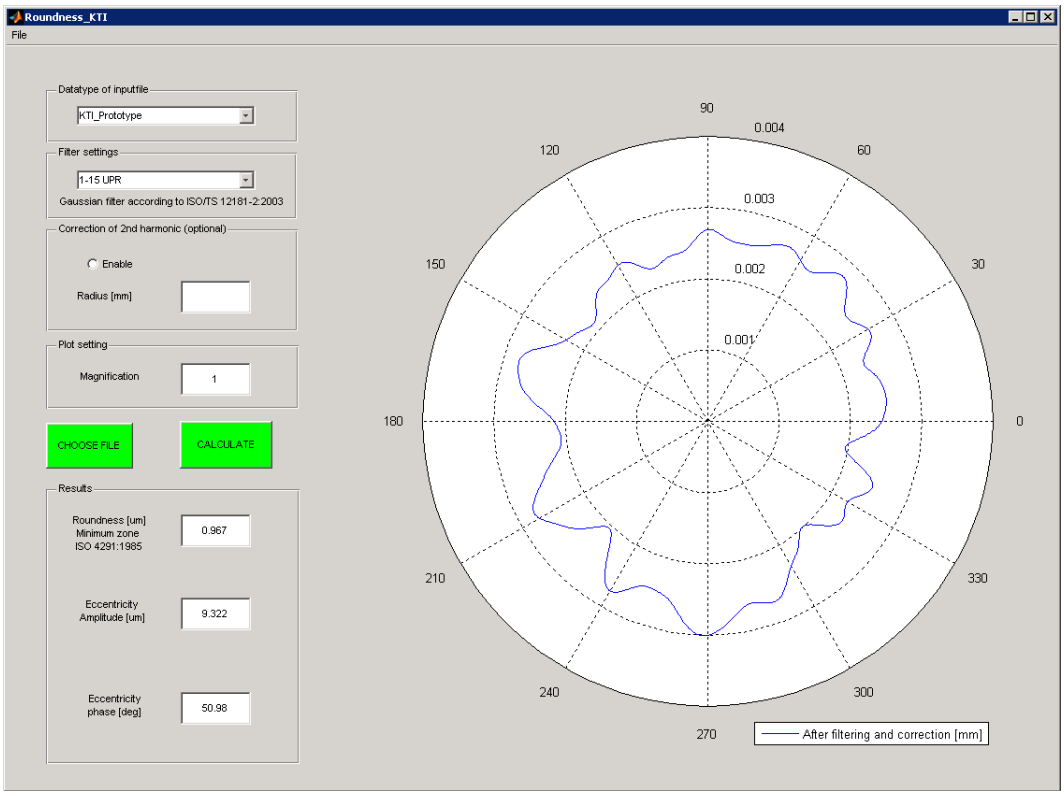

Fig.6.10: Graphical User Interface of the new developed SW-Module.

Also this module has been programmed in MATLAB (Version 2008a) and compiled as a .dll-File, for use with other programs. The function is able to calculate out of raw data, the roundness as well as the amplitude and the phase of the eccentricity. In addition, Gaussian filtering can be used to smooth the effect of high frequencies signals.
To have an advantage in measuring work pieces with deviations by round contour, such us grooves, flats, etc., the software is able to find automatically if there are missing parts in the raw data and fills the missing part with regression points.

In the next subparagraphs a description of the developed software and related algorithms is reported.

6.4.1 Correction of eccentricity

The effect of the eccentricity between workpiece and MCS on measured profile can be deleted using the frequency analysis of the signal.
The eccentricity causes as a major effect a first harmonic oscillation, that is visible in the Fourier space of the measured signal. The amplitude of this first harmonic is equal to the eccentricity itself [125], [126] so transforming the signal using the Fast Fourier Transformation *(FFT)* the amplitude and phase of the eccentricity can be found and corrected. Nevertheless, it was found that the eccentricity has also an influence on the second order harmonic, while the effect on higher frequencies than the second harmonic, can be neglected [127].
The influence of the eccentricity on the second harmonic can only be corrected numerically, by the knowledge of the eccentricity itself (obtained by the first harmonic) and the radius of the workpiece. More details related to algorithms used for eccentricity correction are reported in [128].
To evaluate the power of the eccentricity correction, simulations have been made using synthetic data obtained with the Generator described in Section 6.3. The results of this simulation for a workpiece with a nominal radius of 5 mm are shown in Fig. 6.11, where the deviation is calculated between the roundness of the actual profile and how it appears after the eccentricity correction.

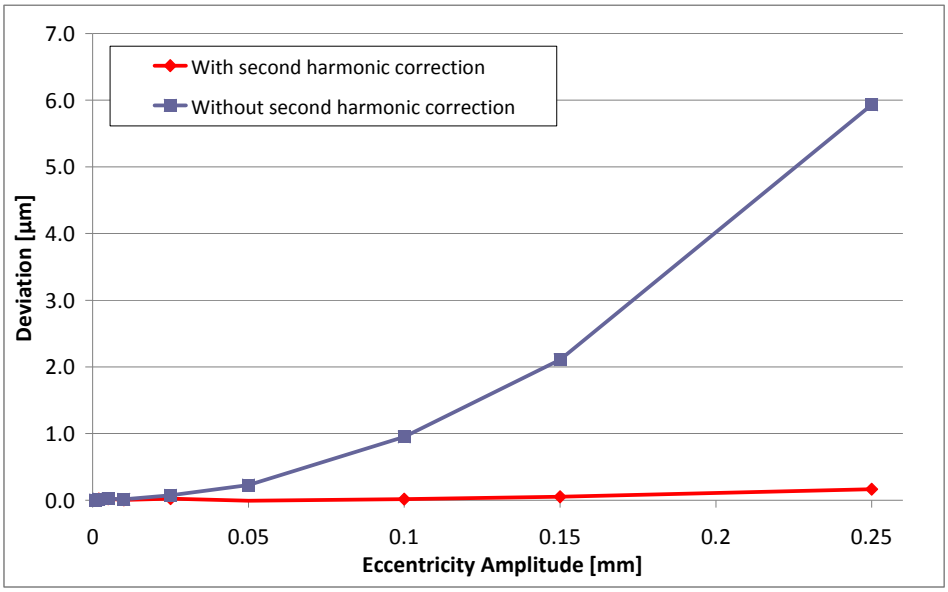

Fig. 6.11: Roundness deviation after eccentricity correction.

The Graph shows as very good results can be obtained for big values of eccentricity using the correction of the second harmonic (deviation within 0.1μm), while neglecting this correction good results are present only for small eccentricity (less than 25 μm).

6.4.2 Roundness calculation

According to the Standard ISO 4291:1985 [123] roundness is calculated following the Tschebyscheff method (minimum zone).
The minimum zone element encloses all points of the profile between two concentric circles (Fig. 6.12). The minimum zone is calculated in a way, the deviation between the two concentric circles becomes the minimum possible deviation. The Tschebyscheff substitute element is a circle directly in the middle of the minimum zone (minimum zone circle).

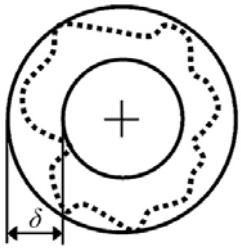

Fig. 6.12: minimum zone.

The following algorithm has been implemented in order to calculate roundness [129]:

(i) An initial solution for the minimum zone is calculated, which approach to the final result. This enables to find a minimum close or equal to the global minimum. For a circle defined by (3), the distance *di* of every point can be calculated by (4):

$$R^2 = (x_i - X_m)^2 + (y_i - Y_m)^2 \tag{3}$$

$$d_i = \sqrt{(x_i - X_m)^2 + (y_i - Y_m)^2} \tag{4}$$

In Eq. 3 and Eq. 4, R is the circle radius, X_m, Y_m are coordinates of circle centre point and (x_i, y_i) are the coordinates of the i_{th} measured point.
The solution of Eq. 5, where (x_1, y_1), (x_2, y_2), (x_3, y_3) are three randomly chosen measured points, leads to an initial solution respect to the three parameters A, B, C (Eq.6).

$$\begin{bmatrix} 1 & -x_1 & -y_1 \\ 1 & -x_2 & -y_2 \\ 1 & -x_3 & -y_3 \end{bmatrix} \cdot \begin{bmatrix} A \\ B \\ C \end{bmatrix} = \begin{bmatrix} -(x_1^2 + y_1^2) \\ -(x_2^2 + y_2^2) \\ -(x_3^2 + y_3^2) \end{bmatrix} \tag{5}$$

$$\begin{bmatrix} A \\ B \\ C \end{bmatrix} = \begin{bmatrix} X_m^2 + Y_m^2 - R^2 \\ 2 * X_m \\ 2 * Y_m \end{bmatrix} \tag{6}$$

(ii) The distance between the centre point of the minimum zone circle (initial solution) and each point can be calculated as described in Eq. 7. By searching the minimum of this distance, it is possible to find the radius of the inner circle (R_i), (Eq. 8) of the minimum zone, by searching the maximum it is possible to find the radius of the outer circle (R_o), (Eq. 9). The difference between R_O and R_I gives the solution for the minimum zone roundness (initial solution).

$$dist = \sqrt{(x_i - X_m)^2 + (y_i - Y_m)^2} \tag{7}$$

$$R_i = \min\{dist\} \tag{8}$$

$$Ro = \max\{dist\} \tag{9}$$

With adequate algorithms, it is possible to search for the minimum of this difference. To find the global minimum, the procedure has to be repeated with different starting points. More details about algorithms and codes are in [128]

6.4.3 Gaussian filtering

The profile of a circular workpiece is composed by three different parts:

- Roughness;
- Waviness;
- Roundness.

These three contribution are characterized by different wavelength and frequency. In order to separate and measure only the roundness of a workpiece, the profile as to be filtered out.
In the new developed software tool, the Gaussian filtering is implemented according to the standard ISO/TS 12281-2:2003 [124]. As input for filtering the cut-

off frequency is asked by the software; the filtration is done oppressing the cut-off frequency with 50% and reducing the higher frequencies as shown in Fig. 6.11.

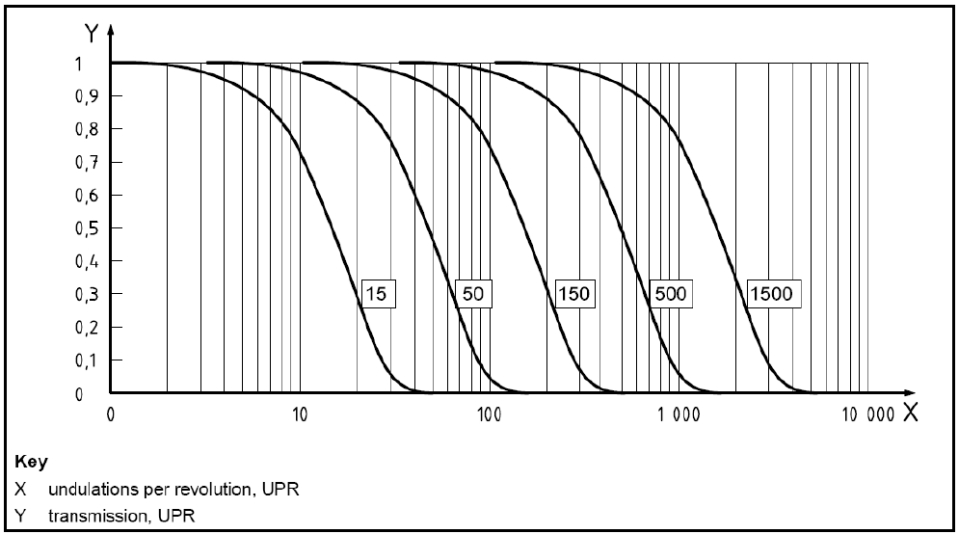

Fig. 6.13: phase correct long wave-pass filter, transmitting characteristic [124].

The attenuation function is given by:

$$\frac{a_1}{a_0} = e^{-\pi(\frac{\alpha * f}{f_c})^2} \tag{1}$$

where

$$\alpha = \sqrt{\frac{\ln(2)}{\pi}} = 0.4697 \tag{2}$$

a_0= amplitude of sine wave undulation before filtering
a_1= amplitude of sine wave undulation after filtering
f_c=cut-off frequency (in UPR)of the long wave-pass filter
f= frequency (in UPR) of the sine-wave

6.4.4 Software validation

In order to validate the new developed SW-Module, a series a test have been performed, involving both comparison with other metrological software on synthetic data and real measurements. In the following parts, the most important results of the tests are reported and discussed.

(i) Comparison between "SW-module" and Quindos

In a first step, 45 different profiles have been generated with the Generator introduced in Section 6.3.1, simulating different roundness deviation (from 340µm to 10µm). These profiles were analysed with the SW-module for the roundness calculation and also with the metrological software Quindos produced by Leitz-Metrology [143]. Objective of the comparison was the evaluation of the algorithms used for roundness calculation and filtering without taking account the eccentricity correction.
In Table 6.1, only a few of the results are shown, where is possible to see as the two software are in good agreement as a maximum deviation of 0.03 µm have been found.

	Roundness Tschebyscheff [µm] : SW-module					Roundness Tschebyscheff [µm] : Quindos				
	Profiles without missing parts									
	15UPR	50UPR	150UPR	500UPR	Without	15UPR	50UPR	150UPR	500UPR	Without
Nr. 1	265.49	307.23	333.82	338.22	339.05	265.52	307.24	333.84	338.24	339.09
Nr. 5	7.02	8.43	9.69	11.47	12.11	7.02	8.43	9.69	11.45	12.11
Nr. 10	7.03	8.41	9.53	11.16	11.73	7.03	8.40	9.53	11.16	11.73
Nr. 15	7.02	8.47	9.49	10.94	11.43	7.01	8.46	9.48	10.94	11.43
Nr. 20	7.03	8.55	9.65	11.35	12.60	7.03	8.55	9.65	11.37	12.60
Nr. 25	7.00	8.46	9.50	11.09	11.72	6.99	8.45	9.50	11.09	11.72
Nr. 30	7.02	8.47	9.53	10.87	11.21	7.01	8.47	9.53	10.87	11.21
Nr. 35	7.07	8.60	9.84	11.32	12.18	7.07	8.60	9.84	11.32	12.17
Nr. 40	7.05	8.51	9.66	11.17	11.85	7.04	8.51	9.66	11.17	11.84
Nr. 45	7.02	8.47	9.51	10.96	11.48	7.01	8.46	9.51	10.96	11.48

Table 6.1: comparison between SW-Module and Quindos.

(ii) Comparison between "SW-Module" and Talyrond 300

The second step for the validation of the SW-Module has regarded the test of algorithms used for eccentricity correction. To do that, a series of real measurements were taken on an existing artefact (see Fig. 6.14) using the dedicated roundness system Talyrond 300 [131] produced by the company Taylor Hobson (Fig. 6.15)

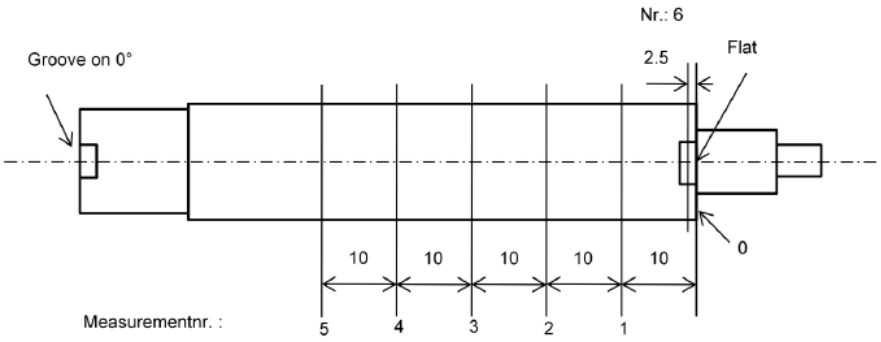

Fig. 6.14: artefact used for the measurements and numbered profiles.

Fig. 6.15: Talyrond 300.

Then results between the SW-Module and the roundness system have been compared; the most important ones are summarized in Table 6.2.
Roundness has been calculated using the Minimum Zone principle and using the following Gaussian filter: 15 UPR, 50 UPR, 150 UPR, 500 UPR and without filter.
In addition a comparison based on raw data with missing parts has been made.
For circular profiles with no missing part, the deviation in all the comparison was in maximum 0.01μm while for the profiles with missing parts, the maximum error was below 0.1μm. Considering these results, the algorithms of the SW-module for the correction of eccentricity and the roundness calculation was considered as correct. In Fig. 6.16 and 6.17 a comparison of roundness plot between the two software is reported for a profile with a missing part.

Profiles without missing parts					
Profile	Filter	Roundness SW-module	Roundness Talyrond 300		Difference [µm]
1	15	0.23	0.22		0.01
	150	0.80	0.80		0.00
	without	1.03	1.03		0.00
2	15	0.24	0.23		0.01
	150	0.63	0.63		0
	without	0.86	0.86		0
3	15	0.22	0.21		0.01
	150	0.69	0.69		0
	without	1.03	1.03		0
4	15	0.35	0.35		0
	150	0.74	0.74		0
	without	1.16	1.17		-0.01
5	15	0.44	0.44		0
	150	0.78	0.78		0
	without	1.08	1.07		0.01
				Max [µm]:	0.01

Profiles with missing parts					
Profile	Filter	Roundness SW-module	Roundness Talyrond 300		Difference [µm]
6	15	0.64	0.54		0.10
	50	0.97	0.92		0.05
	150	1.17	1.15		0.02
	500	1.32	1.32		0.00
	without	1.41	1.41		0.00
				Max [µm]:	0.10

Table 6.2: comparison between SW-Module and Talyrond 300.

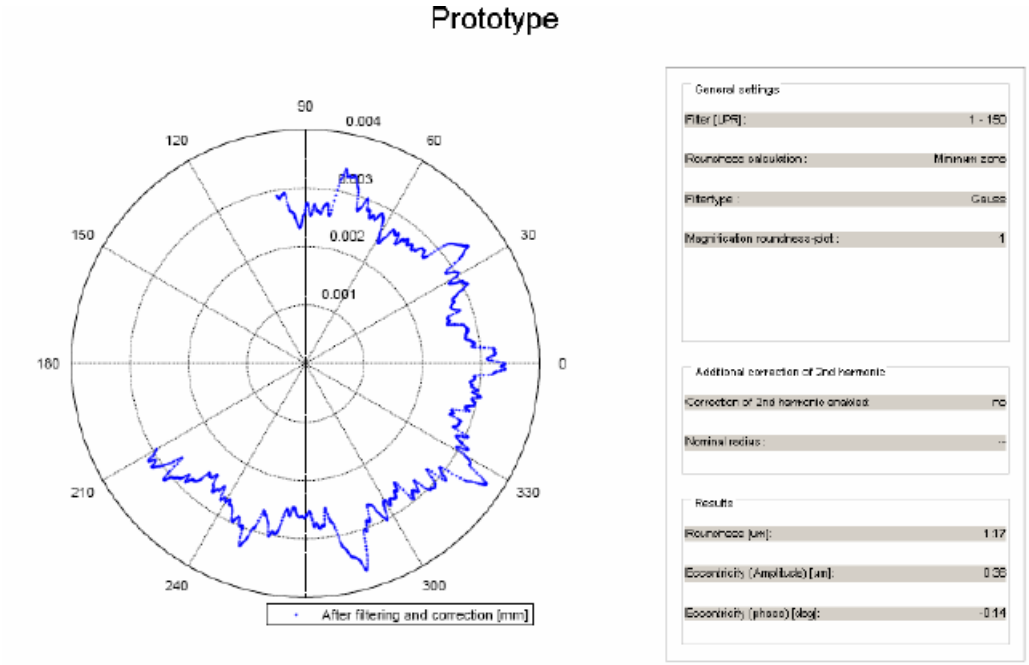

Fig. 6.16: Roundness profile as it appears in SW-Module.

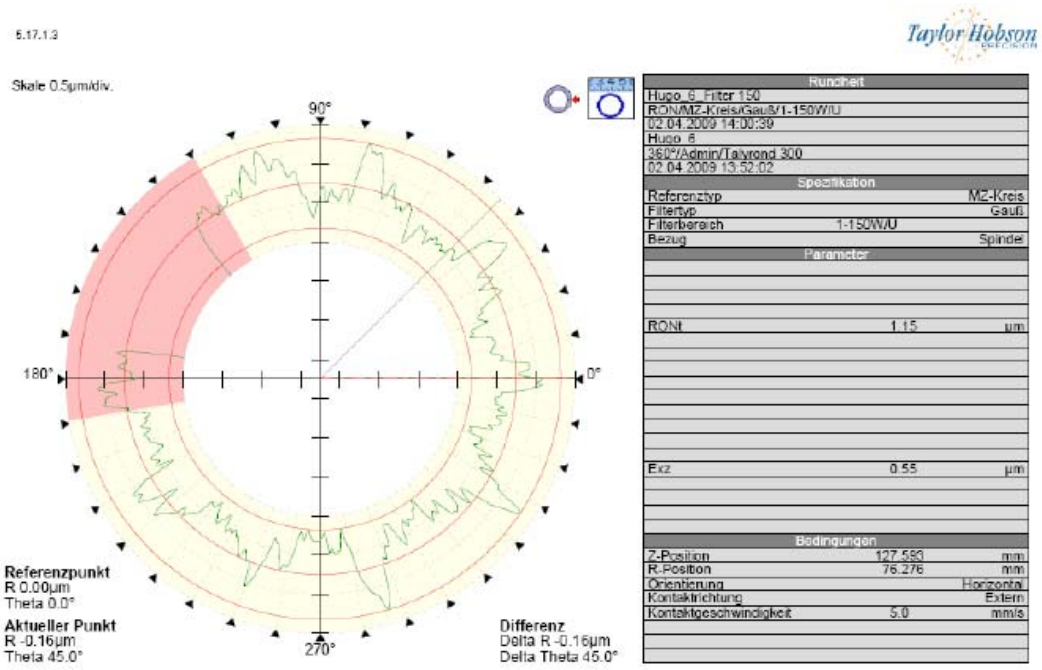

Fig. 6.17: The same profile shown in Fig. 6.14 as it appears in Taylorond 300.

(iii) Comparison between "SW-module" and Mahr MMQ 200

To have an additional comparison for roundness results on profiles with missing parts, an additional comparison have been performer between the "SW-module" and the dedicated roundness system Mahr MMQ 200 [132], reported in Fig 6.18.
The measurements were done on three different positions on a calibrated sphere and excluding a part of the profile, to simulate an unwanted part (such as grooves or flats). The raw data were then analyzed by the "SW-module" and the software of the Mahr MMQ 200. Roundness has been calculated using the Minimum Zone principle and using the following Gaussian filter: 15 UPR, 50 UPR, 150 UPR, 500 UPR and without filter. Results are summarized in Table 6.3 where it is possible to notice as also in this case deviations were below 0.1μm, showing a good agreement between the software.

	Roundness Tschebyscheff [μm] : SW-module					Roundness Tschebyscheff [μm] : Mahr MMQ 200				
	Profiles with missing parts									
	15UPR	50UPR	150UPR	500UPR	without	15UPR	50UPR	150UPR	500UPR	without
Top	0.28	0.30	0.32	0.33	0.38	0.25	0.27	0.29	0.31	0.36
Middle	0.42	0.46	0.46	0.47	0.48	0.24	0.26	0.27	0.29	0.37
Bottom	0.29	0.32	0.33	0.34	0.36	0.21	0.23	0.27	0.30	0.36

Table 6.3: comparison between SW-Module and Mahr MMQ 200.

(iv) Evaluation of real data of the CGM Prototype

The last test have been related to the evaluation of real data acquired on the CGM Prototype system (Fig. 6.1-Fig. 6.2) and their comparison with actual measurement performer on the Talyrond300 system (Fig. 6.15)
A series of measurements have been performed with both the systems on a dedicated steel workpiece with different profiles (Fig.6.1 and Fig. 6.18).

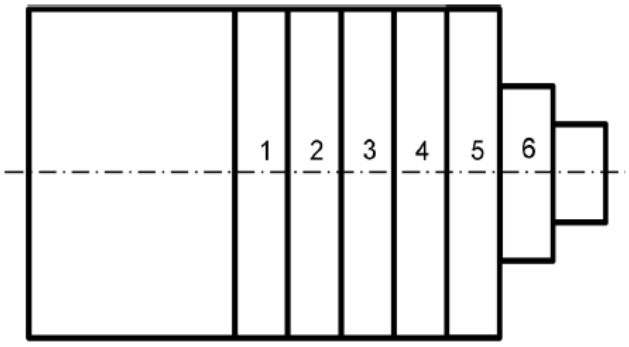

Profiles Nr. 1 – Nr. 5:
different surface, each profile with 0.1mm less in radius then the previous
Profile Nr. 4 + Nr. 5:
Cos-waves, amplitude 10 μm
Profile Nr. 6:
Profile with smaller radius

Fig. 6.18: Sketch of the "workpiece with different profiles".

The measurements taken on the two systems have been both calculated with the "SW-module" and compared. In order to be comparable, all the measurements

have been calculated using a Gaussian filter of 1-50 UPR. Results are summarized in Fig. 6.19, and Fig. 6.20, with the expanded results of the two systems.

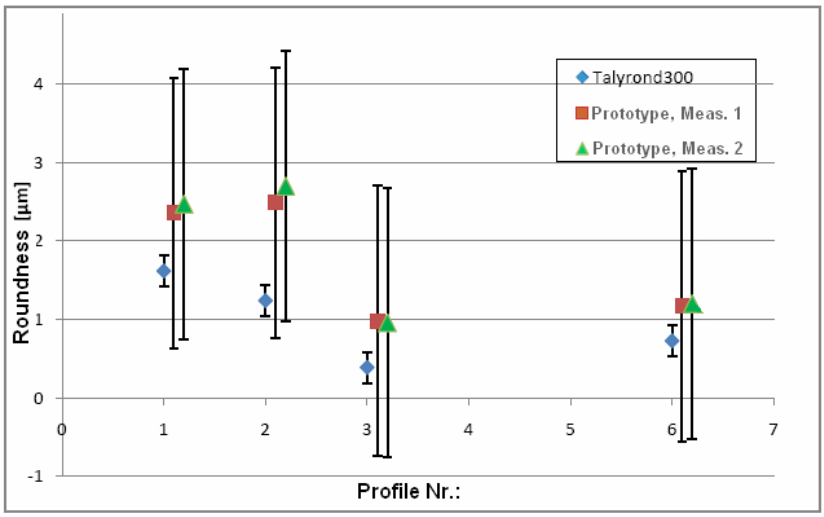

Fig. 6.19: Comparison between CGM Prototype and Talyrond300 (Profile 1, 3, 4, 6).

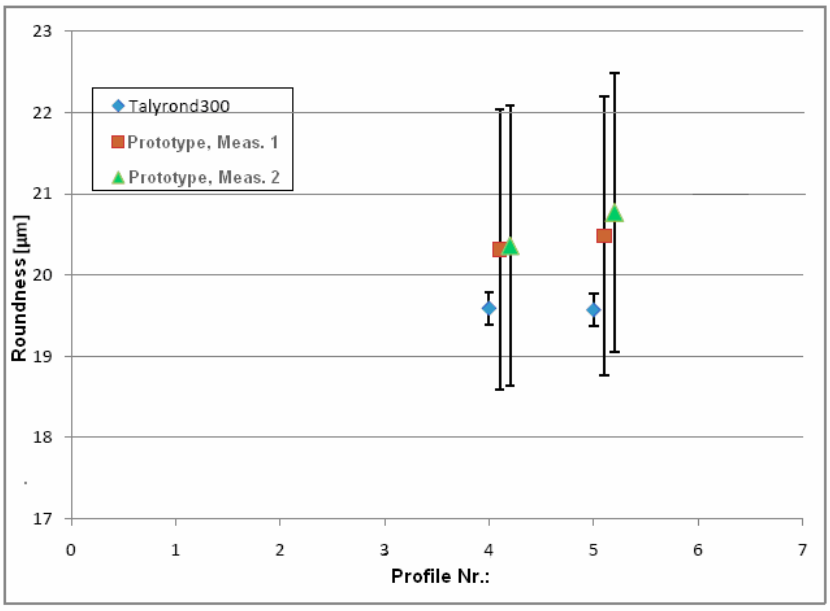

Fig. 6.20: Comparison between CGM Prototype and Talyrond300 (Profile 4, 5).

For the roundness measurements performed with the CGM Prototype, an expanded uncertainty of 1.7µm as been calculated by an uncertainty budget as reported in [128]. Even if measuring results reported in the diagrams are all within the estimated uncertainty, it has to be considered, that for this measurements no specific calibration has been done for the chromatic sensor. The

calculation has been done without correction of the sensor displacement and based only on the calibration factors according to the manufacturer. To improve the results and reduce the uncertainty in measurement, an adequate calibration procedure is necessary. The use of the Flick Standard artefact [133] (Fig. 6.21) has been suggested by the author for this purpose. Using this kind of artefact, in fact, a calibration factor can be determined for all the components of the signal in the Fourier Space and used to compensate both the calibration of the sensor and its misalignment [128].
The effect of calibration by mean of a Flick Standard on the roundness measurement has been simulated and evaluated by the author. In fig. 6.22, results related to an increasing misalignment of the sensors on the measurement of a roundness value of 300µm is shown. As it is possible to notice, the misalignment of the sensor causes an error that is proportional to the entity of the misalignment itself; using the indicated calibration procedure this effect can be completely corrected.

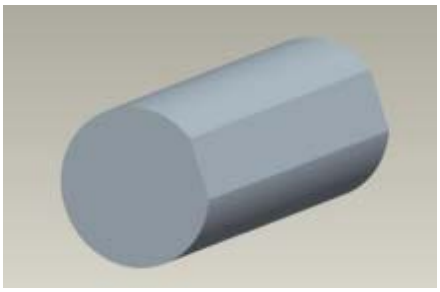

Fig. 6.21: Artefact for sensor calibration and correction of sensor misalignment.

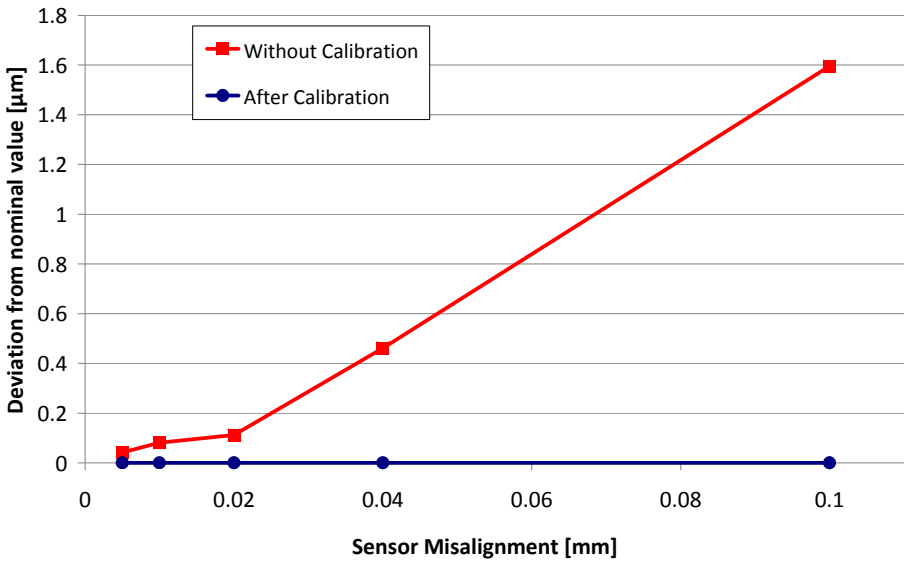

Fig. 6.21: Effect of sensor misalignment on roundness calculation

6.5 CONCLUSIONS

One of the most important advantages of optical sensor is that they can be used directly for quality control and measurements into the production line. In this Chapter an industrial application related to the integration of a chromatic sensor into a high precision grinding machine has been presented.
The author of this Thesis participated to the Project during a 3 months period spent at NTB, working directly to the development of a software tool for in-line measurement of roundness of grinded part. The activities was aimed to the development of a tool able to separate from data collected by the sensor the contribution due to error sources (such as eccentricity of the workpiece, sensor misalignment and noise) from the form error of the workpiece itself. In order to evaluate the contribution of the error sources due to measuring equipment, a model of the error sources have been developed to generate synthetic data representative of the most common situation. Data generated from the simulator have been used to tested the roundness software tool. Results obtained from the analysis have been validated by comparison with dedicated roundness equipment and metrological software showing to be in good agreement. As final contribution of the author, a method for the calibration of the system and improvement of measuring results have been presented.

Chapter 7

VideoAUDIT: Industrial inter-laboratory comparison of CMMs equipped with optical sensors

Traceability of coordinate measurements can be obtained on different levels using a large variety of methods. Documentation of the results given by a CMM can be partially obtained by participation in an audit as e.g. [134],[135],[136]. In an audit, the participants measure items that have been calibrated by a pilot laboratory. The measurements are compared to the reference values and to the results of the other participants. In this Chapter the main results of an industrial inter-laboratory comparison for Coordinate Measuring Machines equipped with optical sensors are presented. The comparison, named *VideoAUDIT*, has been organized and coordinated by the Laboratory of Industrial and Geometrical Metrology of the University of Padova and carried out in Europe from August 2007 to January 2009. A total of 21 CMMs participated in the Project, using different kinds of optical sensors. Participants, mainly small-medium size industrial companies, have been asked to measure a set of calibrated artefacts with measurement tasks of different complexity. They include both 1D/2D standards (glass scale and optomechanical hole plate) and 3D injection moulded workpieces of different colours (four plastic Lego bricks).
Beside the evaluation of actual metrological performances of optical CMMs in industry, an important aim of the comparison was to investigate the validity of measurement uncertainty statements provided by participants. The focus of this investigation was on the additional error sources that emerge when using optical CMMs. Results demonstrate that: (i) the interactions of the optical sensor with the material and surface of the part are among the most important error sources; (ii) the user of the optical CMM in most cases is not aware of the magnitude of these effects; (iii) specific uncertainty evaluation procedures, suitable for industrial users of optical CMM measurements, are needed.

7.1 AIM OF THE PROJECT

The *VideoAUDIT* Project has been developed with the following aims:

- map ability of industrial companies to perform optical CMM measurements and to evaluate limits and problems;
- provide users with artefacts and procedure for testing the accuracy of their measurements;
- test the ability to state uncertainties;
- create an international network of optical CMMs users;
- share information on development of new standards and techniques.

7.2 PARTICIPANTS

A total of 21 CMMs have been participating in the comparison, distributed in 4 European countries as reported in Table 7.1. In order to create a network between different levels of utilizations, the comparison has been extended not only to final users but also to systems manufacturers and Research Institutes. The final composition of the participants is shown in Table 7.2.

Country	Participants	CMM
Italy	12	12
Switzerland	1	2
Denmark	5	6
Spain	1	1
Total	19	21

Table 7.1: Number of participants and CMMs.

Category	Participants
Industrial users of measuring systems	12
Manufacturers of measuring systems	5
Research institutions	4

Table 7.2 Type of participants.

7.3 TIME TABLE AND SCHEDULING

The comparison has been developed in two different phases: the first part, from August 2007 to July 2008, has involved CMMs and companies from Italy and Switzerland [137] while in the second one, from August 2008 to January 2009, the comparison has been extended also to Spain and Denmark [138], [140].
In order to limit the duration of the Project, the circulation has been arranged in a circular path: after each participant finished all the measurements, the comparison package was forwarded to the next participant and the results were sent to the Coordinator, leaving the responsibility to the participants to take care of the

transportation. An alternative option could have been to use the so called "petal path" in which the comparison items are re-measured by the pilot laboratory after each participants to have a better understanding about their stability. In our case, to check the stability of the artefacts, three calibrations have been repeated by the author, respectively before, at the middle and at the end of the circulation. To save the time needed to understand the measuring tasks, all the documents necessary to perform the measurements and to collect the data have been sent to each participant before the arrival of the items. All the documents were available to the participants at the Website of the comparison: www.dimeg.unipd.it/videoaudit. To preserve the confidentiality of the results, an identification number has been given to each participant to compare the measuring results without being recognizable by others. The number of participants has been chosen in order to give to each of them a reasonable period of time (3 weeks) to perform the requested measurements and to elaborate the results. Generally the participants have respected the scheduled time table, allowing to finish the comparison without any delay.

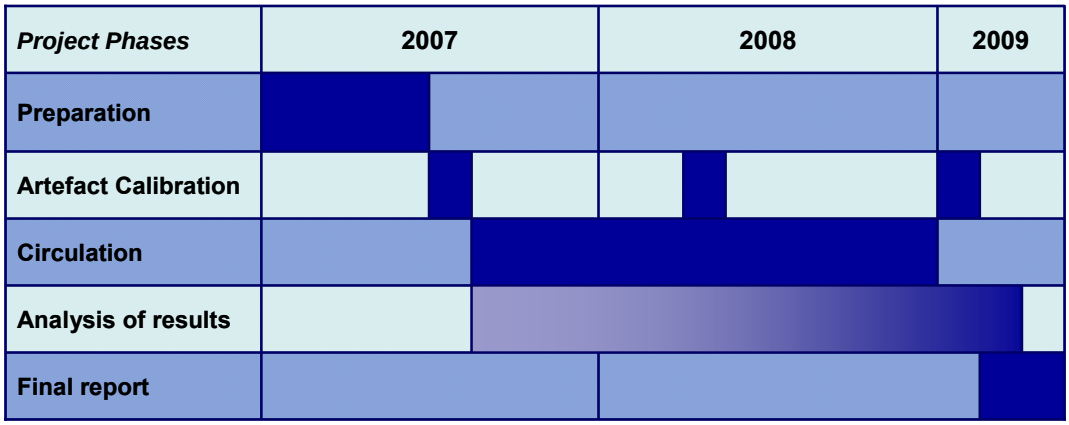

Fig. 7.1: Time table.

7.4 AUDIT ITEMS

In previous comparisons, involving contact CMMs, mainly artefacts for performance verification have been used as audit items [134]. In other cases also special steel parts with form error close to actual workpieces have been used [140], [141]. In this comparison the aim to investigate the performance of optical CMMs, as well as the quality of measurements on actual industrial products, has resulted in the decision to use a set of calibrated artefacts composed by three items, different in form, material and size. Moreover the artefacts have been chosen in order to allow to be measured by different kinds of optical sensors and to cover a large variety of geometrical tolerances according to ISO 1101 [119]. One of the most important requirement to assure a good result of an

intercomparison is to verify that dimensional and geometrical stability of the artefact used as comparison items is respected [142].
Starting from this consideration and taking into account the working volume of the CMMs to be investigated, the following artefacts have been individuated:

- 1D Artefact (Fig. 7.2a): a 300mm glass scale. Here, measuring targets are the calibrated distances between the rectangular chromium depositions. The glass scale was calibrated with expanded calibration uncertainty of (0.5+L/900)μm (L in mm). Dimensional stability of this kind of artefact is well known from literature and experience, nevertheless it was checked during and after the comparison, with measured deviations within the calibration uncertainty.
- 2D Artefact: an optomechanical hole plate (Fig. 1b) [49]. Measuring tasks for this artefact are typically the distances between the centres of 25 holes on a steel sheet of 0.1 mm thickness; however, for the purposes of the present comparison, participants were also asked to measure diameters as well as roundness of 3 selected holes, simulating in this way an industrial inspection of holes on a workpiece. Calibration was performed by contact probing with expanded calibration uncertainty of 1.2μm on holes positions and 1.5μm on diameter and roundness of the 3 selected holes. Stability of the artefact was previously demonstrated [49] and was also checked during and after the comparison, with deviations within the calibration uncertainty.
- 3D Artefacts: a set of 4 polymeric bricks of different colours (Fig. 1c). Measuring targets are dimensions, distances and geometrical tolerances on flat and cylindrical elements. These 3D artefacts were chosen for the availability in different colours and because optical sensors are commonly used to measure plastic parts like these in industry. Reference values were determined using contact probing with an expanded calibration uncertainty of 1.9μm for the longest side of the bricks (examples are reported in Table 7.3). For the calibration a dedicated procedure has been performed by the author, using a reversal method [93],[143]. Stability of the selected 3D artefacts was found to be acceptable for the purposes of the circulation. Repeating the calibration after the circulation deviations were found to be within 2μm for size and within 3μm for form features. To take into account these changes, the uncertainties of the reference values have been set to 3μm for size and 4μm for form features.

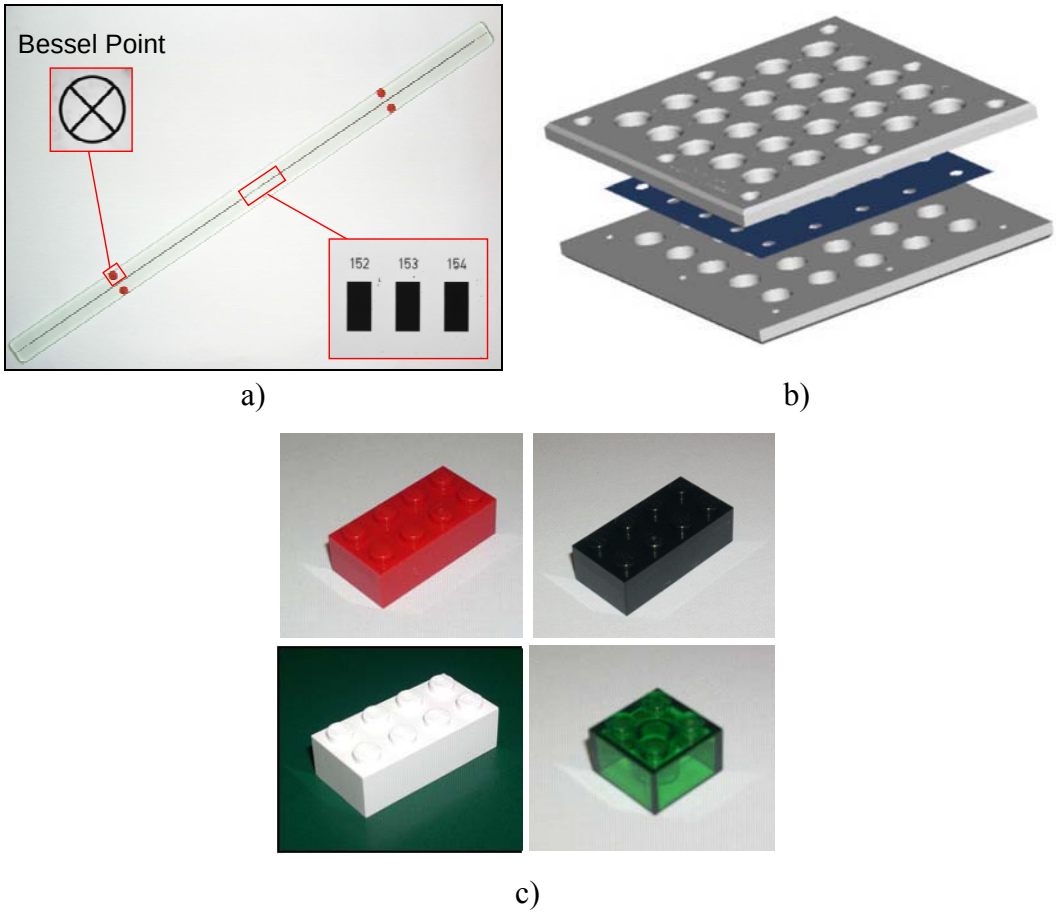

Fig.7.2: audit items. a) Glass Scale, b) Hole Plate, c) Plastic Bricks.

	Before the circulation		After the circulation	
	Calibration	**Uncertainty**	**Calibration**	**Uncertainty**
Length Side A	31.7192	1.6	31.7181	1.9
Length Side B	15.7815	1.5	15.7827	1.6
Length Side C	31.7399	1.5	31.7385	1.8
Length Side D	15.8084	1.3	15.8071	1.3
Diameter 1	4.9079	0.9	4.9076	1.0
Straightness Side	0.0093	1.1	0.0088	0.8
Straightness Side	0.0084	1.5	0.0075	1.0
Straightness Side	0.0093	0.3	0.0084	0.6
Straightness Side	0.0080	0.7	0.0080	0.7
Perpendicularity	0.0108	0.3	0.0110	0.3
Parallelism A_C	0.0228	1.1	0.0215	1.3
Flatness Plane 1	0.0105	0.9	0.0128	1.0

Table 7.3: Example of calibration results for the white plastic Brick (in mm).

7.5 MEASURING PROCEDURES

For each artefact a proper measuring procedure has been studied in order to extract the maximum number of information from the measurements and, when possible, to make the measurement feasible for the different sensors involved. Table 7.3 resumes the features that were asked to be measured chosen in such a way to represent a large variety of geometrical tolerances according to ISO 1101 [119]. They reflect the aim of the project in checking both the machine and the capability of the operator to understand specific measuring tasks. In these procedures the number, location, and distribution of sampling points are detailed described as well as the alignment of the workpiece. Only for the diameter and the roundness of one hole on the 2D artefact the strategy has been left to the own choice of the participants (Table 7.4). Moreover all measurement results were asked to be reported at 20°C. The thermal coefficient of expansion for the materials was stated in the procedures but no instructions were given as how to calculate the correction or the uncertainty associated with the correction. This very restrictive procedure was chosen to achieve comparable results.

	Glass Scale	Hole Plate	Polymeric Bricks
Dimension	10 bidirectional lengths	1 distance between 2 holes 3 internal diameters	4 point to point distances 1 point to plane distance 1 external diameter
Position	-	(X,Y) coordinates of 25 holes centres	(X,Y) coordinates of 8 knobs centres
Roundness	-	3 internal roundness	1 external roundness
Flatness	-	-	1 flatness
Straightness	-	-	4 straightness
Perpendicularity	-	-	1 between two sides
Parallelism	-	-	1 between two sides

Table 7.4: requested measurement

The measuring procedures for the 1D and the 2D artefacts were defined like procedures for interim checks of optical CMMs. Going into detail, for the glass

scale, 10 bidirectional lengths have been requested (fig. 7.3), following the procedure indicated by the draft ISO 10360-7 [58]. In this case, only one repetition of the measurements was asked, without requiring a specific position of the artefacts on the working volume. For the 2D artefacts (fig. 7.4), the participants were asked to determined the (X,Y) coordinate of the centres of the 25 holes, using the same alignment used for the hole-plate calibration, following two different paths: first an in-going spiral and then an outgoing spiral. In this way not only geometrical errors of the machine can be determined, but also the effects of drift or hysteresis errors [49].

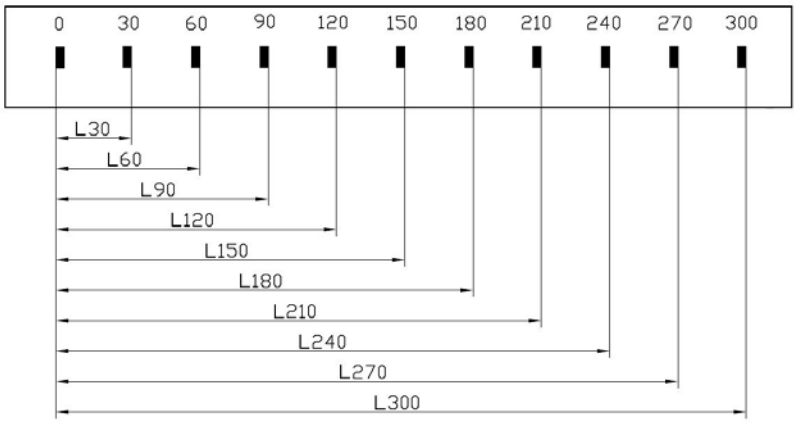

Fig. 7.3: bidirectional measurements on Glass Scale.

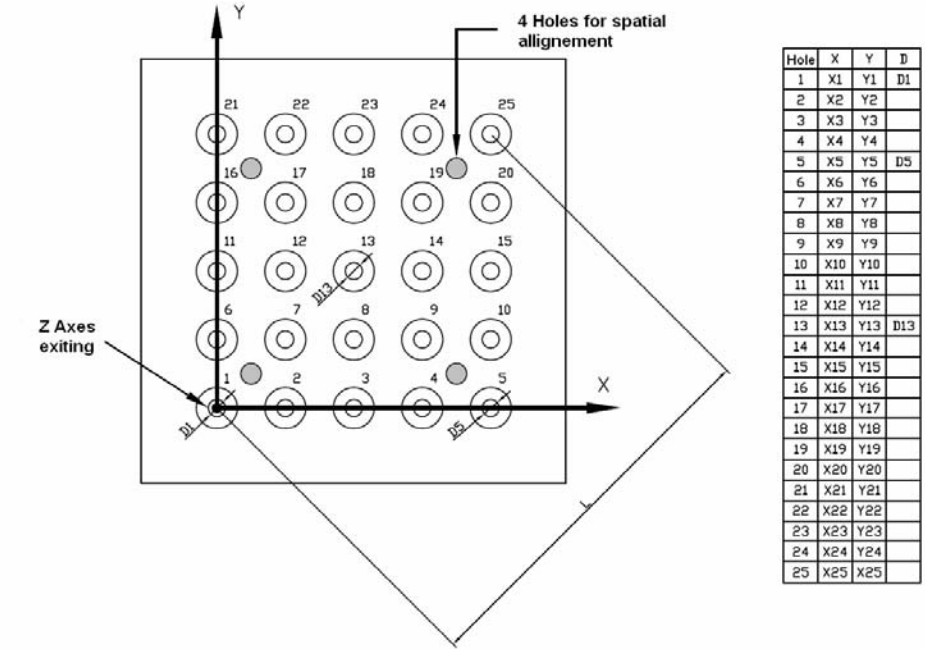

Hole	X	Y	D
1	X1	Y1	D1
2	X2	Y2	
3	X3	Y3	
4	X4	Y4	
5	X5	Y5	D5
6	X6	Y6	
7	X7	Y7	
8	X8	Y8	
9	X9	Y9	
10	X10	Y10	
11	X11	Y11	
12	X12	Y12	
13	X13	Y13	D13
14	X14	Y14	
15	X15	Y15	
16	X16	Y16	
17	X17	Y17	
18	X18	Y18	
19	X19	Y19	
20	X20	Y20	
21	X21	Y21	
22	X22	Y22	
23	X23	Y23	
24	X24	Y24	
25	X25	X25	

Fig. 7.4: measurements and alignment on the Hole Plate.

7.6 UNCERTAINTY EVALUATION

As one of the main objectives of the comparison was to state the ability of the participants to determine the uncertainty of their measurements, for each measured feature, the participants were asked to express the related measuring uncertainty following one of the methods listed below (in order of preference):

- UA) Uncertainty budget determined through analytical calculation of uncertainty contributors (GUM [81] approach);
- UB) Uncertainty calculated according to the substitution method (ISO 15530-3 [78] approach);
- UC) Uncertainty assessment based on the experience of the participant;
- UD) Uncertainty assessment based on system specifications stated by the manufacturer.

The main idea was to test if participant are familiar with task related uncertainty: the ISO standard and the VDI guidelines [37],[58],[59], in fact, use the length measurement uncertainty as specification and testing criteria for the performance of the CMM but this statement only regards length measurement as, for example, performed on gauge blocks or step gauges (two opposite faces). On the other hand, most operators have a good feeling as to the actual uncertainty of a measurement task. This feeling can be based upon experience or knowledge about uncertainties for similar measurement tasks and was to be reported as UC, but in some cases they have not idea about uncertainty calculation and method described by International standards.
In this direction, the comparison acted as learning experience, living the participants the opportunity to learn and test other methods for uncertainty calculation.

7.7 RESULTS

Once all the measuring data were collected by the Coordinator, the results were reported to the participants in two ways. In the first, for each measured feature, the deviation of the measurement performed by the participant respect to the reference value was plotted together with the stated uncertainty. The results of all the participants were plotted in a diagram in order to compare the results with the reference value as well as with the results of other participants. An example of this kind of diagram is shown in Fig. 7.5. To get the results comparable, for the participants that have performed more than one measurement for each features, the mean values have been plotted. If a result is only shown with a dot, this implies that no uncertainty was stated by the participant.
As the comparison of the results comprised both the measured features and the stated uncertainties, in the second kind of reporting, the results are compared putting more attention to the stated uncertainty. One way to do that is to calculate

the normalized error (E_N-value) that combine deviation and uncertainty into one number. This is very useful to communicate the quality of the results to the participants. For all the companies that stated the uncertainty values, the E_N-value was calculated as:

$$E_N = \frac{|Value(lab) - Value(ref)|}{\sqrt{U(lab)^2 + U(ref)^2}}$$

The E_N-value describes the difference between the results obtained by the participants and the reference value, compared to the stated uncertainty. If $E_N < 1$, there is a good agreement between the two results; if $E_N > 1$, the results are not in good agreement. Of course a very big stated uncertainty also causes small E_N so in this case the normalized error might give an erroneous picture of the situation. The E_N-value can be said to combine deviation and uncertainty into one number, thus reducing the dimensionality of the data material. The E_N-value is not only interesting when comparing uncertainties, but it is very useful for communicating results to the participants.
The results of each single participant have been analyzed in order to demonstrate to the single participants the information content provided by the measurements. For the participants that have measured the glass scale in different positions, a report for each position has been produced to allow the identification of the specific scale error and eventually to evaluate the squareness errors. On the basis of the hole plate measurements, a map of the CMM geometrical errors in the XY plane has been calculated and presented to each participant (see Fig. 7.9).
Overall results are presented in the following paragraphs where the measuring systems were classified in four groups, according to type of sensor and manufacturer specifications (Table 7.5). An identification number has been assigned and communicated to each participant to compare the measuring results without being recognizable by others. CMMs equipped with laser triangulation sensors were investigated on the plastic bricks only, since the other artefacts are designed for lateral measurements only. All the results related to the comparison are collected in [144].

Group	Optical sensor	Length measuring capability for 300 mm*	No. of CMMs
A	Image processing	Up to 3 µm	5
B	Image processing	3 - 4 µm	6
C	Image processing	over 4 µm	6
D	Laser triangulation	-	4

*according to the manufacturer specifications for XY plane

Table 7.5: Grouping of participating CMMs

Together with the overall comparison results, the results of each single participant have been analyzed separately in order to show to the single participants the information reachable by the measurements of the single artefacts. For the participants that have measured the glass scale in different positions, a report for each position has been produced to allow the identification of the specific scale error and eventually to evaluate the squareness errors. In the case of the Hole Plate measurements, also a map of the geometrical error in the XY plane has been calculated and presented to each participants.
The participants have shown different capabilities in the measurements of the artefacts, in some cases measuring only some of them (Table 7.6). This can be due to the difficulty of the task or to physical limit of the device used for the measurement. The Green Brick, in particular, being semi-transparent gave more problems than the other artefacts.
In the following paragraphs a detailed analysis of the most important results achieved from the comparison are reported and discussed.

	Glass Scale	**Hole Plate**	**White Brick**	**Red Brick**	**Black Brick**	**Green Brick**
N. Companies	17	17	15	12	12	11

Table 7.6: Numbers of companies that have measured each artefact.

7.8.1 Glass Scale

The participants were asked to measure the glass scale in at least one position into the measuring volume. Following the draft ISO 10360-7 [59], a series of 10 bidirectional measurements between chromium depositions were asked to be measured. In this case the participants had the opportunity to evaluate the presence of systematic linear error of their machine and, repeating the measurements in different positions, to quantify the squareness error between coordinate axis.
The main results concerning the measurement of the glass scale are summarized in Figure 7.5 and in Fig. 7.6. In Figure 7.5 the deviations of the measurements respect to the reference values and the related uncertainties are presented for three selected nominal lengths: 30mm (L30), 120mm (L120) and 210mm (L210).
They reveal a general good ability of most participants in performing simple and well defined bidirectional measurements of length, as well as in determining the associated measurement uncertainty. As expected, a nice correlation with the accuracy class of the CMM has been found: Group A is performing better than B and C.
The average value of the deviations calculated between the participants was observed to be very close to 0 for all the 10 measurements, indicating that alignment and measurement procedures were adequate. Nevertheless, the

Standard Deviation of the results increases with the increasing of the dimension to be measured, confirming the influence of the scale errors. The measurements were not thermally compensated by the participants in some cases, but, considering the low CLT of the glass, the higher deviations are surely due to specific problems of some participants, mainly related to uncorrected geometrical errors and bad verification of the CMMs. This aspect confirm that the glass scale could be used successfully for quick checks of optical CMMs.

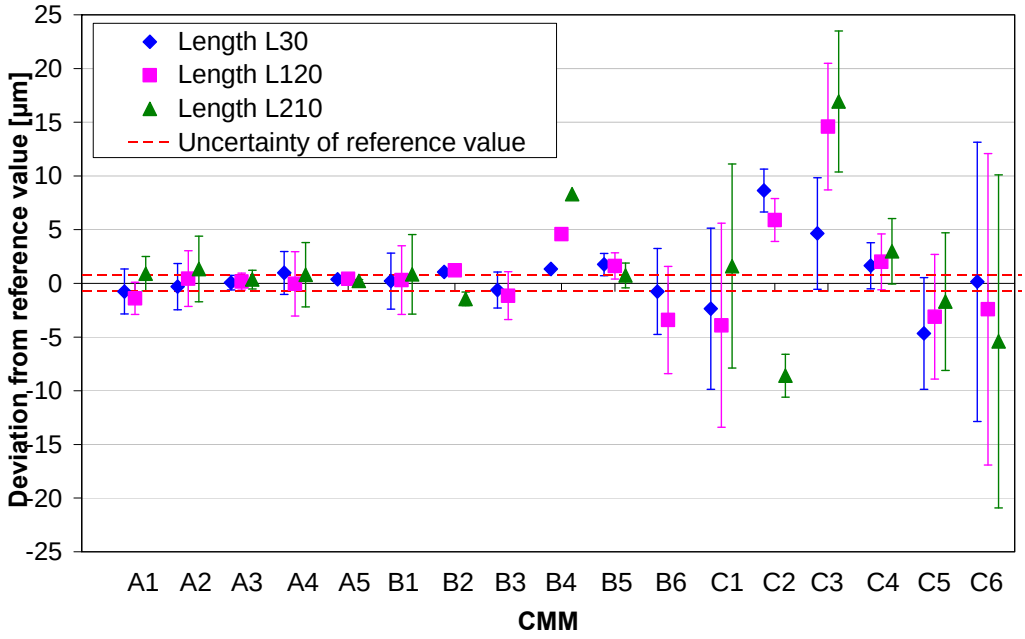

Fig. 7.5: Summary of results from the Glass scale measurements. For the participants that have performed more repetitions, the mean value of the repetitions is reported. Error bars refer to uncertainty stated by the participants.

In Fig. 7.6 the E_N values calculated for the participants that have expressed an uncertainty are shown. The comparison results show that estimation of uncertainty of simple length measurement is possible for industry as only one participant didn't calculate any value (B4). Generally the uncertainty stated by the participants was based on the indication given by the manufacturer, resulting in $E_N>1$ only in few cases (Fig. 7.6). Concerning the method used for the calculation of the measuring uncertainty, 8 participants used the method UD (based on specifications of the manufacturer), 5 participants used the method UA (uncertainty budget, even though in some cases only the repeatability was taken into account), 2 participant followed the method UB (substitution method) and only one the method UC (based on experience).

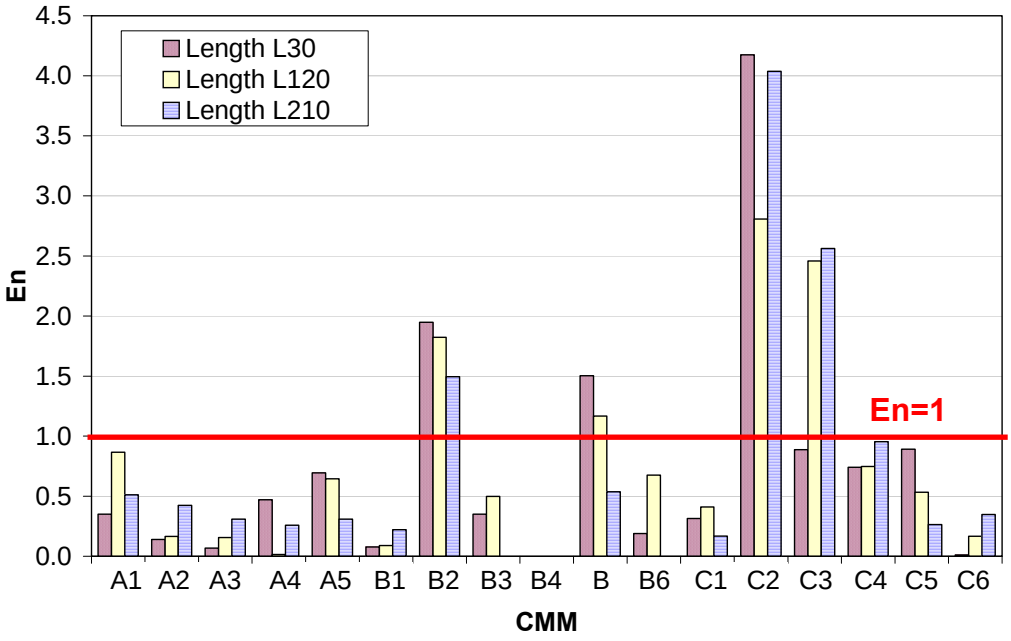

Fig. 7.6: Summary of results from the Glass scale measurements: E_N value.

7.8.2 Hole Plate

Results obtained for the measurement of the Hole Plate are generally worst than the measurements on the glass scale. In the measurements of the position of the holes, in fact, more effects contribute to the final results: first of all the geometrical errors of both the coordinate axis, errors due to the alignment and, thanks to repeated measurements required by the measuring procedure, also on drift and hysteresis. This aspect is shown in Fig. 7.7 where the distance between two holes along the diagonal of the hole plate is taken as performance indicator. In particular results obtained for the distance between the centre of Hole 1 and the centre of Hole 25 can be compared (for similarity of the nominal value) with the results obtained for the Length L120 in Fig. 7.5. In this case, the correlation between the accuracy class of the CMM and measurement results is less visible than in the previous case. Generally, in fact, Group A is performing better than the others but a bigger dispersion is now present inside the same groups.
This aspect is also visible in Fig. 7.8 where the E_N values are shown for the previous measurements. Moreover, Fig. 7.8 shows as the increasing complexity of the measuring task also leads to a bigger difficulty in uncertainty assessment as 3 participants didn't state any value.

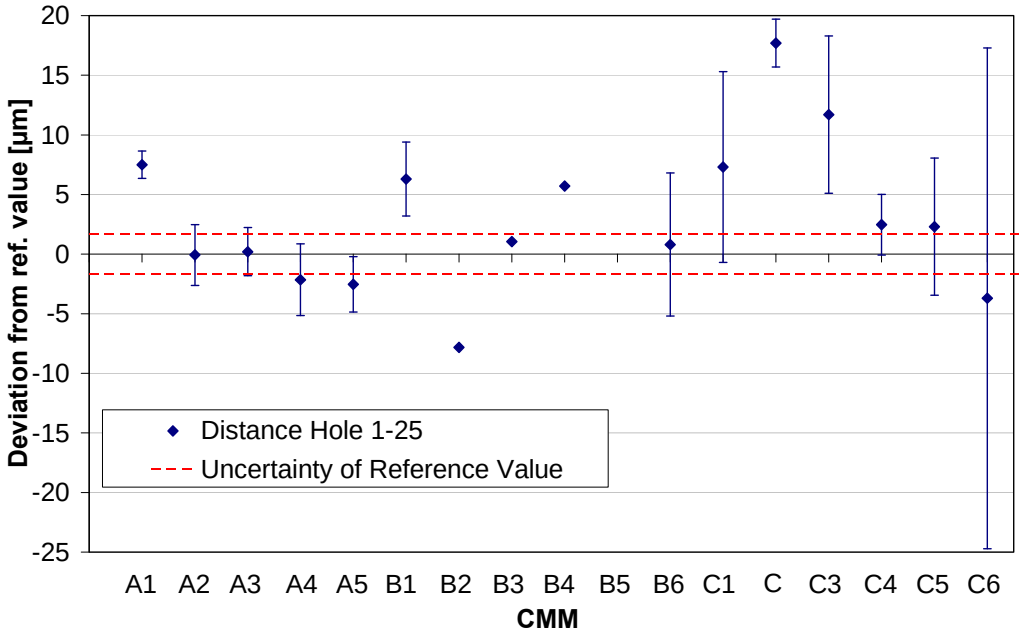

Fig. 7.7: Results obtained from the measurement of the distance between Hole 1 and Hole 25 on the Hole Plate. Error bars represent the uncertainty reported by the participants.

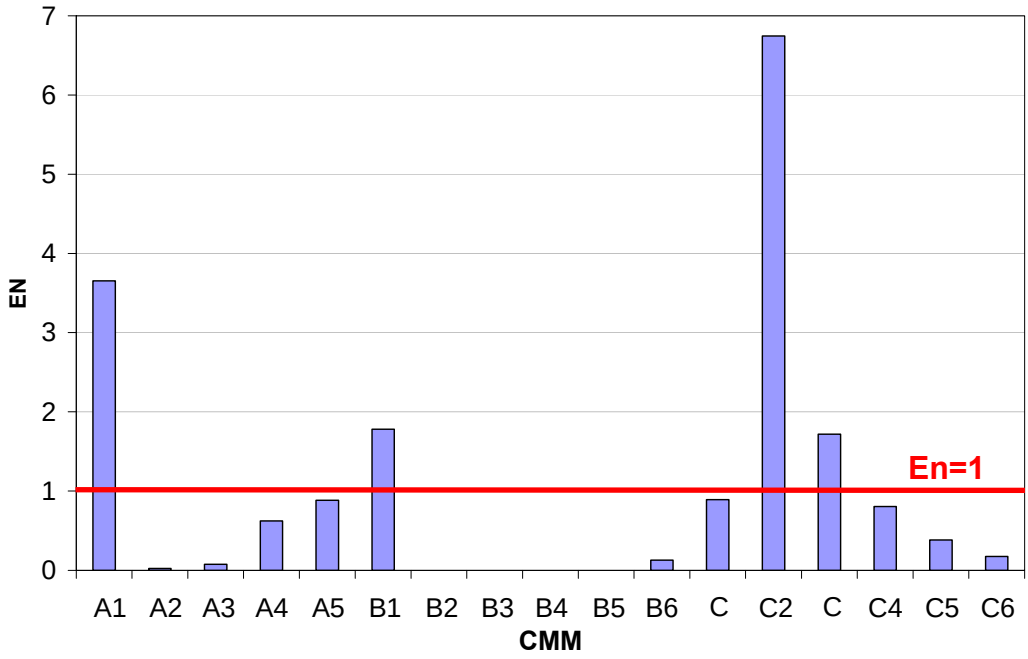

Fig. 7.8: Results obtained from the measurement of the distance between Hole 1 and Hole 25 on the Hole Plate: E_N value.

A better understanding of the errors of each participant can be obtained plotting the map of the deviation of each single hole as shown in Fig. 7.9, in which a squareness error of the axis of the machine is visible.

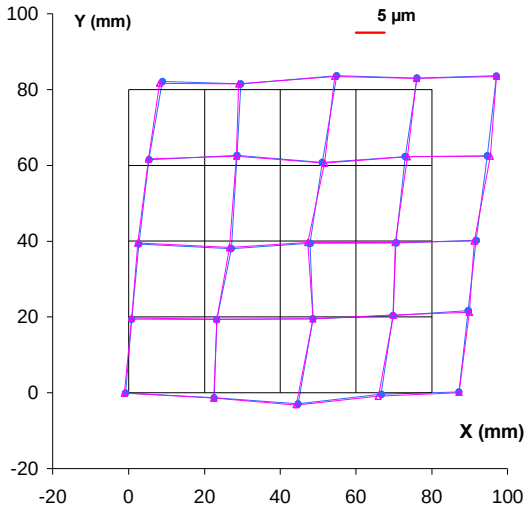

Fig. 7.9: Example of measurement deviations obtained by Participant C3 for the measurement of centres positions on the Hole Plate. The presence of a squareness error is clearly visible in this case.

For the purposes of comparison, however, it is also of big interest to analyse bidirectional measurements task, such as the diameters of 3 selected holes, that are closer to an industrial inspection task. The nominal diameter of holes is 5.5 mm while their calibrated roundness is (2±1)µm.
Participants were asked to follow three different strategies:

- Hole 1: 25 points with movement of the measuring sensor;
- Hole 5: 25 points without movement of the measuring sensor;
- Hole 13: free measuring strategy.

Figure 7.10 shows the summary of results obtained for the diameter measurements of the three selected holes.

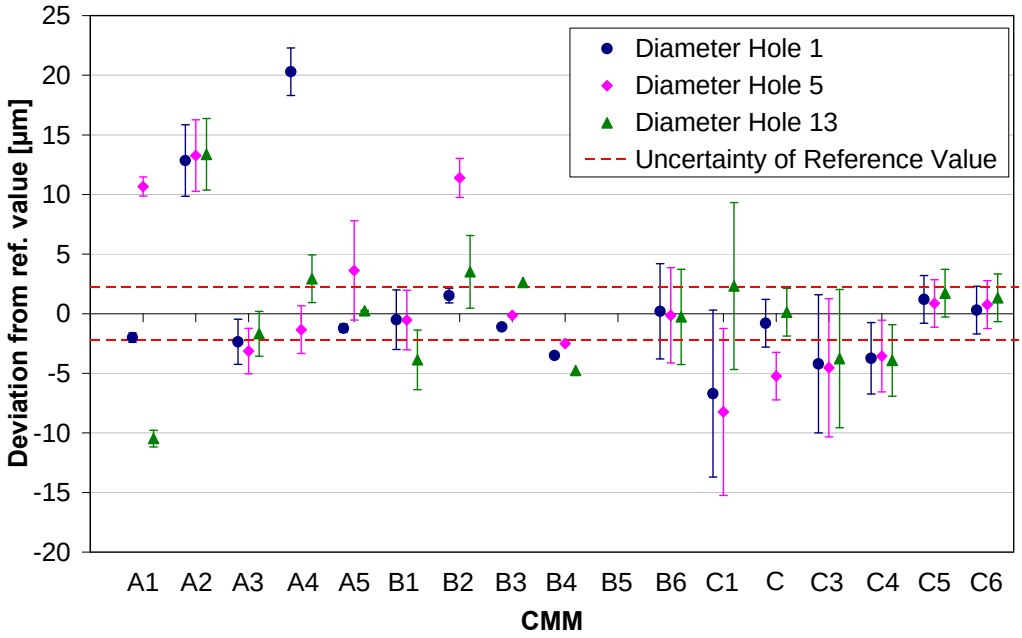

Fig. 7.10: Results obtained from the measurement of diameter for Hole 1, 5 and 13. Error bars represent the uncertainty reported by the participants.

It is worth to notice that, in contrast to the results in Figure 7.5, there is no correlation between quality of the diameter measurement and length measuring performance of the machine, since other length-independent error sources are dominating in this case. One of the most significant error sources that are active in this case is the presence of small dust particles on the holes. The holes are much more difficult to clean than the glass scale. In this case, diameter measurement is very much influenced by image processing and filtering algorithms used by the optical CMM. Furthermore, the hole plate thickness, which is 0.1 mm and hence higher than the tiny chromium depositions on the glass scale, may affect the results, making the holes measurements more sensitive to the type of illumination used. As clearly visible from Fig. 7.10, a number of participants did not properly manage these effects, resulting in non compatible measurements.
As the hole plate has been calibrated using an high accuracy tactile CMM, results from the comparison can also be used to evaluate differences between contact and optical systems. In Fig. 7.11, results related to the measurements of the roundness of the three holes. Also in this case the presence of error sources evaluated in the measurement of diameters is clearly visible, as roundness error is generally overestimated by participants, while the effect of the measurement strategy is not so significant.

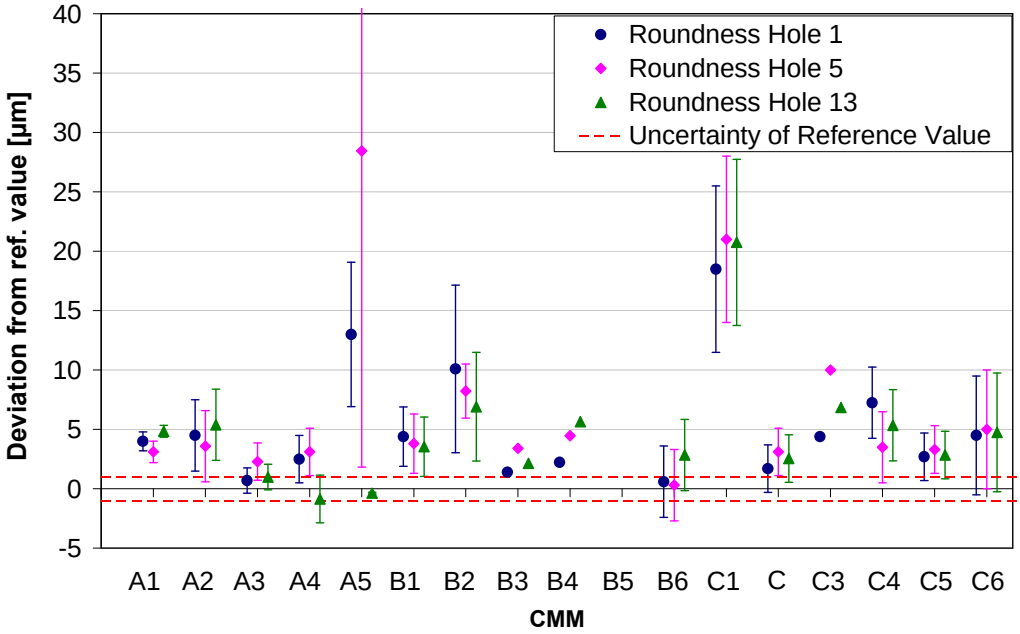

Fig. 7.11: Results obtained from the measurement of roundness for Hole 1, 5 and 13. Error bars represent the uncertainty reported by the participants.

In table 7.7 also is possible to notice that the increasingly complexity of the measurement task has lead also to more difficulties in uncertainty calculation, mainly in the evaluation of form errors. Also in this case the UD method (based on specifications of the manufacturer) has been chosen from the bigger part of the participant (see Table 7.8), without taking into account the task-specific uncertainty.

	Nr. of participants	E_N <1	E_N >1	No Unc.
Position*	16	10	3	3
Length 1-25	16	9	4	3
Diameter Hole 1	16	11	3	2
Diameter Hole 5	16	8	6	2
Diameter Hole 13	16	10	4	2
Roundness Hole 1	15	3	9	3
Roundness Hole 5	15	1	11	3
Roundness Hole 13	15	4	8	3

Table 7.7: Summary of results obtained from the Hole Plate measurements. (*) The parameter *Position* is calculated as mean value of the absolute deviations of the measured X and Y coordinates of the centres.

7.8.3 Plastic Bricks

The measurements on the plastic bricks were analysed taking into account the effect of the different colours and optical properties, as well as the type of features to be measured.

In Fig. 7.12 and 7.13 a summary on the results of the measurement of sizes is presented, where deviations are calculated as the average value of the absolute values of the deviations of the 4 measured lengths of the bricks sides. In Fig 7.12, the values obtained by the calibration in contact mode have been used as reference, while in Fig. 7.13 reference values are the median values calculated between participants. From the comparison of the two graphs, it is possible to see that the large deviations are not due to calibration method employed.

Considering that the nominal value of the length was 32mm or 16mm, the results can be compared with the results shown in Fig. 7.5 for the Length L30. It is possible to notice that in the measurements of the plastic bricks, generally, the results are worse than in the measurements of the glass scale and that there is not a clear correlation with the class of accuracy.

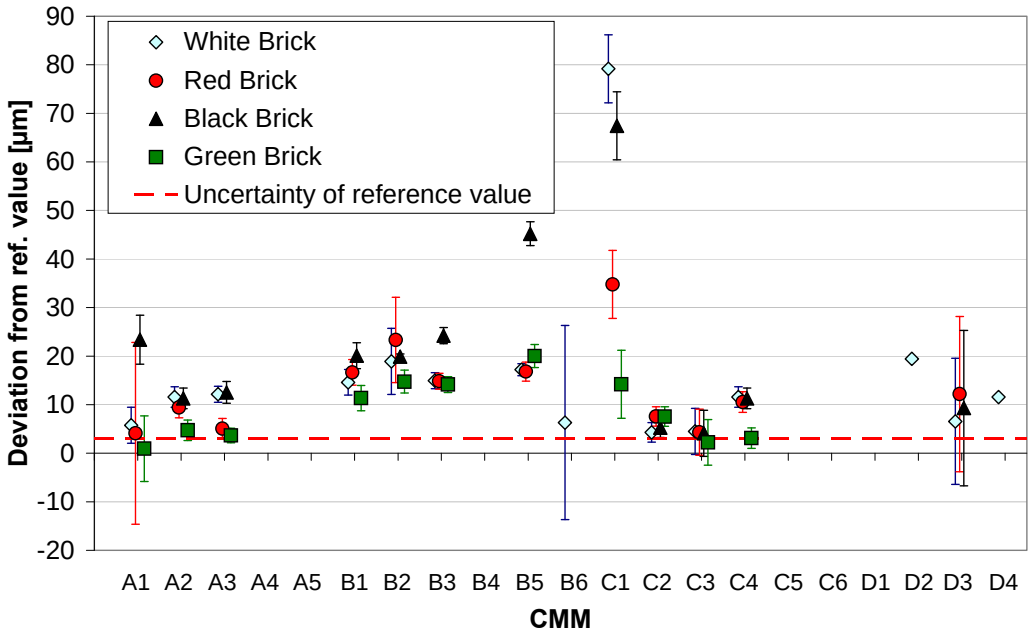

Fig. 7.12: Summary of results for the measurement of sizes on Plastic Bricks. Error bars represent the uncertainty reported by the participant. Reference values are results of calibration with contact CMM.

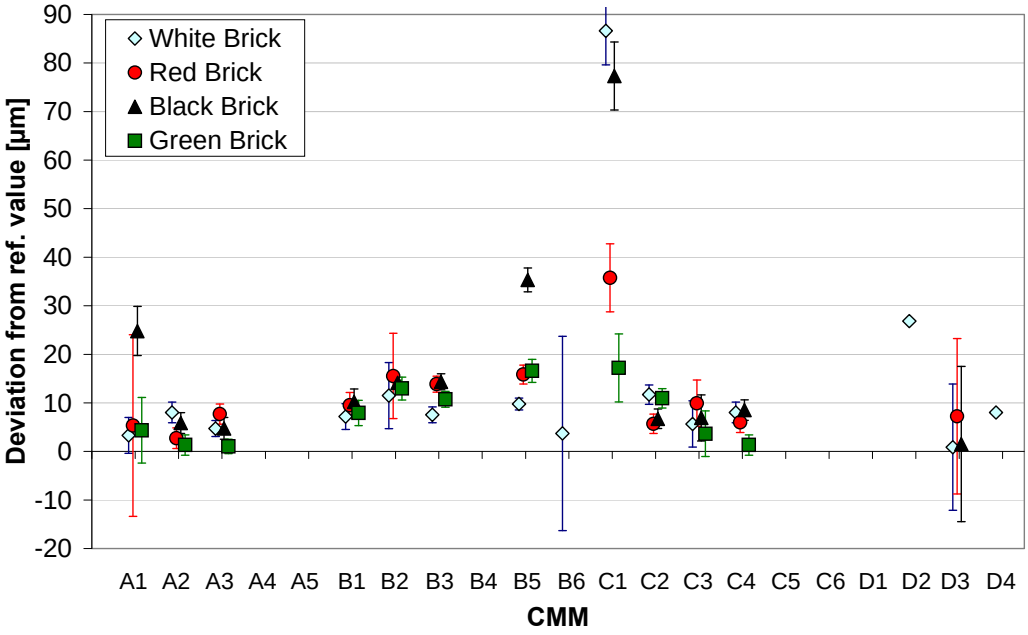

Fig. 7.13: Summary of results for the measurement of sizes on Plastic Bricks. Error bars represent the uncertainty reported by the participant. Reference values are the median values calculated between participants.

These results can be explained taking into account that:

- translucent materials (such as plastic) can transmit or reflect the light depending on the material properties (e.g. colour) and on the type of light used, causing an effect of shrinkage or distortion of the measured features;
- the 4 planes constituting the 4 sides of the bricks are sloped of few degrees and the acquisition of points at the indicated height could be difficult for some kind of sensors;
- the plastic bricks are more sensitive to thermal effects than other artefacts, due to much higher CTE ($8 \cdot 10^{-5}$ K^{-1}). When the measurements are not corrected for temperature difference, a bigger deviation can take place compared with the previous cases.

Figure 7.14 shows a summary of external diameter measurements on top knobs (nominal diameter is 4.9mm, roundness up to 7µm). Also in this case, results are worse than in previous situations, mainly if compared with diameter measurements on the hole plate (Fig. 10). Beside the reasons listed for the measurement of sizes, in fact, it has to be taken into account that the measured

cylindrical knobs do not have sharp edges (edges are rounded off with radii of about 0.1mm) and this makes the measurements more difficult for image processing sensors. This is true although the participants measured according to a well defined procedure prescribing number and position of measured points.

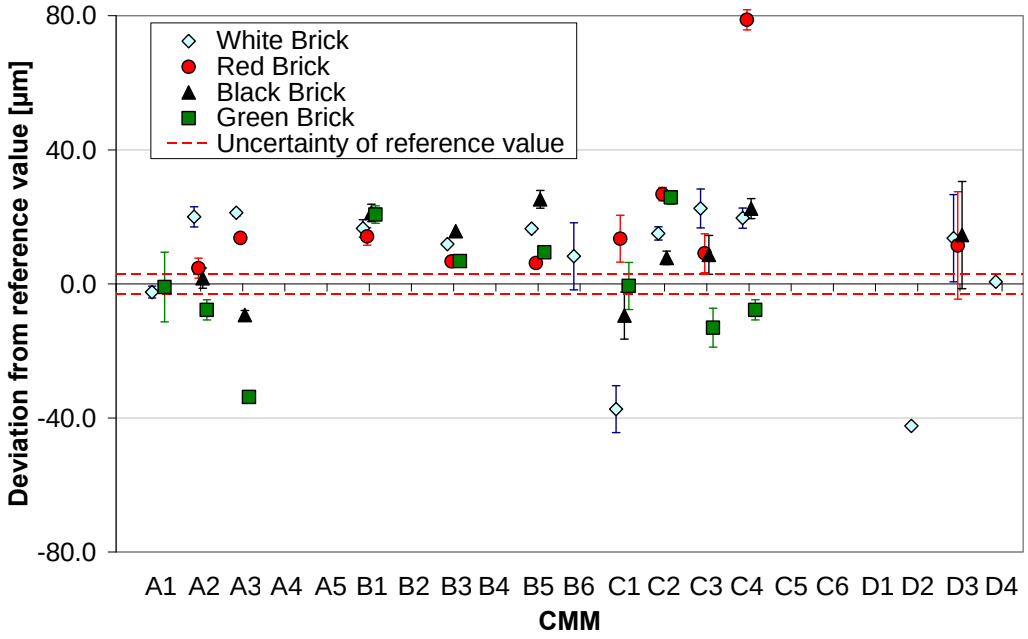

Fig. 7.14: Summary of diameter results on the plastic bricks. Error bars represent the uncertainty reported by the participant. (A1 is out of range with Red and Black Bricks, B2 is out of range with all the Bricks; A4, A5, B4, C5, C6 and D1 did not measure).

Big deviations have been found not only for dimensional measurements but also for geometrical ones, as in presented in Figure 7.15 where a summary of roundness measurements is reported. In this case, the roundness error is generally overestimated respect to the reference value obtained in contact mode. This aspect confirms the bigger influence of external error sources in optical measurements if compared with tactile ones, the effects of image processing and filtering.

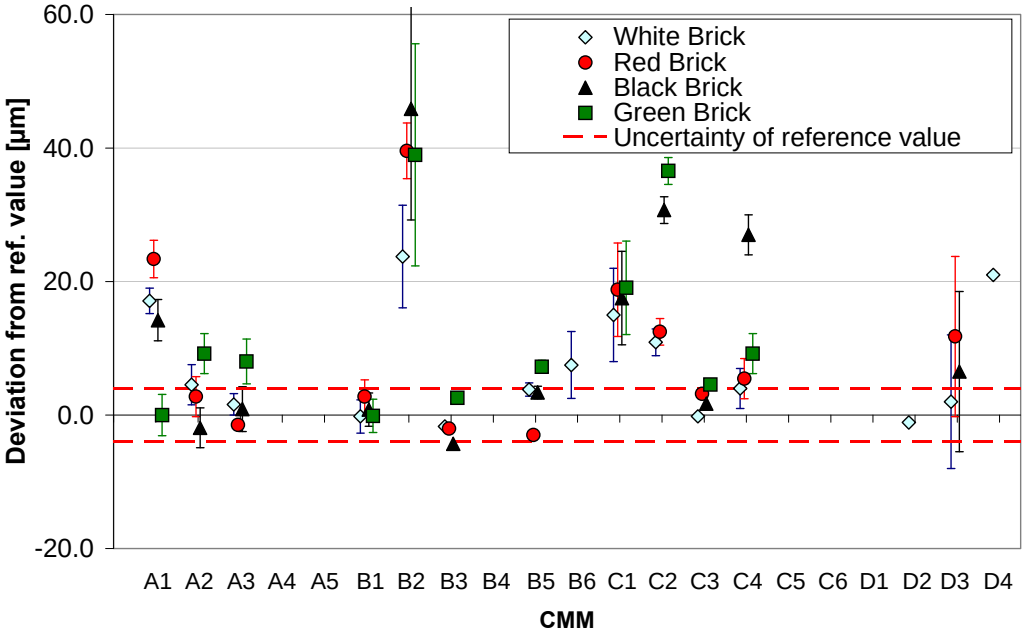

Fig. 7.15: Summary of roundness results on the plastic bricks. Error bars represent the uncertainty reported by the participant. (A4, A5, B4, C5, C6 and D1 did not measure).

The above mentioned error sources were not taken into account by most participants and actually very few measurements are compatible. Figures from 7.12 to 7.15 clearly show a larger scatter of results if compared with the other artefacts, proving that the 3D artefacts are more problematic for the participants. This is reflected also by the procedure that participants declared to follow for uncertainty evaluation. Table 7.8 shows the summary of methods used by the participants to evaluate the uncertainty related to the measurands shown on Figures 7.5, 7.10, 7.15. It appears evident that a large portion of industrial users did not implement task-specific evaluation of measuring uncertainty. In 67% of the cases, the participants that performed the measurements on the 3D artefacts provided an uncertainty statement based only on manufacturer specifications or was not able to state the uncertainty.

Procedure	Glass scale	Hole plate	Plastic bricks
UA) Uncertainty budget	5	4	3
UB) Use of calibrated items and substitution	2	2	1
UC) Experience of the participant	1	2	1
UD) Manufacturer system specifications	8	7	7
No statement	1	2	3

Table 7.8 Summary of procedures for the evaluation of uncertainty.

7.8 CONCLUSIONS

Metrological performance of optical coordinate measuring machines under industrial conditions has been investigated by a comparison carried out in the period from August 2007 to January 2009. The comparison involved 21 optical CMMs of different companies in Europe, mainly equipped with image processing sensors. A set of 3 different items has been selected, including both artefacts for performance verification and common industrial workpieces. All items demonstrated adequate dimensional stability during the circulation.

Measurements on the glass scale revealed a good ability of the participants in performing simple and well defined measurements of length, as well as in determining the associated measurement uncertainty.

Distance measurements on the hole plate confirmed the results obtained on the glass scale. On the other hand, for holes diameter measurements, the presence of length-independent error sources was observed, with effects that were not properly managed by some participants, resulting in non compatible measurements.

Results on the plastic bricks revealed the influence of many different quantities, resulting in larger scatter of data if compared with the other artefacts. Deviations from the reference mechanical values are up to one order of magnitude larger than the corresponding CMM length measuring performance; however participants in most cases were not able to take into account the additional error sources.

The comparison proved that the quality of dimensional measurement results on real industrial workpieces is largely independent on the CMM length measurement performance, as well as the limited ability of most participants to properly evaluate task-specific measurement uncertainty.

ACKNOWLEDGEMENTS

The authorwish to thank Prof. L. De Chiffre for fruitful discussions and his continuous enthusiastic support to the project. The participation of the following organisations is gratefully acknowledged by the author: 3Shape A/S (DK), ACC Elettromeccanica SpA (I), Calearo Antenne SpA (I), Diamond SA (CH), Technical University of Denmark (DK), Hexagon Metrology SpA (I), Mallinkrodt DAR (CH), Metris Italia (I), Metrologic ApS (DK), OGP Italia Srl (I), Omega Officine Meccaniche SpA (I), Palmer scarl (I), Radiometer Medical ApS (DK), Riverplast Srl (I), Tecnologie Diesel & Sistemi Frenanti SpA (I), TQM Itaca srl (I), Universidad Politecnica de Madrid (E).

Conclusions

The main conclusions of the Ph.D. project are summarized in the following. They are subdivided in three parts. The first part contains a study of the state of the art in Optical Metrology and related industrial requirements. The second part is dedicated to the review of methods and artefacts for performance verification and traceability establishment of optical Coordinate Measuring Systems (CMSs). Finally, the third part includes three case studies of optical metrology in industrial environment.

In the first part of the Thesis (Chapter 1 and 2), special attention has been paid to the current industrial requirements for Productive Metrology. Modern production, in fact, is characterized by increasing complexity, related both to dimensions of products and materials used for goods. Recently, as reported in Chapter 2, a large number a new instruments and sensors based on non contact technology has been developed. These sensors and instruments present all the characteristics to satisfy the industrial requirements for quality assurance: absence of contact, fast acquisition, possibility of being used directly for in line application. Nevertheless there are still some limitations regarding their use and integration into mature systems such as Coordinate Measuring Systems (CMS). For now, in fact, their accuracy is generally one order lower than contact systems, especially for 3D systems, and error sources are still not well known to final users. Another big limitation regards the normative aspect as only in the last years the International Organization for Standardization has started to put more attention to the optical systems, both for dimensional and roughness measurements. Without clear and full accepted methods and procedures for testing and verify metrological performances of optical systems, in fact, their advantages risk to be useless.

In the second part of the Thesis a study on the technical and scientific state-of-the-art on methods and artefacts for performance verification of optical Coordinate Measuring Systems was carried out including examples of measurements on own machines. In particular, error sources in optical coordinate metrology have been examined, considering separately the main aspects related to lateral sensors and

distance sensors. The influence of measuring parameters, such as illumination, windows size and magnification have been discussed through experimental investigations performed by the author using a Video CMM, while the effect of relative slope between optical axis and surface to be measured has been quantified for a conoscopic holography laser.
In Chapter 3 guidelines, standards and initiatives for standardization of performances verification of optical CMS have been introduced and discussed. Even if well defined and accepted procedures are necessary to allow the employment of new measuring equipment in production, for now no internationally standardized rules exist for non-contact systems. The main consequences of this lack in the normative field can be summarized in the following points: (i) specifications provided by manufacturers of different systems are defined on the basis of non-comparable verification procedures, (ii) users have difficulties in comparing systems based on different principles, (iii) metrological performances of optical CMS cannot be checked properly along the time. In addition, the characteristic uncertainty contributors for non-contact methods are often not well known or documented. Therefore, new methods and artefacts for testing optical systems and for making optical measurements comparable with mechanical measurement are required. To fulfil this lack of standardization, the international cooperation "OSIS" (Optical Sensor Interface Standard), has been started among the main manufacturers of CMMs and optical sensors. In order to contribute to the standardization of methods and artefacts, tests proposed by the OSIS Project have been performed by the author on an high accuracy multisensor CMM.
Another problem concerning performance verification of optical systems concerns the availability of suited artefacts. In particular artefacts for performance verification of optical CMS have to fulfil some requirements: they must be stable, easy to be calibrated, cheap and, in particular, to be measured by different optical sensors. The influence of the object properties (material and surface characteristics) on the measurement results, in fact, is much stronger and more difficult to assess for optical sensors than for tactile ones. To allow the comparison among different optical CMS the artefact properties should have no significant effect on the parameters to be determined. Starting from these considerations an experimental investigation on artefacts for optical systems have been presented in Chapter 4. In particular optical properties of cooperative-lambertian surfaces have been studied, mainly related to application with laser triangulation sensor. As result of the investigation, some artefacts made of acid etched steel have been developed.

In the third part of the Thesis a series of results related to experimental investigations and applications of optical measuring machines and equipment in industrial environment are reported and discussed. Going into detail, in Chapter 5

results related to activities performed within the European Co-operative Research Project OP3MET have been presented and discussed. The Project, carried out between November 2006 and November 2008, was aimed to the development of a new 3D laser scanner to be employed directly for in-line measurement. The author participated to the Project with activities related to performance verification and traceability of the newly developed system. In particular, the activities have regarded: (i) the use of cooperative artefacts, (ii) implementation and testing of new procedures for performance verification starting from existing national standards, (iii) development of procedures for uncertainty evaluation and traceability of measurements, (iv) testing of the newly developed metrological software. Results of the activities related to performance evaluation has been used to move some interesting comments about the national standard VDI/VDE 2617-6.2:2005.

In Chapter 6 results from an industrial project related to the integration of a chromatic sensor into a high precision grinding machine are reported. The author participated to this project working directly to the development of a software tool for in-line measurement of roundness of grinded part, able to separate from the data collected by the sensor the contribution due to error sources (such as eccentricity of the workpiece, sensor misalignment and noise) from the roundness of the workpiece itself. Based on the mathematical model related to the influence of error sources, a Generator of synthetic data was developed. Data generated from simulations have been used to test the roundness software module. Results obtained from the analysis have been validated by comparison with dedicated roundness equipments and software showing to be in good agreement.

Finally, in the last Chapter, the most important results from the inter-laboratory comparison *VideoAUDIT* have been reported and discussed. Metrological performances of optical coordinate measuring machines under industrial conditions has been investigated by a comparison carried out in the period from August 2007 to January 2009. The comparison involved 21 optical CMMs of different companies in Europe, mainly equipped with image processing sensors. A set of 3 different items has been selected, including both artefacts for performance verification (a 300mm glass scale and an optomechanical hole plate) and common industrial workpieces (a set of 4 plastic bricks). All items demonstrated adequate dimensional stability during the circulation. Measurements on the glass scale revealed a good ability of the participants in performing simple and well defined measurements of length, as well as in determining the associated measurement uncertainty. Distance measurements on the hole plate confirmed the results obtained on the glass scale. On the other hand, for holes diameter measurements, the presence of length-independent error sources was observed, with effects that were not properly managed by some participants, resulting in non compatible measurements.

Results on the plastic bricks revealed the influence of many different quantities, resulting in larger scatter of data if compared with the other artefacts. Deviations from the reference mechanical values are up to one order of magnitude larger than the corresponding CMM length measuring performance; however, participants in most cases were not able to take into account the additional error sources. The comparison proved that the quality of dimensional measurement results on real industrial workpieces is largely independent on the CMM length measurement performance, as well as the limited ability of most participants to properly evaluate task-specific measurement uncertainty.

References

[1] Küpper, H. U., "Produktion" in: Dichtl, E., Issing, O. (Hrsg./Edt.): Vahlens grosses Wirtschaeftslexikon, Verlag Franz Vahlen, München, 1987.

[2] Kunzmann H. , Pfeifer T., Schmitt R., Schwenke H., Weckenmann A., "Productive Metrology - Adding Value to Manufacture", CIRP Annals: 51, p. 685-699, 2002.

[3] Dance, D. L., "Cost of Ownership for Metrology Tools", American Institute of Physics, 1996.

[4] Cullen J., Hollingum J., "Implementing Total Quality", IFS (Publications) Ltd., United Kingdom, 1987.

[5] Pfeifer T., Imkamp D., Schmitt R., "Coordinate Metrology and Cax-Application in Industrial Production", Carl Hanser Verlag, Munich, ISBN-10: 3-446-40134-2, 2006.

[6] Sardella A., "Advanced processes, controls and inspection innovations for prefilled syringes", http://www.ondrugdelivery.com, 2009.

[7] Murphy S. D., "In-process measurement and control", Marcel Dekker Inc, US, ISBN 0-8247-8130-9, 1990.

[8] National Research Council - CPSMA, "Harnessing light: Optical Science and Engineering for the 21st Century", National Academy Press, Washington D.C., ISBN 0-30905991-7, 1998.

[9] Frost & Sullivan Report, "Market engineering research for the total European industrial vision system market", Frost & Sullivan, 2000.

[10] Neumann, H.J., "Koordinatenmesstechnik heute and morgen", QZ Qualität und Zuverlässigkeit, Carl Hanser Verlag, Munich, Nr. 9, S.1013-1017, 1997.

[11] Bosch J.A. (ed.), "Coordinate measuring machines and systems", Marcel Dekker, New York, USA, 1995.

[12] Neumann H.J., “Coordinate metrology. Technology and applications”, Verlag moderne industrie, Germany, 1990.

[13] Kunzmann H., Wäldele F., “Performance of CMMs”, Annals of the CIRP, Vol.37/2, p.633-640, 1988.

[14] Bariani P., “Dimensional Metrology for Microtechnology”, Ph.D. Thesis, Technical University of Denmark, Lyngby, 2004.

[15] Vermeulen MMPA, Rosielle PCJN, Schellekens PHJ, “Design of a high-precision 3D-Coordinate Measuring Machine, Annals of the CIRP, Vol. 47/1, p. 447-450, 1998.

[16] Bergmans RH. “Metrology for nanotechnology”, Proc. Euspen, 557-560, 2002.

[17] Website IBS Precision Engineering: www.ibspe.com

[18] Peggs GN, Lewis AJ, Oldfield S., “Design for a Compact High-Accuracy CMM”, Annals of the CIRP, Vol. 48/1, p. 417-420, 1999.

[19] Leach RK., Haycocks J., Jackson K., Lewis A., Oldfield S.,Yacoot A., “Advances in traceable nanometrology at the National Physical Laboratory, Nanotechnology, Vol. 12/1, R1-R6, 2001.

[20] Schwenke H, Wäldele F, Weiskirch C, Kunzmann H., “Opto-Tactile Sensor for 2 D and 3 D Measurement of Small Structures on Coordinate Measuring Machines”, Annals of the CIRP; 50 /1:, p.361-364, 2001.

[21] Bütefisch S, Büttgenbach S, Kleine-Besten T, Brand U., “Micromechanical three-axial force sensor for micromaterial characterisation”, Microsystem Technologies; 7: 171-174, 2001.

[22] Schwenke, H., Neuschaefer-Rube, U., Pfeifer, T., Kunzmann, H., “Optical Methods for Dimensional Metrology in Production Metrology”, CIRP Annals, Volume 51, Pages 685-699, 2002.

[23] Neumann H.J., “Coordinate metrology. Technology and application”, Verlag Moderne Industrie, Germany, 1990.

[24] Schwenke, H., Wäldele, F., Weiskirch, C., Kunzmann, H., 2001, “Opto-tactile sensor for 2D and 3D measurement of small structures on coordinate measuring machines”, Annals of the CIRP, Vol.50/1, 361-364, 2001.

[25] Christoph R., Neumann H.J., “Multisensor coordinate metrology” Verlag moderneindustrie, Munich, Germany, 2004.

[26] ISO 9000-9004, “Quality Management Systems and supporting documents”, ISO, Geneva, 2000.

[27] ISO/IEC 17025:2005/Cor 2006, "General Requirements for the competence of testing and calibration laboratories", ISO, Geneva, 2005/Cor 2006.

[28] JCGM 200:2008, International vocabulary of basic and general terms in metrology, (VIM), 2008.

[29] Simone Carmignato, "Traceability of coordinate measurements on complex surfaces, Ph.D. Thesis, University of Padova, Padova, 2005.

[30] VDI/VDE 2617 - 6.2: 2005, "Accuracy of CMMs - Characteristics and their testing - Guideline for the application of DIN EN ISO 10360 to CMMs with optical distance sensors", VDI, Düsseldorf, 2005.

[31] De Chiffre L., Carmignato S., "Industrial requirements to optical measurements in part verification and process control", IV Metromeet International Conference, 2008.

[32] Gava, A., "Modelling of the micro injection molding process, Ph.D. Thesis, University of Padova, Padova, 2009.

[33] Savio E, De Chiffre L, Schmitt R., "Metrology of freeform shaped parts", Annals of the CIRP, 56(2):810–35, 2005.

[34] Website Battenfeld: http://www.battenfeld-imt.com

[35] Van Gestel, N., Cuypers, S., Bleys, P., Kruth, J.P. "A performance evaluation test for laser line scanners on CMMs", Optics and Lasers in Engineering, Volume 47, Pages 336-342, 2009.

[36] Website OSIS: http://www.ntb.ch/3422.html

[37] VDI/VDE 2617 Blatt 6: 1997, "Accuracy of coordinate measuring machines – Characteristic parameters and their verification – CMMs with optical probes – basics", VDI, 1997.

[38] VDI/VDE 2617 Blatt 6.1: 2005, "Accuracy of coordinate measuring machines – Characteristic parameters and their verification – CMMs with optical probes – Sensors for 2D measurement", VDI, 2005.

[39] Sirat, G. Psaltis, D., "Conoscopic Holography", Optics Letters, Vol.10, Number 1, pp. 4-6. 1985.

[40] Losano F., Marinsek G., Merlo A.M., Ricci M., "Computer tomography in the automotive field: development of a new engine head case study", Proceedings of International Symposium on Computerized Tomography for Industrial Applications and Image Processing in Radiology, DGZfP, BB 67-CD: paper 10, 1999.

[41] Dastarac D., "Industrial Computed Tomography: Control and Digitalisation", Proceedings of International Symposium on Computerized

Tomography for Industrial Applications and Image Processing in Radiology, DGZfP, BB 67-CD, 1999.

[42] Obrist A., Flisch A., Hofmann J., Wirth J., "First Article Inspection Based on Industrial X-ray Computed Tomography", Proceedings of International Conference on Material Testing and Research, AMA Service GmbH, 2001.

[43] ISO 14253-1:1998, "Geometrical Product Specifications (GPS) – Inspection by measurement of workpieces and measuring instruments – Part 1: Decision rules for proving conformance or non-conformance with specification", ISO, Geneva, 1998.

[44] ISO 14253-2:1999, "Geometrical Product Specifications (GPS) – Inspection by measurement of workpieces and measuring instruments – Part 2: Guide to the estimation of uncertainty in GPS measurement, in calibration of measuring equipment and in product verification", ISO, Geneva, 1999.

[45] Hüser-Teuchert D., Trapet E., Garces A., Torres-Leza F., Pfeifer T., Scharsich P., "Performance test procedures for optical coordinate measuring probes. Final project report. Part 1", BCR report No EUR 15315 EN, Luxembourg 1994.

[46] Hüser-Teuchert D., Trapet E., Garces A., Torres-Leza F., Pfeifer T., Scharsich P., "Performance test procedures for optical coordinate measuring probes. Final project report. Part 2", BCR report No EUR 15315 EN, Luxembourg 1994.

[47] Carmignato S., Voltan A., Savio E., "Quantification of uncertainty contributors in coordinate measurements using video probes", Proc. of 7th EUSPEN Int. Conf., Bremen, May 2007.

[48] Morace R. E., "Traceability of measurements on optical coordinate measuring machines", Ph.D. Thesis, University of Naples Federico II, Naples, 2004.

[49] Hansen H. N., "Verification and calibration of coordinate measuring machines", Ph.D. Thesis, Technical University of Denmark, Lyngby, 1997.

[50] De Chiffre L., Hansen H.N., "Metrological limitations of optical probe techniques for dimensional measurements", Annals of CIRP, Vol. 44/1, p. 501-504, 1995.

[51] Morace R. E., Hansen H. N., De Chiffre L., "Uncertainty contributions due to different measurement strategies applied to optomechanical hole plate", Proc. of the Euspen International Topical Conference, Aachen, Germany, 2003.

[52] Morace R. E., Hansen H. N., De Chiffre L., " Uncertainty budget for optical coordinate measurements of circle diameter", Proc. of the 8th IMEKO International Symposium on Measurement and Quality Control in Production, Erlangen, Germany, 2004.

[53] De Chiffre, L., Hansen, H. N., Morace R. E., "Comparison of Coordinate Measuring Machines using an Optomechanical Hole Plate", Annals of the CIRP, 54/1:479-482, 2005.

[54] Huser, D., Pfeifer, T., Scharsich, P., Trapet, E., "A survey of the errors of optical coordinate measuring probes, Utraprecision in manufacturing engineering", Verlag Franz Rhiem, Duisburg, 11-14, ISBN 3-926832-1 1-8, 1994.

[55] Buzinski, M., Levine, A., Stevenson, W.H., "Performance characteristics of range sensors utilizing optical triangulation", IEEE/AESS Proc. of National Aerospace and Electronics Conference, pp. 1230-1236, 1992.

[56] Website Optimet: http://www.optimet.com.

[57] Paviotti A., Carmignato S., Voltan A., Laurenti N., Cortelazzo G., "Estimating angle-dependent systematic error and measurement uncertainty for a conoscopic holography measurement system", Proc. SPIE, Vol. 7239, 72390Z, DOI:10.1117/12.805972, 2009.

[58] ISO/DIS 10360-7 (2009-02-11), "GPS – Acceptance test and reverification test for CMMs - Part 7: CMMs equipped with video probing systems", ISO, Geneva, 2009.

[59] ISO 10360-2: 2001, "GPS – Acceptance tests and reverifications test for coordinate measuring machines (CMM) – Part 2: CMMs used for measuring sizes", ISO, Geneva, 2001.

[60] ISO/CD 10360-8, (2009-08-17) "GPS – Acceptance and reverification tests for coordinate measuring machines (CMM) – Part 8: CMMs with optical distance sensors", ISO, Geneva, 2009.

[61] ISO 10360-5: 2000, "GPS -- Acceptance and reverification tests for coordinate measuring machines (CMM) -- Part 5: CMMs using multiple-stylus probing systems", ISO, Geneva, 2000.

[62] ISO/CD 10360-9, (2009-08-17) "GPS – Acceptance and reverification tests for coordinate measuring machines (CMM) – Part 9: CMMs with multiple probing systems", ISO, Geneva, 2009.

[63] VDI/VDE 2617 Blatt 6.2: 1999, "Accuracy of coordinate measuring machines – Characteristic parameters and their verification – Coordinate

measuring machines with optical probes – Optical sensors for one-dimensional distance measurement", Verein Deutscher Ingenieure, 1999.

[64] ANSI/ASME B89.4.1-1997, "Methods for performance evaluation of coordinate measuring machine", American National Standards Institute, 1997.

[65] ANSI/ASME B89.4.14-1998 Draft, "Method for performance evaluation of noncontact probes for CMMs", American National Standards Institute, 1998.

[66] VDI/VDE 2634 - Part 1:2002, "Optical 3D measuring systems – Image systems with point by point probing", Verein Deutscher Ingenieure, 2002.

[67] VDI/VDE 2634 - Part 2:2002, "Optical 3D measuring systems – Optical systems based on area scanning", Verein Deutscher Ingenieure, 2002.

[68] DIN 32877:2000-08, "Optoelektronische Abstands-, Profil- und Formmessung", Beuth Verlag, Berlin, August 2000.

[69] Carmignato, S., Neuschaefer-Rube, U., Schwenke, H., Wendt, K., "Tests and artefacts for determining the structural resolution of optical distance sensors for coordinate measurement", Proc. of the 6th euspen International Conference, Baden, Wien, 2006.

[70] Trapet, E., "Measuring with Vision System: Industry Standards for Acceptance and Verification Tests", Proceedings of "3rd EMVA Business Conference", Palermo, 2005.

[71] Keferstein, C. P., Züst, R., "Minimizing technical and financial risk when integrating and applying optical sensors for in-process measurement", IMS International Forum; p. 475-482., 2004.

[72] Website IACMM: http://www.iacmm.org

[73] OSIS WG1: Mechanical / Electrical interface, "Documentation, Issue 1.0", 2003.

[74] OSIS WG2: Data integration, "Documentation, Release V1.0, 06.08.2003

[75] OSIS WG3: Specification, classifications and performance verification, Documentation, Release 1.1, 25.01.2006.

[76] ISO 10360-4: 2000, "GPS -- Acceptance and reverification tests for coordinate measuring machines (CMM) -- Part 4: CMMs used in scanning measuring mode", ISO, Geneva

[77] Voltan A., Carmignato S., Savio E., "Performance Verification of Coordinate Measuring Machines Equipped with Optical Sensors", Proceedings of 8th AMST Int. Conf., Udine, Italy, 2008.

[78] ISO/TS 15530-3: 2004, “GPS - CMMs: Technique for determining the uncertainty of measurement - Part 3: Use of calibrated workpieces or standards”, ISO, Geneva, 2004.

[79] ISO/TS 15530-4: 2008, “GPS - CMMs: Technique for determining the uncertainty of measurement - Part 4: Evaluating task-specific measurement uncertainty using simulation”, ISO, Geneva, 2008.

[80] ISO/CD TS Draft 15530-2, “GPS - Coordinate measuring machines (CMM): Technique for determining the uncertainty of measurement - Part 2: Use of multiple measurements strategies in calibration artefacts”, ISO, 2007

[81] JCGM 100:2008, Evaluation of measurement data - Guide to the expression of uncertainty in measurement (GUM).

[82] Pfeifer T., Spur G., “Task specific gauge for the inspection of coordinate measuring machines”, Annals of the CIRP, 43/1:465-468, 1994.

[83] Sammartini M., De Chiffre L., “A task specific gauge for pitch measurement of cylindrical gears”, 6th ISMQC (IMEKO), 1998.

[84] Sammartini M., De Chiffre L., “Development and validation of a new reference cylindrical gear for pitch measurement”, Precision Engineering, 24:302-309, 2000.

[85] Savio, E., “Traceability of free-form measurements on coordinate measuring machines”, Ph.D.Thesis, University of Padova, Padova, 1999

[86] Savio E., De Chiffre L., “An artefact for traceable freeform measurements on coordinate measuring machines”, Precision Engineering, 26: 58-68, 2002.

[87] Trapet E., Waldele F., “The Virtual CMM Concept”, In Advanced Mathematical Tools in Metrology II, World Scientific, 238-247, 1996.

[88] Kunzmann, H., Trapet, E., Waldele, F., “Concept for the Traceability of Measurements with Coordinate Measuring Machines”, Proc. 7th IPES, Kobe, Japan, 41-52, 1993.

[89] Haitjema, H., van Dorp, B., Morel, M., Schellekens, P.H.J., “Uncertainty estimation by the concept of virtual instruments”, Proc. SPIE 4401 Recent Developments in Traceable Dimensional Measurements, J.E. Decker and N. Brown, Eds., SPIE, 2001.

[90] Phillips S.D., et al., “The Calculation of CMM Measurement Uncertainty via the Method of Simulation by Constraints”, Am. Soc. for Precision Engineering, 16:443- 446, 1997.

[91] Balsamo A., et al., “Evaluation of CMM uncertainty through Monte Carlo simulations”, Annals of the CIRP, 48/1:425-428, 1999.

[92] Schwenke H., et al., “Assessment of uncertainties in dimensional metrology by Monte Carlo simulation: proposal of a modular and visual software”, Annals of the CIRP, 49/1:395-398, 2000.

[93] Voltan A., Carmignato S., “Calibration of Plastic Parts Using Video Probes”, Proceedings of 8th AMST Int. Conf., Udine, Italy, 2008.

[94] Salsbury J.G., “A Simplified Methodology for the Uncertainty Analysis of CMM Measurements”, Tech. Paper, Conf. On Precision Metrology/Applying Imaging and Sensoring, Society of Manufacturing Engineers, Indianapolis, IN, IQ95- 155:1-22, 1995.

[95] Website Trapet Precision Engineering: http://www.trapet.de

[96] Blondeau, J., “Method for calibrating measuring instrument for thickness and external diameter”, United States Patent 6505495, 2003

[97] Lartigue C, Contri A, Bourdet P., “Digitised point quality in relation with point exploitation” Measurement;32:193–203, 2002.

[98] Che C., Ni J., “A ball-target-based extrinsic calibration technique for high accuracy 3-D metrology using off-the-shelf laser-stripe sensors”. Precision Engineering; 24:210–9, 2000.

[99] Feng H, Liu Y, Xi F. “Analysis of digitizing errors of a laser scanning system”, Precision Engineering, 25:185–91, 2001

[100] Kusnoto, B., Evans, C.A., “Reliability of a 3D surface leser scanner for orthodontic applications”, American Journal of Orthodontics and Dentofacial Orthopedics, Volume 122, 2002

[101] De la Perrelle, E. T., Herbert, H., “The measurement of absorptivity and reflectivity”, Aeronautical research council, C.P. No. 601, 1962.

[102] Ehrig, W., Neuschaefer-Rube, U., “Artefacts with rough surfaces for verification of optical microsensors”, Proc. SPIE 6616/1 661626–1–9, 2007.

[103] Forest Collado, J., “New methods for triangulation-based shape acquisition using laser scanners”, ISBN 84-689-3091-1, 2005.

[104] Website 3Shape A/S: http://www.3shape.com

[105] Murakami, F., “Accuracy Assessment of a laser triangulation Sensor”, IEEE 0-7803-1880-3, 1994.

[106] Keferstein, C. P., Marxer, M., “Testing bench for laser triangulation sensors”, Volume 18 Number 3 pp. 183-187, ISSN 0260-2288, 1998.

[107] Boehler, W., Bordas Vicent, M., Marbs, A., "Investigating laser scanner accuracy", XIXth CIPA Simposium at Antalya, Turkey, 2003.

[108] Novello, R., "Sviluppo di campioni e procedure per la verifica metrologica di uno scanner laser 3D", M M.Sc.-thesis, DIMEG - Università di Padova, Padova, 2008.

[109] Brotto, M., "Verifica delle prestazioni metrologiche di sistemi di misura a coordinate con sensore laser", M.Sc.-thesis, DIMEG - Università di Padova, Padova, (in Italian) 2008.

[110] Fisker, R., Clausen, T., Deichmann, N., Oejelund, H., "Adaptive 3D Scanning", Patent WO2006007855, 2006.

[111] Carmignato, S., De Chiffre, L., Fisker, R., Hollenbeck, K., Savio E., "Development of an innovative laser scanner for geometrical verification of metallic and parts", 18th IMEKO TC2 Symposium on Photonics in Measurements. Prague, ISBN/ISSN: 978-80-86742-24-3, 2008.

[112] Wang, G. , Zheng, B., Li, X., Houkes, Z., Regtien, P.P.L., "Modeling and calibration of the laser beam-scanning triangulation measurement system", Robotics and Autonomous Systems, 40, 267-277, 2002.

[113] Smith, K.B., Zheng, Y.F., "Point laser Triangulation Probe Calibration for Coordinate Metrology", Journal of Manufacturing Science and Engineering, Vol.122 pp. 582-593, 2000.

[114] Zexiao, X., Jianguo, W., Ming, J., "Study on a full field of view laser scanning system", International Journal of Machine Tools & Manufacture 47 33-43, 2006.

[115] Beraldin, J.-A., El-Hakim, S. F., Blais, F., "Performance evaluation of three active vision systems built at the National Research Council of Canada", Optical 3-D Measurement Techniques III, Vienna, pp.352-361, 1995.

[116] El-Hakim, S. F., Beraldin, J.-A., Blais, F., "A Comparative Evaluation of the Performance of Passive and Active 3-D Vision Systems", Proc.: St. Petersburg Conference on Digital Photogrammetry, St. Petersburg, Russia, 1995.

[117] Carmignato, S., Savio, E., "Investigation on performance verification of coordinate measuring systems with optical distance sensors", 18th IMEKO TC2 Symposium on Photonics in Measurements. Prague, ISBN/ISSN: 978-80-86742-24-3, 2008

[118] Greif, N., Schrepf, H., Richter, D., "Software validation in metrology: A case study for a GUM-supporting software", Measurement, Volume 39, 849-855, 2006

[119] ISO 1101:2004, “Geometrical Product Specifications (GPS) - Geometrical tolerancing - Tolerances of form, orientation, location and run-out”, ISO, Geneva, 2004.

[120] Finetto, A., “Sviluppo ed implementazione di test per la verifica di software per metrologia geometrica”, M.Sc.-thesis, DIMEG - Università di Padova, Padova, (in Italian) 2008.

[121] Tonshoff, H. K., Friemuth, T., Becker, J. C., “Process Monitoring in Grinding.”, Annals of the CIRP 51(2):551–571, 2002.

[122] Keferstein, C. P., Honegger, D., Thurnherr, H., Gschwend, B., “Process monitoring in non-circular grinding with optical sensor”, Annals of CIRP, 57, 533–536, 2008

[123] ISO 4291:1995, “Methods for the assessement of departure from roundness - Measurement of variations in radius”, ISO, Geneva, 1995.

[124] ISO/TS 12181-2:2003, “GPS - Roundness - Part 2: Specification operators”, ISO, Geneva, 2003.

[125] Cho, N., Tu, J., “Roundness modeling of machined parts for tolerance analysis”, Precision Engineering, 5, 35–47, 2001.

[126] Hii, K.F., Vallance, R., Grejda, R. D., Marsh, E. R., “Error motion of a kinematic spindle”, Precision Engineering 28, 204–21, 2004.

[127] Zakharov, O. V., Brzhozovskii, B. M., “Accuracy of centering during measurement by roundness gauges”, Measurement Techniques, Vol. 49, No. 11, 2006

[128] Voltan, A., Götti, R., “Development of a SW-module for roundness calculation: final report”, NTB, Buchs, 2009

[129] Goch, G., Lubke, K., “Tschebyscheff approximation for the calculation of maximum inscribed/ minimum circumscribed geometry elements and form deviations”, Annals of the CIRP, 57, 517–520, 2008.

[130] Website Leitz-Metrology: http://www.leitz-metrology.com

[131] Website Taylor-Hobson Ltd: http://www.taylor-hobson.com

[132] Website Mahr GmbH: http://www.mahr.com

[133] Nielsen, H.S., Malburg, M.C.: Traceability and correlation in roundness measurement, Precision Engineering. 19, 1996.

[134] Kunzmann H., Trapet E., Wäldele F., EAL Interlaboratory comparison M16 “Ball plate calibration”, Final report, Physikalisch-Technische Bundesanstalt, Braunschweig, Germany, September ,1995.

[135] Kunzmann H., Trapet E., Wäldele F., Results of the international comparison of ball plate measurements in CIRP and WECC, Annals of the CIRP Vol. 44, p. 479-482, 1995

[136] Tikka H., Method for determining uncertainty of specified coordinate measurement, Dr.Sc.-thesis, Tampere University of Technology, Finland, 1992.

[137] Carmignato S. Voltan A., "An industrial comparison of coordinate measuring systems equipped with optical sensors: the VideoAUDIT Project", Proc. SPIE, Vol. 7239, 72390F, DOI:10.1117/12.805980, 2009

[138] Voltan A., Carmignato S., Savio E., "Industrial comparison of optical Coordinate Measuring Systems", Proceedings of 9th Euspen International Conference. San Sebastian, Spain, 2009

[139] Carmignato, S., Voltan, A., Savio, E., "Metrological performance of optical coordinate measuring machines under industrial conditions", submitted to CIRP, 2010

[140] Hansen H. N., De Chiffre L., "An industrial comparison of coordinate measuring machines in Scandinavia with focus on uncertainty statements", Precision Engineering, 23:185–195, 1999

[141] Meneghello R., De Chiffre L., Balsamo A., "Precision of Coordinate Measurements in Industry: Audit Italiano", Proceedings of 2nd Euspen International Conference, Turin, Italy, Spain, 2001

[142] Nielsen, H.S., "Inter-laboratory comparisons, the tool to establish mutual confidence in measurement and calibration services", Proc. of Metromeet Conference, Bilbao, Spain, 2008

[143] Evans C.J., Hocken R.J., Estler W. T., "Self-Calibration: Reversal, Redundancy, Error Separation, and 'Absolute Testing'", Keynote paper, Annals of the CIRP, 45/2:617-634, 1996.

[144] Carmignato S., Voltan A., Savio E., "VideoAUDIT Industrial interlaboratory comparison of CMMs equipped with optical sensors. Final report". Laboratory of Industrial and Geometrical Metrology, University of Padova, Padova, Italy, 2009.